

Image Cover Sheet

CLASSIFICATION**SYSTEM NUMBER**

501263

UNCLASSIFIED

**TITLE**

ON THE PREDICTION OF MECHANICAL BEHAVIOR OF PARTICULATE COMPOSITES USING AN
IMPROVED MORI-TANAKA METHOD

System Number:**Patron Number:****Requester:****Notes:****DSIS Use only:****Deliver to:**

UNCLASSIFIED

DEFENCE RESEARCH ESTABLISHMENT
CENTRE DE RECHERCHES POUR LA DÉFENSE
VALCARTIER, QUÉBEC

DREV – R-9514

Unlimited Distribution/Distribution illimitée

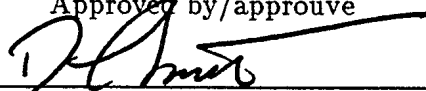
ON THE PREDICTION OF MECHANICAL BEHAVIOR
OF PARTICULATE COMPOSITES
USING AN IMPROVED MORI-TANAKA METHOD

by

F.C. Wong

January/janvier 1997

Approved by/approuvé



Chief Scientist/Scientifique en chef

10 Dec '96

Date

SANS CLASSIFICATION

UNCLASSIFIED

i

ABSTRACT

New micromechanical models for the prediction of particulate composite mechanical behavior have been developed. The models use an energy balance concept to account for nonlinear behavior due to particle debonding and incorporate a composite modulus prediction routine based on an improved Mori-Tanaka method. This method permits particle interaction effects to be taken into account and allows the stiffness matrix for voids or vacuoles to be explicitly stated in the model. To demonstrate the characteristics of the improved Mori-Tanaka method, comparisons with 2-phase and 3-phase modulus data were made. The micromechanical models developed for void and vacuole formation were evaluated against available mechanical behavior data. Comparisons showed that the model derived for vacuole formation predicted the mechanical behavior correctly for two types of model composites which contained inclusion volume fractions ranging from 0.2 to 0.5. The inability of the models to predict the initial stress-strain behavior of a composite containing a volume fraction of 0.22 of well-bonded particles suggests that the nonlinear matrix effects need to be included in the present model formulation.

RÉSUMÉ

Les nouveaux modèles micromécaniques pour la prédiction de comportement des composites chargés ont été développés. Les modèles utilisent un concept d'énergie pour tenir compte de la perte due aux décollements de particules. Les modèles emploient aussi une technique créée par Mori et Tanaka pour calculer le module de composite. Grâce à cette méthode, on peut inclure dans nos équations les effets d'interaction entre les particules et les effets de types de décollement soit les vides ou les vacuoles. Pour démontrer les caractéristiques de cette nouvelle méthode Mori-Tanaka, on a effectué des comparaisons avec les composites de 2 et 3 phases. Les modèles micromécaniques ont été évalués avec les données de comportement mécaniques disponibles. Les comparaisons ont démontré que le modèle pour les vacuoles a calculé correctement les comportements pour deux types de composites chargés avec 0,2 jusqu'à 0,5 fraction volume de particule. Le fait qu'il y avait des problèmes avec les prédictions de module initial pour le composite chargé avec 0,22 fraction volume de particule indique que l'effet de la non-linéarité de la matrice devrait être inclus dans la composition actuelle.

UNCLASSIFIED

iii

TABLE OF CONTENTS

ABSTRACT/RÉSUMÉ	i
EXECUTIVE SUMMARY	v
NOMENCLATURE	vii
1.0 INTRODUCTION	1
2.0 COMPOSITE MODULUS PREDICTION	2
2.1 Eshelby's Equivalent Inclusion Method	3
2.2 The Mori-Tanaka Method	6
2.3 Correction for Particle-Particle Interaction	8
3.0 ELASTIC PROPERTIES OF A TWO-PHASE COMPOSITE	10
4.0 ELASTIC PROPERTIES OF A THREE-PHASE COMPOSITE	11
5.0 CRITICAL STRAIN FOR ORTHOTROPIC COMPOSITES	15
6.0 MODULUS PREDICTION PERFORMANCE	17
6.1 Comparison with Glass/Epoxy Composite	17
6.2 Comparison with Tungsten-Carbide/Cobalt Composite	18
6.3 Comparison with Glass/Polyurethane Composite	19
6.4 Comparison for Three-Phase Composites	20
7.0 PREDICTION OF MECHANICAL BEHAVIOR	23
7.1 Model Characteristics	24
7.2 Glass Bead/Polyurethane Composite	25
7.3 Glass Bead/Polyethylene Composite	26
8.0 SUMMARY	29
9.0 REFERENCES	32

FIGURES 1 to 22

TABLES I to III

UNCLASSIFIED

iv

APPENDIX A- Mathematica Listing for 3-Phase Modulus Model A.1

APPENDIX B- FORTRAN Listing for Micromechanical Model B.1

UNCLASSIFIED

v

EXECUTIVE SUMMARY

Propellants are presently characterized from a macroscopic point of view. This means that the mechanisms that govern material behavior are lumped together and measured as a unit to produce a material property. This approach does not provide the quantitative information required for modifying a formulation. To meet this need, an analytical model that predicts the material properties from knowledge of factors such as particle size distribution, volume fraction of particles, adhesion energy and polymer properties is required. This ability to predict mechanical properties has important consequences for the determination of rocket motor service life. If the properties of the motor grain can be predicted before the propellant is cast, motor service life can be determined. If the calculated service life is deemed too short, the model can be used to guide the type of adjustments that need to be made to extend the service life of the motor. This capability would represent major savings in development and life cycle management costs because service life related problems could be resolved before the motor is fielded.

In recent years, researchers in the propellant industry have begun to use composite materials concepts for predicting the stress-strain behavior of propellants. These concepts, based on a microscopic point of view, take into account the size, shape and quantity of filler introduced into polymeric matrices. Previously, the strengths and weaknesses of the Anderson-Farris micromechanical model were examined using experimentally derived data. This model was based on an energy balance concept and calculated composite modulus using a differential scheme. It was shown that the model could predict the mechanical behavior of highly loaded composites if a representative value of adhesion energy was available.

In this report, new micromechanical models for the prediction of propellant mechanical behavior have been developed. The models again use energy balance to account for nonlinear behavior due to particle debonding. However, composite modulus is predicted using a routine based on an improved Mori-Tanaka method. This method permits particle interaction effects to be taken into account and allows the stiffness matrix for voids or vacuoles to be explicitly stated in the model. Comparisons with literature modulus data showed that tensile modulus could be predicted accurately with the improved Mori-Tanaka method. Comparisons with literature stress-strain data also showed that the model derived for vacuole formation predicted the mechanical behavior correctly for two types of model propellants which contained inclusion volume fractions ranging from 0.2 to 0.5.

UNCLASSIFIED

vii

NOMENCLATURE $L \equiv \text{length}$ $F \equiv \text{force}$

square brackets [] denote dimensions of the quantity

A_{ijkl}	=	$(C_{ijmn}^i - C_{ijmn}^o)^{-1} \cdot C_{mnkl}^o$, $[FL^{-2}]$
B_{ijkl}	=	$(C_{ijmn}^v - C_{ijmn}^o)^{-1} \cdot C_{mnkl}^o$, $[FL^{-2}]$
\bar{C}_{ijkl}	-	average elastic constants of composite, $[FL^{-2}]$
C_{ijkl}^o	-	elastic constants of comparison material, $[FL^{-2}]$
C_{ijkl}^r	-	elastic constants of phase-r material, $[FL^{-2}]$
c^i	-	volume fraction of inclusions, $[-]$
c_o^i	-	initial volume fraction of inclusions, $[-]$
c^r	-	volume fraction of phase-r inclusion, $[-]$
c^v	-	volume fraction of voids or vacuoles, $[-]$
\bar{E}	-	average composite tensile modulus, $[FL^{-2}]$
E_c	-	average composite tensile modulus, $[FL^{-2}]$
E_i	-	inclusion tensile modulus, $[FL^{-2}]$
E_m	-	matrix tensile modulus, $[FL^{-2}]$
$\bar{\mathcal{E}}$	-	composite energy, $[FL]$
\mathcal{E}_{int}	-	interaction energy, $[FL]$
\mathcal{E}_o	-	comparison material energy, $[FL]$
G_c	-	adhesion energy, $[FL]$
I_{ijkl}	-	identity matrix, $[-]$
\bar{K}	-	average composite bulk modulus, $[FL^{-2}]$
P_f	-	maximum packing fraction, $[-]$
S	-	surface area of inclusion, $[L^2]$
S_{ijkl}^r	-	Eshelby matrix of phase-r material, $[-]$
u_{ij}^A	-	prescribed surface displacement, $[L]$
u_{ij}^c	-	constrained displacement, $[L]$
V	-	volume of inclusion $[L^3]$,
Y	-	interaction function $[-]$,
Y_m	-	interaction function multiplier, $[-]$
δ_{ij}	-	Kronecker delta, $[-]$
ϵ_{cr}	-	critical strain, $[L/L]$
$\bar{\epsilon}_{ij}$	-	average composite strain, $[L/L]$
$\tilde{\epsilon}_{ij}$	-	average perturbed strain, $[L/L]$

UNCLASSIFIED

viii

ϵ_{ij}^c	-	constrained strain, $[L/L]$
ϵ_{ij}^*	-	eigenstrain, $[L/L]$
$\epsilon_{ij\ c}^{*r}$	-	corrected eigenstrain of phase-r material, $[L/L]$
$\epsilon_{ij\ u}^{*r}$	-	uncorrected eigenstrain of phase-r material, $[L/L]$
Γ_{ijkl}^r	-	correction matrix of phase-r material, $[-]$
λ, μ	-	Lamé constants, $[FL^{-2}]$
$\bar{\mu}$	-	average composite shear modulus, $[FL^{-2}]$
$\bar{\nu}$	-	average composite Poisson ratio, $[-]$
$\tilde{\sigma}_{ij}$	-	average perturbed stress, $[FL^{-2}]$
σ_{ij}^A	-	prescribed surface stress, $[FL^{-2}]$
σ_{ij}^c	-	constrained stress, $[FL^{-2}]$
$\sigma_{ij\ r}^c$	-	constrained stress of phase-r material, $[FL^{-2}]$
σ_{ij}^i	-	inclusion stress, $[FL^{-2}]$
$\sigma_{ij\ r}^i$	-	inclusion stress of phase-r material, $[FL^{-2}]$
σ_{ij}^*	-	eigenstress, $[FL^{-2}]$

UNCLASSIFIED

1

1.0 INTRODUCTION

The use of micromechanics for predicting material properties is not new in the field of composite materials (Refs. 1–9). In recent years, researchers in the solid propellant industry have begun using composite materials concepts for predicting the stress-strain behavior of oxidizer/binder type propellants to assess the impact that a formulation may have on a propellant's final mechanical properties (Refs. 10 and 11).

In Refs. 12 and 13, the authors hypothesized that nonlinear mechanical behavior in filled polymers was caused by the debonding of inclusions from the matrix. They modeled this process through an energy balance model which decreased inclusion concentration and increased void concentration. The composite's mechanical behavior was determined by the resulting composite modulus. An evaluation of their technique was made in Refs. 14 and 15. It was concluded that their model could predict the mechanical behavior of highly loaded composites if a representative adhesion energy was available.

Refs. 12 and 14 calculated composite modulus using the Farber-Farris (F-F) routine (Ref. 16). This routine is an incremental scheme based on a model that was developed for the prediction of viscosity of highly concentrated suspensions. In this article, the F-F routine has been replaced by a modulus prediction routine which is based on the Mori-Tanaka (M-T) method (Ref. 17). This method has received much attention recently because it permits closed-form solutions for multiphase anisotropic composites (Refs. 18 and 19). By including recent work from Ju and Chen into the M-T method, particle-particle interaction effects can be taken into account (Refs. 20 and 21). This results in an improved modulus prediction routine and subsequently, an improved micromechanical model for the prediction of mechanical behavior of particulate-filled composites.

UNCLASSIFIED

2

The characteristics of the improved M-T modulus prediction routine will be examined and compared with modulus data available in the literature. As well, comparisons will be made with F-F predictions to illustrate the differences between the two routines. The consequences of using the improved M-T routine for prediction of mechanical behavior of model particulate composites will be shown for two cases. The first case will model debonded particles using spherical voids to simulate completely debonded inclusions. The second case will model debonded particles using orthotropic inclusion properties to simulate spherical inclusions entrapped by spheroidal voids. Comparisons will be made between theoretical predictions of mechanical behavior and available literature data. This study was undertaken at DREV between January 1994 and March 1995 under PSC 32C, Rockets and Missiles.

2.0 COMPOSITE MODULUS PREDICTION

Mori and Tanaka showed that the internal stress at any point in a medium containing a finite concentration of inclusions was comprised of an average uniform stress and local fluctuating stresses which were found near the inclusions (Ref. 17). They also showed that the average of all the local fluctuating stresses in the matrix was zero. A key feature in their presentation was the use of Eshelby's equivalent inclusion method (Ref. 22).

Given the importance of the Eshelby and Mori-Tanaka methods to the current work, it would be appropriate to begin with an overview of Eshelby's concepts and a discussion of the salient points leading to the Mori-Tanaka formulation.

UNCLASSIFIED

3

2.1 Eshelby's Equivalent Inclusion Method

Eshelby developed a theory to examine how a far field uniform applied stress or strain is disturbed by a single inclusion in an infinite elastic matrix. He presented it in the form of a simple series of cutting, straining and rewelding operations. Conceptually, the steps were:

1. Remove the inclusion from the matrix and allow it to undergo a uniform stress-free strain, ϵ_{ij}^* . The stress-free strain is also known as the transformation strain or eigen-strain. The transformation or eigenstress due to the transformation strain would be,

$$\sigma_{ij}^* = \lambda \epsilon_{kk}^* \delta_{ij} + 2\mu \epsilon_{ij}^*$$

where λ and μ are the matrix Lamé constants.

2. Apply a surface stress $-\sigma_{ij}^* n_j$ to the inclusion to bring it back to its original shape. Embed the particle back into the matrix. Consider this as the zero strain point for the inclusion and the matrix.
3. Allow the surface stress $-\sigma_{ij}^* n_j$ to relax. The inclusion will see a change in stress of $-\sigma_{ij}^* n_j + \Delta \sigma_{ij} n_j$ while the matrix will see an equal and opposite stress of $\sigma_{ij}^* n_j - \Delta \sigma_{ij} n_j$.

The fact that the inclusion had different properties than the surrounding matrix gave rise to relaxed or constrained strains, ϵ_{ij}^c , in the matrix or inclusion. The relaxed or constrained stresses in the matrix in terms of the matrix properties were shown to be $\sigma_{ij}^c = \lambda \epsilon_{kk}^c \delta_{ij} + 2\mu \epsilon_{ij}^c$. Thus, the stresses in the inclusion, σ_{ij}^i , were

UNCLASSIFIED

4

$$\begin{aligned}
 \sigma_{ij}^i &= \sigma_{ij}^c - \sigma_{ij}^* \\
 &= \lambda(\epsilon_{kk}^c - \epsilon_{kk}^*)\delta_{ij} + 2\mu(\epsilon_{ij}^c - \epsilon_{ij}^*)
 \end{aligned} \tag{1}$$

By examining the elastic field in an ellipsoidal inclusion, Eshelby arrived at an important relationship between the constrained strains and the eigenstrains,

$$\epsilon_{ij}^c = S_{ijkl}\epsilon_{kl}^* \tag{2}$$

where S_{ijkl} is known as the Eshelby tensor. The tensor is a function of the matrix Poisson ratio and the shape of the inclusion.

Eshelby had also shown that the interaction energy between the constrained elastic field u_i^c with an applied elastic field u_i^A could be defined as

$$\mathcal{E}_{int} = \frac{1}{2} \int_S (\sigma_{ij}^c u_i^A - \sigma_{ij}^A u_i^c) dS_j \tag{3}$$

where

- S = surface area of inclusion,
- σ_{ij}^c = constrained inclusion or matrix stress,
- σ_{ij}^A = prescribed surface stresses,
- u_i^c = constrained inclusion or matrix strain,
- u_i^A = prescribed surface displacements.

Using the continuity of σ_{ij}^c and σ_{ij}^i across the inclusion surface, Gauss' theorem, the equivalence $\sigma_{ij}^A \epsilon_{ij}^c = \sigma_{ij}^c \epsilon_{ij}^A$ and eq. 1, eq. 3 could be written as

$$\mathcal{E}_{int} = -\frac{1}{2} \int_V \sigma_{ij}^* \epsilon_{ij}^A dV \tag{4}$$

$$= -\frac{1}{2} \int_V \sigma_{ij}^A \epsilon_{ij}^* dV \tag{5}$$

where

UNCLASSIFIED

5

$$\begin{aligned}
V &= \text{volume of inclusion,} \\
\sigma_{ij}^A &= \text{prescribed surface stresses,} \\
\sigma_{ij}^* &= \text{inclusion eigenstresses,} \\
\epsilon_{ij}^A &= \text{prescribed surface strains.} \\
\epsilon_{ij}^* &= \text{inclusion eigenstrains.}
\end{aligned}$$

The interaction energy \mathcal{E}_{int} was useful because it could be used to find the elastic constants of a composite. Using a comparison material with stiffness properties $C_{ijkl}^o{}^{-1}$ along with eq. 5, the energy of the composite, $\bar{\mathcal{E}}$, for prescribed stresses was

$$\begin{aligned}
\bar{\mathcal{E}} &= \mathcal{E}_o - \mathcal{E}_{int} \\
\frac{1}{2} \bar{C}_{ijkl}{}^{-1} \sigma_{ij}^A \sigma_{kl}^A &= \frac{1}{2} C_{ijkl}^o{}^{-1} \sigma_{ij}^A \sigma_{kl}^A + \frac{1}{2} \int_V \sigma_{ij}^A \epsilon_{ij}^* dV
\end{aligned} \tag{6}$$

For prescribed strains, the energy of the composite was

$$\begin{aligned}
\bar{\mathcal{E}} &= \mathcal{E}_o + \mathcal{E}_{int} \\
\frac{1}{2} \bar{C}_{ijkl} \epsilon_{ij}^A \epsilon_{kl}^A &= \frac{1}{2} C_{ijkl}^o \epsilon_{ij}^A \epsilon_{kl}^A - \frac{1}{2} \int_V \sigma_{ij}^A \epsilon_{ij}^* dV
\end{aligned} \tag{7}$$

The meaning of the energy equations may be interpreted in the following manner. For hard inclusions ($\lambda_i > \lambda_o$ and $\mu_i > \mu_o$), the inclusion deforms less than the comparison material for a prescribed strain ϵ_{ij}^A . This is equivalent to Eshelby's case where an inclusion spontaneously contracts ($-\epsilon_{ij}^*$) in an elastic medium due to phase or temperature change. From eq. 7, the negative transformation strain signifies that the composite material has an increased capacity to store energy in relation to the comparison material. Thus, the elastic constants of the composite are greater than that of the comparison material. For soft inclusions ($\lambda_i < \lambda_o$ and $\mu_i < \mu_o$), the inclusion deforms more than the comparison material. Thus, the composite has a decreased capacity to store energy. This leads to a composite with elastic constants which are less than those of the comparison material. A similar argument can be used with eq. 6.

UNCLASSIFIED

6

Using the definitions $\bar{\epsilon}_{kl} = \bar{C}_{ijkl}^{-1} \sigma_{ij}^A$ and $\epsilon_{kl}^o = C_{ijkl}^o^{-1} \sigma_{ij}^A$, eq. 6 may be used to show that the average composite strain is

$$\bar{\epsilon}_{kl} = \epsilon_{kl}^o + c \epsilon_{kl}^* \quad [8]$$

where

- $\bar{\epsilon}_{kl}$ = average composite strain,
- ϵ_{kl}^o = comparison material strain,
- c = volume fraction of the inclusion,
- ϵ_{kl}^* = eigenstrain of the inclusion.

Conversely, it can be shown with eq. 7 that the average composite stress is

$$\bar{\sigma}_{ij} = \sigma_{ij}^o - c \sigma_{ij}^* \quad [9]$$

where

- $\bar{\sigma}_{ij}$ = average composite stress,
- σ_{ij}^o = comparison material stress,
- c = volume fraction of the inclusion,
- σ_{ij}^* = eigenstress of the inclusion.

2.2 The Mori-Tanaka Method

The Mori-Tanaka method has been used to analyze a series of problems ranging from the determination of composite elastic constants (Ref. 19) to the determination of stresses in and around inclusions (Ref. 23). Following Weng (Ref. 18), the term "phase" will be applied to a collection of inclusions whose shape, orientation and elastic moduli are identical. The superscript r will be used to identify an r -th phase of inclusions.

The development of the Mori-Tanaka method proceeds as follows (Ref. 23). For a prescribed stress σ_{ij}^A , let the average strain produced in an elastic composite and comparison

UNCLASSIFIED

7

material be defined as

$$\sigma_{ij}^A = \bar{C}_{ijkl} \bar{\epsilon}_{kl} \quad [10]$$

$$\sigma_{ij}^A = C_{ijkl}^o \epsilon_{kl}^o \quad [11]$$

where

$$\begin{aligned} \sigma_{ij}^A &= \text{prescribed surface stresses,} \\ \bar{C}_{ijkl} &= \text{average elastic constants of the composite,} \\ \bar{\epsilon}_{kl} &= \text{average composite strain,} \\ C_{ijkl}^o &= \text{elastic constants of the comparison material,} \\ \epsilon_{kl}^o &= \text{comparison material strain.} \end{aligned}$$

Letting the average perturbed stress due to the presence of all inclusions be defined as $\tilde{\sigma}_{ij}$, the corresponding perturbed strains are $\tilde{\epsilon}_{ij}$. The overall stress in the comparison material is

$$\sigma_{ij}^A + \tilde{\sigma}_{ij} = C_{ijkl}^o (\epsilon_{kl}^o + \tilde{\epsilon}_{kl}) \quad [12]$$

Looking at the stresses in the inclusion, it will differ from the stresses in the comparison material by an amount equivalent to Eshelby's constrained stresses due to the difference in material properties. The inclusion stresses in terms of the inclusion properties C_{ijkl}^r are

$$\sigma_{ij}^{i,r} = \sigma_{ij}^A + \tilde{\sigma}_{ij} + \sigma_{ij}^c = C_{ijkl}^r (\epsilon_{kl}^o + \tilde{\epsilon}_{kl} + \epsilon_{kl}^c) \quad [13]$$

Using Eshelby's inclusion method eq. 1, the inclusion stresses in terms of the eigenstrains are

$$\sigma_{ij}^{i,r} = \sigma_{ij}^A + \tilde{\sigma}_{ij} + \sigma_{ij}^c = C_{ijkl}^o (\epsilon_{kl}^o + \tilde{\epsilon}_{kl} + \epsilon_{kl}^c - \epsilon_{kl}^*) \quad [14]$$

Mori and Tanaka showed that the volume integral of all perturbed stresses in a representative volume element (RVE) was zero. In other words, the perturbed stresses were

UNCLASSIFIED

8

in equilibrium with the constrained stresses. Assuming that all particles in the RVE were equally stressed, equilibrium required

$$\tilde{\sigma}_{ij} + \sum c^r \sigma_{ij}^{c,r} = 0 \quad [15]$$

Subtracting eq. 12 from eq. 14 and using eq. 2 for phase r ,

$$\sigma_{ij}^{c,r} = C_{ijkl}^o (S_{klmn}^r \epsilon_{mn}^{*,r} - \epsilon_{kl}^{*,r}) \quad [16]$$

Defining the identity tensor as $I_{ijkl} = \frac{1}{2}(\delta_{ik}\delta_{jl} + \delta_{il}\delta_{jk})$ and using eqs. 11, 12 and 16 in eq. 15, the perturbed strains are

$$\tilde{\epsilon}_{kl} = - \sum c^r (S_{klmn}^r - I_{klmn}) \epsilon_{mn}^{*,r} \quad [17]$$

By setting the third term in eq. 13 equal to the third term in eq. 14 and making use of the definitions for comparison strains in eq. 11, constrained strains in eq. 2 and perturbed strains in eq. 17, the governing equation for the composite is

$$\begin{aligned} (C_{ijkl}^o - C_{ijkl}^r) \epsilon_{kl}^o &= (C_{ijkl}^r - C_{ijkl}^o) [S_{klpq}^r \epsilon_{pq}^{*,r} \\ &\quad - \sum c^r (S_{klmn}^r - I_{klmn}) \epsilon_{mn}^{*,r}] + C_{ijkl}^o \epsilon_{kl}^{*,r} \end{aligned} \quad [18]$$

2.3 Correction for Particle-Particle Interaction

Ju and Chen (Ref. 21) formulated new ensemble-averaged constitutive equations based on Eshelby's equivalent inclusion principle. The equations took into account particle-particle interaction effects. Previously, Weng (Ref. 18) had shown that the Mori-Tanaka (M-T) method could be reduced to give the Hashin-Shtrikman (H-S) lower bound as a special case. Experimental data has shown that the M-T method and the H-S lower bound

UNCLASSIFIED

underestimated slightly composite modulus (Refs. 24 and 25). Ju and Chen showed that by accounting for particle interaction, their model could reproduce experimental data more closely. As a special case, their model reduced to the M-T equations when particle interaction was ignored. This meant that the M-T results and the H-S lower bounds corresponded to a micromechanical model with non-interacting particles.

The solution in Ref. 21 for particle interaction comes in a form convenient for inclusion in a M-T formulation. Since the theory is based on Eshelby's equivalent inclusion principle, the correction matrix, Γ^r , could be cast in terms of the uncorrected eigenstrain solution. From this point on, braces will be used to denote vectors and brackets will be used to denote square matrices. The corrected eigenstrain vector of phase-r was shown to be

$$\{\epsilon_c^{*r}\} = [\Gamma^r]\{\epsilon_u^{*r}\} \quad [19]$$

where

$$\begin{aligned} \{\epsilon_c^{*r}\} &= \text{interacting or corrected eigenstrain of phase-r,} \\ [\Gamma^r] &= [I] + \frac{5c^r}{4\beta^2} Y[W^r], \\ \{\epsilon_u^{*r}\} &= \text{non-interacting or uncorrected eigenstrain of phase-r,} \\ [I] &= \text{identity matrix,} \\ c^r &= \text{volume fraction of phase-r,} \\ Y &= \text{interaction factor,} \\ [W^r] &= \zeta_1 \delta_{ij} \delta_{kl} + \zeta_2 (\delta_{ik} \delta_{jl} + \delta_{il} \delta_{jk}), \\ \zeta_1 &= 12(13\nu_o - 14\nu_o^2) - \frac{96\alpha}{3\alpha+2\beta} (1 - 2\nu_o)(1 + \nu_o), \\ \zeta_2 &= 6(25 - 34\nu_o + 22\nu_o^2) - \frac{36\alpha}{3\alpha+2\beta} (1 - 2\nu_o)(1 + \nu_o), \\ \alpha &= 2(5\nu_o - 1) + 10(1 - \nu_o) \left(\frac{K_o}{K_r - K_o} - \frac{\mu_o}{\mu_r - \mu_o} \right), \\ \beta &= 2(4 - 5\nu_o) + 15(1 - \nu_o) \left(\frac{\mu_o}{\mu_r - \mu_o} \right), \\ \nu_o &= \text{Poisson's ratio of comparison material,} \\ K_o, K_r &= \text{bulk modulus of comparison and phase-r inclusion,} \\ \mu_o, \mu_r &= \text{shear modulus of comparison and phase-r inclusion.} \end{aligned}$$

In eq. 19 the inter-particle effects are quantified by the second term in $[\Gamma^r]$. As explained in Ref. 21, this matrix was derived from the analysis of probabilistic pairwise particle

UNCLASSIFIED

10

interaction of two identical and randomly located elastic spheres which are embedded in a comparison material.

The factor Y (Ref. 21) is related to the microstructure of the composite and is characterized by a radial distribution function, $g(r)$. For a statistically uniform radial distribution function where $g(r) = 1$, $Y = 1/24$. It will be shown later that $[\Gamma^r]$ causes certain problems in the recovery of $[C^r]$ when $c^r = 1$. This can be remedied by selecting a modified form of Y . This point will be discussed further in Sec. 6.0.

3.0 ELASTIC PROPERTIES OF A TWO-PHASE COMPOSITE

The average composite modulus for an elastic medium containing a finite concentration of inclusions may be calculated using the energy equation that Eshelby developed but extended for multiple inclusions. If the domain of integration in eq. 6 is extended for finite concentrations of inclusions of phase r , then the following equation can be written

$$\frac{1}{2} \bar{C}_{ijkl}^{-1} \sigma_{kl}^A \sigma_{ij}^A = \frac{1}{2} C_{ijkl}^o^{-1} \sigma_{kl}^A \sigma_{ij}^A + \frac{1}{2} \sum \int_{V^r} \sigma_{ij}^A \epsilon_{ij}^{*r} dV^r \quad [20]$$

This leads naturally to a modified form of eq. 8 which denotes that all particles of phase r are taken into account,

$$\{\bar{\epsilon}\} = \{\epsilon^o\} + \sum c^r \{\epsilon_c^{*r}\} \quad [21]$$

where $\{\epsilon_c^{*r}\}$ is defined in Sec. 2.3. The form of eq. 21 is slightly different than that found in Ref. 18. Here the interacting eigenstrain is used. However, if $[\Gamma^r]$ is set equal to $[I]$, the non-interacting eigenstrain is easily recovered. This would give an average composite strain identical to that found in Ref. 18.

The average elastic constants for a two-phase composite can be determined in a

UNCLASSIFIED

11

two-step process using the equations discussed in Secs. 2.2 and 2.3. First, eqs. 18 and 19 are used in eq. 21 to obtain

$$\{\epsilon^{*r}\} = -(c^r[I - S^r] + [S^r] + [C^r - C^o]^{-1} \cdot [C^o] - c^r[\Gamma^r])^{-1} \{\bar{\epsilon}\} \quad [22]$$

Note that ϵ_{kl}^{*r} in eq. 18 is identical to $\{\epsilon_u^{*r}\}$ in eq. 19. Second, solving eq. 21 for $\{\epsilon^o\}$ and substituting it into eq. 11 gives

$$\{\sigma^A\} = [C^o] \cdot (\{\bar{\epsilon}\} - c^r \{\epsilon^{*r}\}) \quad [23]$$

Then using eqs. 19 and 22 into eq. 23 and making a sign change, the average elastic properties can be expressed as

$$[\bar{C}] = [C^o] \cdot ([I] + c^r[\Gamma^r](c^r[I - S^r - \Gamma^r] + [S^r] + [C^r - C^o]^{-1} \cdot [C^o])^{-1}) \quad [24]$$

Comparison of eq. 24 with that of eq. 53 in Ref. 21 shows that the two are not identical for the case where particle interaction is taken into account. The difference occurs because Ref. 20 derived the volume-averaged strain tensor by integrating Green's function over a representative volume element to arrive at a definition that was a function of the uniform far-field strains, the eigenstrains and a depolarization tensor.

4.0 ELASTIC PROPERTIES OF A THREE-PHASE COMPOSITE

In order to predict the mechanical behavior of a particulate composite, the model in Refs. 12 and 14 required new elastic moduli be calculated each time a group of inclusions are debonded. The elastic modulus of a composite with bonded and debonded inclusions was assumed equivalent to the elastic modulus of a composite which contains inclusions and voids. Thus, the case of a three-phase composite is of special interest here because the

UNCLASSIFIED

12

debonding process in the above assumption changes the initial two-phase composite where all inclusions are bonded to the matrix into a three-phase composite where some particles become debonded thereby creating voids or vacuoles. The distinction between a void and vacuole is that a void is a spherical air bubble while a vacuole is a spheroidal air pocket which surrounds a debonded inclusion.

The average elastic properties for a 3-phase composite can be derived using the procedure outlined in Sec. 3.0. The only difference is that the summation of phases will now be used. Therefore, eq. 18 is modified by explicitly specifying the number of phases in eq. 17. The two resulting equations from consideration of each phase are

$$-\{\epsilon^o\} = (c^i[I - S^i] + [S^i] + [A])\{\epsilon^{*i}\} + c^v[I - S^v]\{\epsilon^{*v}\} \quad [25]$$

$$-\{\epsilon^o\} = (c^v[I - S^v] + [S^v] + [B])\{\epsilon^{*v}\} + c^i[I - S^i]\{\epsilon^{*i}\} \quad [26]$$

where

$$\begin{aligned} [A] &= [C^i - C^o]^{-1} \cdot [C^o], \\ [B] &= [C^v - C^o]^{-1} \cdot [C^o], \\ i &= \text{parameters relating to inclusions,} \\ v &= \text{parameters relating to voids or vacuoles.} \end{aligned}$$

Subtracting eq. 26 from eq. 25 gives the relationship between $\{\epsilon^{*i}\}$ and $\{\epsilon^{*v}\}$,

$$([S^i] + [A])\{\epsilon^{*i}\} - ([S^v] + [B])\{\epsilon^{*v}\} = \{0\} \quad [27]$$

Following the procedure outlined in Sec. 3.0, the non-interacting eigenstrains for the inclusion and void or vacuole are

$$\begin{aligned} \{\epsilon_u^{*i}\} &= -(c^i[I - S^i - \Gamma^i] + [S^i] + [A] \\ &\quad + c^v[I - S^v - \Gamma^v] \cdot [S^v + B]^{-1} \cdot [S^i + A])^{-1} \{\bar{\epsilon}\} \end{aligned} \quad [28]$$

UNCLASSIFIED

13

$$\begin{aligned} \{\epsilon_u^{*v}\} = & -(c^v[I - S^v - \Gamma^v] + [S^v] + [B]) \\ & + c^i[I - S^i - \Gamma^i] \cdot [S^i + A]^{-1} \cdot [S^v + B])^{-1} \{\bar{\epsilon}\} \end{aligned} \quad [29]$$

As before, starting from eq. 11, the substitution of eqs. 21, 19, 28 and 29 gives the average elastic properties of a 3-phase composite as

$$\begin{aligned} [\bar{C}] = [C^o] \cdot ([I] + & c^i[\Gamma^i](c^i[I - S^i - \Gamma^i] + [S^i] + [A]) \\ & + c^v[I - S^v - \Gamma^v] \cdot [S^v + B]^{-1} \cdot [S^i + A])^{-1} \\ & + c^v[\Gamma^v](c^v[I - S^v - \Gamma^v] + [S^v] + [B]) \\ & + c^i[I - S^i - \Gamma^i] \cdot [S^i + A]^{-1} \cdot [S^v + B])^{-1}) \end{aligned} \quad [30]$$

As mentioned in Sec. 2.1, the Eshelby tensor $[S]$ is dependent on the matrix Poisson ratio ν_o and the inclusion shape. Reference 23 gives $[S]$ for spheroidal inclusions. For spherical inclusions $[S]$ is defined by Ref. 21 as

$$S_{ijkl} = \frac{1}{15(1 - \nu_o)} ((5\nu_o - 1)\delta_{ij}\delta_{kl} + (4 - 5\nu_o)(\delta_{ik}\delta_{jl} + \delta_{il}\delta_{jk})) \quad [31]$$

For the case where the debonded inclusions are modeled by equivalent sized spherical voids, the property matrix $[C^v]$ can be set to zero. Alternatively, isotropic void properties can be specified to simulate partially debonded inclusions. This technique was used in Ref. 12. In either case, the average composite properties remains isotropic so the usual engineering elastic constants like bulk, shear and tensile modulus and Poisson's ratio may be found from eq. 30 using

UNCLASSIFIED

14

$$\begin{aligned}
\bar{K} &= (1/3)(\bar{C}_{1111} + 2\bar{C}_{1122}) \\
\bar{\mu} &= (1/2)(\bar{C}_{1111} + \bar{C}_{1122}) \\
\bar{E} &= \bar{C}_{1111} - \frac{2\bar{C}_{1122}\bar{C}_{2211}}{\bar{C}_{2222} + \bar{C}_{2233}} \\
\bar{\nu} &= \frac{\bar{C}_{2211}}{\bar{C}_{2222} + \bar{C}_{2233}}
\end{aligned} \tag{32}$$

In the case of modeling vacuoles, Mochida (Ref. 26) suggested that the boundary conditions around a debonded inclusion may be specified as

$$0 = \sigma_{ii}^v = C_{iikl}^v(\epsilon_{kl}^o + \tilde{\epsilon}_{kl} + \epsilon_{kl}^c) \tag{33}$$

$$0 = \epsilon_{jj}^o + \tilde{\epsilon}_{jj} + \epsilon_{jj}^c \tag{34}$$

Assuming the load is applied in the ii -direction and the equator of the particle is represented by the jj -direction, eqs. 33 and 34 state that no stresses are experienced by the inclusion in the loading direction and no lateral contraction is allowed around the equator.

Attempting to apply Mochida's boundary conditions to the present formulation results in a trivial solution where $\{\epsilon^*\} = \{0\}$ because application of eqs. 33 and 34 to eqs. 13 and 14 leads one to conclude that

$$\{0\} = \{\epsilon^o + \tilde{\epsilon} + \epsilon^c\}$$

$$\{0\} = \{\epsilon^o + \tilde{\epsilon} + \epsilon^c - \epsilon^*\}$$

An alternative to Mochida's method is to model the debonded phase as a spherical inclusion with orthotropic properties. A low or zero modulus value in the loading direction can be used to represent the debonded condition and a high or inclusion modulus value in the equator direction can be used to enforce the lateral constraint condition. Since the

UNCLASSIFIED

15

M-T formulation can be applied equally well to inclusions with orthotropic properties as to inclusions with isotropic properties, this approach can be implemented by modifying the definition of the debonded particle's material matrix. The property matrix for the normal components of an orthotropic material is (Ref. 27)

$$[C^v] = m \begin{bmatrix} E_{11}(1 - \nu_{23}\nu_{32}) & E_{11}(\nu_{21} + \nu_{23}\nu_{31}) & E_{11}(\nu_{31} + \nu_{21}\nu_{32}) \\ E_{22}(\nu_{12} + \nu_{13}\nu_{32}) & E_{22}(1 - \nu_{13}\nu_{31}) & E_{22}(\nu_{32} + \nu_{12}\nu_{31}) \\ E_{33}(\nu_{13} + \nu_{12}\nu_{23}) & E_{33}(\nu_{23} + \nu_{13}\nu_{21}) & E_{33}(1 - \nu_{12}\nu_{21}) \end{bmatrix} \quad [35]$$

where

$$\begin{aligned} m &= (1 - \nu_{12}\nu_{21} - \nu_{13}\nu_{31} - \nu_{23}\nu_{32} - \nu_{12}\nu_{23}\nu_{31} - \nu_{13}\nu_{21}\nu_{32})^{-1}, \\ E_{ii} &= \text{tensile modulus of vacuole in the } ii\text{-direction,} \\ \nu_{ij} &= \text{Poisson's ratio of vacuole in the } ij\text{-direction.} \end{aligned}$$

5.0 CRITICAL STRAIN FOR ORTHOTROPIC COMPOSITES

The prediction of mechanical behavior is performed using an energy balance model which is derived in terms of critical strain. Critical strain is defined as the point where the internal strain energy in the composite and the energy released due to particle debonding equals the work put into the composite. This statement can be expressed as (Refs. 12 and 14)

$$2G_c\delta A/V_o = \sigma_{ij}\delta\epsilon_{ij} - \delta\sigma_{ij}\epsilon_{ij} \quad [36]$$

where G_c is the adhesion energy between particle and matrix, δA is the variation in surface area, σ_{ij} is the composite stress, ϵ_{ij} is the composite strain and V_o is the specimen volume.

Examining the case of a uniaxial bar under tension and ambient pressure, eq. 36 can be simplified to (Refs. 12 and 14)

$$2G_c\delta A/V_o = \sigma_{11}^A\delta\epsilon_{cr} - \delta\sigma_{11}^A\epsilon_{cr} \quad [37]$$

UNCLASSIFIED

16

where σ_{11}^A is the applied stress in the 11-direction and ϵ_{cr} the critical strain. The boundary conditions $\sigma_{22} = \sigma_{33} = 0$ and $\epsilon_{22} = \epsilon_{33}$ were used.

By using the same boundary conditions on the constitutive equation for an orthotropic material (eq. 10), the transverse strain is

$$\epsilon_{22} = -\frac{\bar{C}_{2211}}{\bar{C}_{2222} + \bar{C}_{2233}} \epsilon_{cr} \quad [38]$$

Using eq. 38 to solve for σ_{11}^A in eq. 10, the simplified constitutive equation is

$$\sigma_{11}^A = \left(\bar{C}_{1111} - \frac{2\bar{C}_{1122}\bar{C}_{2211}}{\bar{C}_{2222} + \bar{C}_{2233}} \right) \epsilon_{cr} \quad [39]$$

Taking the variation of σ_{11}^A and substituting it and eq. 39 into eq. 37 gives

$$2G_c \delta A / V_o = \left[-\delta \bar{C}_{1111} - 2 \left\{ \frac{\bar{C}_{1122}\bar{C}_{2211}(\delta \bar{C}_{2222} + \delta \bar{C}_{2233})}{(\bar{C}_{2222} + \bar{C}_{2233})^2} \right\} + 2 \left\{ \frac{(\bar{C}_{2222} + \bar{C}_{2233})(\bar{C}_{2211}\delta \bar{C}_{1122} + \bar{C}_{1122}\delta \bar{C}_{2211})}{(\bar{C}_{2222} + \bar{C}_{2233})^2} \right\} \right] \epsilon_{cr}^2 \quad [40]$$

This equation is valid for orthotropic composites under uniaxial tension and ambient pressure. It assumes the RVE is larger than the largest particle so that average stress, strain and modulus can be used. If $[\bar{C}]$ is isotropic then eq. 40 reduces to

$$2G_c \delta A / V_o = -\delta E \epsilon_{cr}^2 \quad [41]$$

where δE is the variation in tensile modulus.

To solve eq. 40 or eq. 41, the variational quantities are changed to incremental quantities based on inclusion concentration. For example, δA would change to $\Delta A / \Delta c^i$. The algorithm to generate the composite's stress-strain behavior has been outlined in Refs. 14 and 15.

UNCLASSIFIED

17

6.0 MODULUS PREDICTION PERFORMANCE

The performance of the energy balance model in Ref. 14 is directly related to the performance of the composite modulus prediction routine employed. Therefore, it is of interest to examine the prediction characteristics of the composite modulus models developed in Secs. 3.0 and 4.0. To accomplish this task, the models will be compared with experimental data obtained from Refs. 25, 29 and 30. As well, they will be compared with the Farber-Farris predictions (Ref. 16). The Farber-Farris routine was originally used in the energy balance model in Ref. 14. The Mathematica (Ref. 28) input file used for generation of the Mori-Tanaka data may be found in Appendix A. A summary of the constituent properties for the composites used in this document are shown in Table I.

6.1 Comparison with Glass/Epoxy Composite

A comparison of the 2-phase composite predictions (eq. 24) with experimental data obtained from Smith (Ref. 29) and theoretical predictions using the Farber-Farris routine is shown in Fig. 1. Smith's composite system consisted of glass spheres embedded in epoxy ($E_i/E_m = 25$). Three variations of the 2-phase model are shown.

The first variation is the Mori-Tanaka model where no particle interaction is accounted for (denoted M-T in Fig. 1, $[I^*] = [I]$ in eq. 24). This variation will be called simply the M-T model. It can be seen that the M-T model underpredicted Smith's data at volume fractions c^i above 0.3. This was not surprising since Ref. 18 showed that the M-T solution was equivalent to the Hashin-Shtrikman lower bounds.

The second variation (called M-T interaction) is the M-T model corrected for par-

UNCLASSIFIED

18

ticle interaction ($[\Gamma^r]$ with $Y = 1/24$). This variation fared better up to $c^i = 0.4$. However, between $0.4 < c^i < 0.63$, the normalized composite modulus, E_c/E_m , rapidly rose. At $c^i = 0.63$, it dropped suddenly. Between $0.63 < c^i < 1$, E_c/E_m rose back up to -2 . It was obvious that this undesirable behavior was being caused by the introduction of the correction matrix $[\Gamma^r]$. An examination of eq. 24 showed that unless $[\Gamma^r] \rightarrow [I]$ as $c^i \rightarrow 1$, the inclusion properties could never be recovered. One way of forcing this behavior was to introduce a factor $1 - c^i$ into the definition of Y in eq. 19.

Thus, the third variation (called M-T modified) is the M-T model corrected using a modified particle interaction factor ($[\Gamma^r]$ with $Y = (1 - c^i)/24$). This model behaved much better and gave good predictions up to $c^i = 0.5$. In comparison with the Farber-Farris predictions in which a maximum packing fraction $P_f = 1$ was used (denoted F-F in Fig. 1), the M-T modified model gave similar results.

An attempt was made to see if $Y = (1 - c^i)/24$ had any significance when compared with the traditional radial distribution function predicted by the Percus-Yevick solution (Refs. 31 and 32). A comparison showed there was no similarity between the two. Thus, the function Y used here only provides a means of recovering inclusion properties and cannot be seen as an indicator of microstructural features as suggested by the authors in Ref. 21.

6.2 Comparison with Tungsten-Carbide/Cobalt Composite

A similar comparison is made using experimental data obtained from Ravichandran (Ref. 25). Here the composite system is a tungsten-carbide/cobalt cermet ($E_i/E_m=3.4$). The results are shown in Fig. 2.

UNCLASSIFIED

19

In contrast to Fig. 1, Fig. 2 shows that the predicted E_c/E_m rises smoothly for the entire range of c^i . This is a consequence of the low inclusion to matrix modular ratio. This material system demonstrates the sensitivity of the M-T interaction solution to the constituent properties.

The M-T modified and Farber-Farris solutions give almost identical results while the M-T solution gives slightly lower modulus values. These three models tended to underpredict the experimental data. The M-T interaction solution shows that it overpredicts modulus in the neighborhood of $c^i = 0.75$ and above.

6.3 Comparison with Glass/Polyurethane Composite

As a final comparison, the experimental data from Yilmazer is used (Ref. 30). The glass bead/polyurethane composite had an $E_i/E_m > 16000$. This material system exhibited behavior that was different than the previous two. At $c^i = 0.5$, the normalized modulus measured by Yilmazer was $E_c/E_m = 13$. When other references (Ref. 25 in Ref. 25, Refs. 29, 33, 34 and 35) were examined, generally $E_c/E_m < 5$ at $c^i = 0.5$.

The Farber-Farris solution underpredicted the experimental results when the maximum packing fraction $P_f = 1$ was used (see Fig. 3). To bring the F-F solution up to the measured data, P_f was set equal to 0.6. The fact that a packing fraction is required indicates that the additional reinforcement seen in this material system is not due to the E_i/E_m alone but includes some other reinforcing mechanism like particle interaction.

As expected the M-T solution underpredicted the experimental data. Again, to reproduce the experimental data, a modification to the definition of Y in eq. 19 was required.

UNCLASSIFIED

20

This time, an interaction factor multiplier $Y_m = 1.26$ was added giving $Y = Y_m(1 - c^i)/24$. The value for Y_m was found through trial and error. Like the maximum packing fraction, Y_m provides an indication of additional reinforcement through particle interaction. As can be seen from Fig. 3, the M-T modified solution reproduces the measured moduli quite well.

6.4 Comparison for Three-Phase Composites

Experimental data for the modulus of three-phase composites is scarce (Ref. 18). A study by Ishai and Cohen on a composite system comprised of sand and voids in a matrix of epoxy is frequently used for evaluation of three-phase models (Ref. 35). The modular ratio for this system is $E_i/E_m = 36$. Huang (Ref. 36) showed that the volume fraction of sand c^i varied with volume fraction of voids c^v according to $c^i = 0.173(1 - c^v)$ for the Ishai and Cohen data. With composites containing void volume fractions of $0.1 < c^v < 0.6$, the inclusion volume fraction was within a narrow range of $0.16 > c^i > 0.07$.

Figure 4 shows a comparison of the Farber-Farris (F-F) model and the 3-phase M-T model (eq. 30). Two variations of the M-T model have been used. The first is the M-T model with no particle interaction (denoted M-T in Fig. 4). The second is the modified M-T model with particle interaction between inclusions and between voids (denoted M-T, Γ^i , Γ^v). An interaction factor of $Y = (1 - c^i)/24$ was used for the inclusions and voids. As Fig. 4 shows, all models predicted the experimental composite moduli well. This was expected since the inclusion loading was fairly low. Small differences between the three models can be seen though. The F-F model tended to predict higher moduli at the lower void concentrations and vice versa at the higher void concentrations. The M-T model predicted higher moduli than the F-F model and the modified M-T model at the higher

void concentrations. The modified M-T model predicted the experimental data over the entire range except at $c^v = 0.4$ where it overpredicted the composite modulus.

A further understanding of the 3-phase M-T model is gained by predicting composite modulus using the Yilmazer glass bead/polyurethane (Ref. 30) and Smith glass bead/epoxy (Ref. 29) property data. Since the energy balance model (Sec. 5.0) assumes debonded inclusions will become voids or vacuoles, the void or vacuole volume fraction varies according to $c^v = c_o^i - c^i$. An initial inclusion volume fraction c_o^i of 0.5 has been selected here. Voids were modeled by setting $[C^v] = [0]$. Vacuoles were modeled by setting $E_{11}^v = 0$ and $\nu_{12}^v = \nu_{13}^v = 0$ in eq. 35 assuming loading was in the 11-direction. A value of $Y = 1.26(1 - c^i)/24$ was used for the generation of the Yilmazer M-T void and M-T vacuole predictions while a value of $Y = (1 - c^i)/24$ was used for the Smith predictions. The interaction multipliers were chosen based on the results obtained in Sec. 6.3.

Figure 5 shows the performance of the F-F and M-T models for the glass/void/polyurethane (PU) data. The M-T solution (no interaction) is shown for reference. For both the M-T void and M-T vacuole results, a larger drop in modulus is predicted when compared to the F-F results ($P_f = 0.6$). However, at $c^i < 0.17$, all models gave similar moduli. The M-T vacuole model gave slightly higher moduli than the M-T void model as $c^i \rightarrow 0$ (see E_{vac}/E_{void} curve). This was expected since the vacuole stiffness matrix $[C^v]$ was partially populated with non-zero values. This behavior was also observed by Mochida in Ref. 26.

The model performance for the glass/void/epoxy data (Fig. 6) showed that as $c^i \rightarrow 0$, the M-T models predicted higher modulus between $0.45 < c^i < 0.5$ then lower moduli down to $c^i = 0.12$ in comparison to the Farber-Farris solution ($P_f = 1$). This was not surprising

UNCLASSIFIED

22

given the 2-phase predictions in Sec. 6.1. The M-T model moduli decreased more rapidly than the F-F modulus but the difference in rates of decrease was not as great as that seen for the glass/PU data. Again, the M-T vacuole model gave a slightly higher moduli than the M-T void model as $c^i \rightarrow 0$.

A comparison of predicted composite Poisson ratio ν_c for the glass/void/PU composite is shown in Fig. 7. The F-F predictions gave a slightly concave-down curve as $c^i \rightarrow 0$. The M-T solutions on the other hand had a curious concave-up shape.

The dependency of the Poisson ratio curvature on the matrix Poisson ratio ν_m is shown in Fig. 8. The solid lines represent the Poisson behavior if the inclusions were assumed to be rigid ($[C^i] = [\infty]$). Reference 20 showed that ν_c was independent of the inclusion Poisson ratio for this case. For a matrix Poisson ratio $\nu_m = 0.2$, it can be seen that the composite Poisson ratio ν_c equalled 0.2 for all c^i . Budiansky (Ref. 37) observed the same behavior in his analysis of elastic moduli of heterogeneous materials. He found that at $c^i = 0.2$, his shear and bulk modulus equations became decoupled. Calculations for $\nu_m > 0.2$ show that with rigid inclusions, ν_c has a concave-up shape. For $\nu_m < 0.2$, ν_c has a concave-down shape. It appears, then, for analyses which use a discrete averaging process such as that given by eqs. 24 and 30 or employed in Refs. 18, 20 or 37, the predicted ν_c will show this kind of behavior.

The dashed lines in Fig. 8 show the ν_c behavior using glass/PU property data. ν_m was varied between 0.1 to 0.3 while $\nu_i = 0.16$. Particle interaction was accounted for and $Y = 1.26(1 - c^i)/24$. The deviation from the 3-phase rigid inclusion prediction at $\nu_m = 0.2$ is caused by $\nu_i \neq 0.2$. For values of $\nu_m \neq 0.2$, the effects of $[\Gamma^r]$ and E_i/E_m come into play. Since $\nu_m = 0.499$ for PU, it is evident why a concave-up curve is predicted in Fig. 7.

UNCLASSIFIED

23

Going back to Fig. 7, the M-T solution gives a higher prediction of ν_c compared with the M-T void and M-T vacuole solutions. In the case of the M-T void results, ν_c eventually converges to the M-T solution since $c^i \rightarrow 0$. The M-T vacuole results demonstrate the restraining power of the $\nu_{12}^v = \nu_{13}^v = 0$ assumption. Numerical trials for glass/void/epoxy showed the same trends.

7.0 PREDICTION OF MECHANICAL BEHAVIOR

The general characteristics of the critical strain equation (eq. 40) will first be examined using the M-T void model. Stress-strain behavior for different volume fractions of inclusions will be shown to illustrate how the model functions. Void volume fraction is calculated from $c^v = c_o^i - c^i$ where c_o^i is the initial inclusion volume fraction.

To examine the consequences of using the critical strain equation based on the M-T void or M-T vacuole models, mechanical behavior predictions will be compared with literature data for two types of model particulate composites. The first composite is a glass bead/polyurethane system which was studied by Yilmazer and Farris (Ref. 30). The second composite is a glass bead/polyethylene system which was studied previously by the author (Ref. 14). Predictions using the Farber-Farris model will be made to highlight the differences between it and the M-T models. The FORTRAN program used for generating the M-T void and vacuole data may be found in Appendix B.

UNCLASSIFIED

24

7.1 Model Characteristics

The results shown in Figs. 9 and 10 were generated using the constituent properties from Ref. 29 (see Table I). $Y = (1 - c^i)/24$ was used (Sec. 6.1) along with an adhesion energy of 5 J/m^2 (Ref. 13). Particle diameter size was set at $50 \text{ }\mu\text{m}$ and the log standard deviation equalled 0.2.

Figure 9 shows how stress-strain behavior changes with initial inclusion volume fraction. As initial volume fraction increased, composite modulus also increased. This trend has been well documented in the literature (Refs. 38, 39 and 40). Examining the volume fraction curves, as long as initial volume fraction remained constant, linear elastic behavior was predicted. Maximum stress was determined by the composite modulus and the initial critical strain values. Once inclusions started to debond, volume fraction decreased and nonlinear behavior was observed. Stress increased or decreased depending on the initial volume of inclusions. Below inclusion volume fractions of 0.05, linear behavior was again predicted. The modulus at this point was determined by the volume of voids in the composite. The current model does not contain a failure criterion so only a portion of the predicted stress-strain curve would be seen in experiments.

The relationship between volume fraction and probability of inclusion survival with strain is shown in Fig. 10. Probability of survival represents the number of well-bonded inclusions remaining in the composite. It can also be thought of as a cumulative size distribution curve where the lefthand side of the figure represents large particle diameters and the righthand side representing small diameters. For the log standard deviation studied, 10% of the total number of particles made up 50% of the inclusion volume. When the inclusion volume fell to < 0.05 , approximately 50% of the total number of particles remained.

UNCLASSIFIED

25

This shows that the larger particles controlled the type of nonlinear behavior predicted and that the smaller particles were almost inconsequential.

7.2 Glass Bead/Polyurethane Composite

In Ref. 30, the authors fabricated glass bead/polyurethane composites with inclusion volume fractions ranging from $c_o^i = 0.0$ to $c_o^i = 0.5$ in steps of 0.1. One set of composites contained untreated glass beads while a second set used glass beads treated with a silane coupling agent. Six out of the twelve composite combinations studied in Ref. 30 have been chosen to demonstrate the performance of the models. In Ref. 13, the authors used void properties and adjusted the matrix modulus and the adhesion energy to obtain agreement between the experimental and predicted values. In this section, only adhesion energy was considered an adjustable parameter. Its value was increased until the experimentally measured maximum stress was obtained (Ref. 14). The matrix modulus was considered a fixed quantity since it was measured. Void properties were set to zero. A value of $Y = 1.26(1 - c^i)/24$ was used in the M-T models since this gave the correct modulus predictions in Sec. 6.3.

Figure 11 shows a comparison of the experimental data for a composite containing $c_o^i = 0.30$ of untreated beads with the F-F model and the M-T void and M-T vacuole models. The parameters used for these predictions may be found in Table II. It can be seen that the M-T vacuole model gave the best prediction for composite behavior. The M-T void model predicted a greater reduction in modulus and as a consequence lower stress at a strain > 0.25 . The F-F model predicted a yield point and a much lower stress at a strain > 0.20 .

UNCLASSIFIED

26

For a composite containing $c_o^i = 0.40$ of untreated beads (Fig. 12), the F-F model predicted the experimental data better. Both the M-T void and M-T vacuole models overpredicted the composite stress after the yield point. The behavior of the composite containing $c_o^i = 0.50$ of untreated beads (Fig. 13) was more accurately predicted by the M-T models than the F-F model. It can be seen that the initial modulus predicted by the M-T models matched the experimental data very well. The predictions after strain > 0.05 cannot be confirmed because the specimen ruptured at that point.

Comparison between the experimental data for the composite containing c_o^i equal to 0.30, 0.40 and 0.50 of treated beads and the models shows that the M-T vacuole model gave the closest predictions (see Figs. 14, 15 and 16). Like the untreated bead composites the M-T void model underpredicted composite stresses slightly. The composite containing $c_o^i = 0.4$ treated beads did not have the large drop in stress like its equivalent with untreated beads. As seen from the previous figures, the M-T models tended to predict this type of behavior. The F-F model predicted a yield point and a large drop in stresses afterwards. Examination of Table II shows that larger adhesion energies G_c were needed in the models for treated beads to account for the improved adhesion due to the silane treatment. These energy values provide a means for evaluating the adhesion characteristics between the constituents without having to measure it experimentally.

7.3 Glass Bead/Polyethylene Composite

In Ref. 14, the author fabricated glass bead/polyethylene composites with approximate inclusion volume fractions of $c_o^i = 0.2$ and $c_o^i = 0.5$. As with Ref. 30, one set of composites contained untreated glass beads while the other set used glass beads treated

UNCLASSIFIED

27

with a silane coupling agent. The six composite combinations studied in Ref. 14 will be used to demonstrate the performance of the models. The matrix modulus was considered a fixed quantity for the M-T models while the interaction factor multiplier, Y_m , had to be considered an adjustable parameter for this material system. This will be discussed shortly. Void properties were set to zero. Adhesion energy was considered an adjustable parameter for all models. It was increased until experimentally measured maximum stress was obtained.

Figure 17 shows a comparison of the experimental data for a composite containing $c_o^i = 0.19$ of 31 μm untreated beads (designated U2520) with the F-F, M-T void and M-T vacuole models. The F-F model predicted a yield point and then a drop in stress. The M-T models provided better predictions when $Y_m = 0.6$ was used. In comparison with $Y_m = 1.26$ for glass/polyurethane composites (Sec. 6.3) where it was suggested that the value of 1.26 indicated the presence of additional reinforcement, the value of 0.6 supports the idea that there was an absence of additional reinforcement due to the poor adhesion between particle and matrix. It can be seen that the M-T vacuole model predicted the behavior of the composite better for strains > 0.025 .

The results for the composite containing $c_o^i = 0.22$ of 31 μm treated beads (T2520) shows that all models had difficulty with the nonlinearity at the beginning of the stress-strain curve (Fig. 18). This was caused by the use of a linear elastic matrix modulus in the models.

The results for T2520 suggest that the nonlinear effects due to matrix nonlinearity were as significant as the nonlinear effects due to inclusion debonding. Two factors allowed this to happen. First, T2520 contained a low volume fraction of inclusions. This permitted

UNCLASSIFIED

28

matrix properties to have a greater influence on overall behavior. Second, the actual stress-strain curve for polyethylene has a concave-down shape up to its maximum stress. This meant that the actual modulus was high initially and then dropped off as maximum stress was reached. The predicted values were based on an average matrix modulus which was defined as the secant modulus measured at 90% of maximum stress (Ref. 14). Thus, composite stresses were underpredicted initially because an average linear elastic matrix modulus was used.

The M-T models for T2520 used a $Y_m = 2.5$. Following the reasoning given previously, this indicates that the silane coupling agent was causing additional reinforcement effects to be seen. The difference in Y_m for the U2520 and T2520 predictions is reflected in the differences found in their overall stress-strain behavior. T2520 has a larger initial modulus and a higher maximum stress than U2520. The untreated and treated glass bead/polyurethane composites ($c_o^i = 0.40$) have similar stress-strain behavior in spite of the fact that one has a surface treatment. This explains why the glass bead/polyethylene composites need an adjustable Y_m while the glass bead/polyurethane composites do not.

Figure 19 for a composite containing $c_o^i = 0.48$ of $31 \mu\text{m}$ untreated beads (U2550) shows that all models could reproduce the experimental data. However, for the F-F model to approximate the experimental behavior, the measured matrix modulus of 187 MPa had to be reduced to 90 MPa. The justification given in Ref. 14 for this reduction was that poor adhesion resulted in loss of reinforcement and lack of strain in the matrix. As with the U2520 composite, the M-T models accounted for this behavior through modification of Y_m . To reproduce the experimental data $Y_m = 0.8$ was used. As before, this value indicates that there was an absence of additional reinforcement due to poor adhesion.

UNCLASSIFIED

29

A comparison of the results for a composite containing $c_o^i = 0.49$ of 31 μm treated beads (T2550) in Fig. 20 shows that the M-T models gave the best prediction of mechanical behavior. $Y_m = 2.5$ was used. As with the T2520 M-T results, this value indicated that additional reinforcement was being produced by the coupling agent. Nonlinearity due to actual matrix behavior was less evident for this composite because there is less matrix volume. This allowed nonlinearity due to inclusion debonding to dominate. The F-F model predicted a yield point and a decline in stress after a strain of 0.075.

Figures 21 and 22 shows a comparison of results for composites containing $c_o^i = 0.19$ and $c_o^i = 0.49$ of 130 μm treated beads respectively. The $c_o^i = 0.19$ T1020 composite (Fig. 21) behaves much like the T2520 composite (Fig. 17). Again the M-T and F-F models underpredict the stresses at strains below 0.035. The reasons given during the discussion of the T2520 results would apply to the T1020 results as well. At strains > 0.035 , it can be seen that the M-T vacuole results follow more closely the experimental results. For the $c_o^i = 0.49$ T1050 composite results (Fig. 22), the M-T predictions follow the experimental data better. The value of $Y_m = 2.5$ indicated that additional reinforcement was present. An examination of Table III shows that larger adhesion energies were required in the models to reflect the improved adhesion due to the silane treated beads. Adhesion energies could not be verified because they were not measured.

8.0 SUMMARY

The theoretical framework for calculating composite modulus using an improved Mori-Tanaka method has been presented. A comparison of 2-phase composite results with experimental data showed that the M-T solution with no particle interaction effects un-

UNCLASSIFIED

30

derpredicted the measured moduli. The inclusion of particle interaction effects through a correction matrix $[\Gamma^*]$ improved predictions but had some undesirable side effects. These side effects were eliminated by making the interaction factor Y a function of the inclusion volume fraction.

A comparison with 3-phase modulus data obtained from the literature showed there was good agreement between the 3-phase M-T model and the Farber-Farris model for low initial inclusion volume fractions. At higher initial inclusion volume fractions, predictions for a hypothetical 3-phase composite showed that the 3-phase M-T model predicted a faster decrease in modulus than the F-F model. Moduli solutions for composites containing vacuoles showed that a slightly higher modulus could be expected when compared to composites containing voids.

Examination of the Poisson ratio results for 3-phase composites showed that a non-monotonic behavior was predicted as inclusion volume fraction was increased. This behavior was restricted to modulus prediction models which were derived using a discrete averaging process to account for the reinforcement of additional inclusions.

Based on the improved M-T method, new micromechanical models for the prediction of particulate composite mechanical behavior were developed. Comparisons between the M-T void and M-T vacuole models and the experimental data for glass/polyurethane and glass/polyethylene composites showed that the M-T vacuole model gave the best results for inclusion volume fractions ranging from $c_o^i = 0.2$ to $c_o^i = 0.4$. This suggests vacuole formation rather than void formation is more representative of the actual debonding process. The composites containing $c_o^i = 0.5$ particles showed that the M-T models generally performed better than the F-F model. The M-T models either predicted the initial modulus

UNCLASSIFIED

31

or the stress after the knee of the stress-strain curve more closely.

The introduction of an interaction factor multiplier Y_m in the M-T models provided a means of evaluating the degree of particle interaction in the glass/polyethylene composites. A low Y_m suggested that there was little interaction due to poor adhesion between the phases. A high Y_m suggested there was greater interaction due to improved adhesion.

The only case where the F-F model performed better than the M-T models was in a glass/polyurethane composite which contained $c_o^i = 0.4$ of untreated beads. The experimental data showed a yield point and a large drop in stress afterwards. Since the F-F predictions tend to have this shape, the F-F model gave good results for this situation. The M-T models tended to show a much more gradual decline in stress. From the composite systems studied, the gradual decline behavior appeared to be more common.

The F-F and M-T models had trouble predicting the mechanical behavior of a glass/polyethylene composite containing $c_o^i = 0.22$ of treated glass beads. The discrepancy between theoretical and experimental results was attributed to the use of linear elastic matrix properties. This shortcoming indicates that improvements to M-T void and M-T vacuole predictions can be made by reformulation of the models to include nonlinear matrix behavior.

UNCLASSIFIED

32

9.0 REFERENCES

1. Hashin, Z., "The Elastic Moduli of Heterogeneous Materials", J. Appl. Mech., Vol. 29, April 1962, pp. 143-150.
2. Brassell, G.W., Wischmann, K.B., "Mechanical and Thermal Expansion Properties of a Particulate Filled Polymer", J. of Mat. Sci., Vol. 9, No. 2, 1974, pp. 307-314.
3. Christensen, R.M., Lo, K.H., "Solutions for Effective Shear Properties in Three Phase Sphere and Cylinder Models", J. Mech. Phys. Solids, Vol. 27, 1979, pp. 315-330.
4. Lene, F., Leguillon, D., "Homogenized Constitutive Law for a Partially Cohesive Composite Material", Int. J. Solids and Structures, Vol. 18, No. 5, 1982, pp. 443-458.
5. Aboudi, J., Benveniste, Y., "Constitutive Relations for Fiber-Reinforced Inelastic Laminated Plates", J. Appl. Mech., Vol. 51, 1984, pp. 107-113.
6. Schapery, R.A., "A Micromechanical Model for Non-Linear Viscoelastic Behavior of Particle Reinforced Rubber with Distributed Damage", Eng. Frac. Mech., Vol. 25, No. 5, May 1986, pp. 845-867.
7. Shikula, E. N., "Strain Properties of Particulate Composites with Microcracks", Int. Appl. Mech., Vol. 29, Sept. 1993, pp. 745-751.
8. Willis, J.R., "Variational and Related Methods for the Overall Properties of Composites", Advances in Applied Mechanics, Vol. 21, 1981.
9. Hashin, Z., "Analysis of Composite Materials - A Survey", J. Appl. Mech., Vol. 50, No. 4, Sept. 1983, pp. 481-505.
10. Sullivan, B.J., Hashin, Z., "Analysis of the Properties of Solid Propellants", Materials Sciences Corp., MSC/TFR/1901/8305, April 1988.
11. Astronautics Laboratory, "Micromechanics of Highly Filled Elastomers - Technical Interchange Meeting", AFAL/TIM-89/10, Oct. 1989.
12. Vratsanos-Anderson, L. L. and Farris, R. J., "A Predictive Model for the Mechanical Behaviour of Particulate Composites. Part I: Model Derivation", Polym. Eng. Sci., Vol. 33, No. 22, 1993, pp. 1458-1465.
13. Vratsanos-Anderson, L. L. and Farris, R. J., "A Predictive Model for the Mechanical Behaviour of Particulate Composites. Part II: Comparison of Model Predictions to Literature Data", Polym. Eng. Sci., Vol. 33, No. 22, 1993, pp. 1466-1474.

UNCLASSIFIED

33

14. Wong, F. C. and Ait-Kadi, A. "Mechanical Behaviour of Particulate Composites: Experiments and Micromechanical Predictions", *J. Appl. Poly. Sci.*, Vol. 55, 1995, pp. 263-278.
15. Wong, F. C., "Mechanical Behaviour of Particulate Composites: Experiments and Micromechanical Predictions", DREV R-9403/94, UNCLASSIFIED.
16. Farber, J. N. and Farris, R. J., "Model for Prediction of the Elastic Response of Reinforced Materials over Wide Ranges of Concentration", *J. of Appl. Poly. Sci.*, Vol. 34, 1987, pp. 2093-2104.
17. Mori, T. and K. Tanaka, "Average Stress in Matrix and Average Elastic Energy of Materials with Misfitting Inclusions", *Acta Metall.*, Vol. 21, 1973, pp. 571-574.
18. Weng, G. J., "Some Elastic Properties of Reinforced Solids, with Special Reference to Isotropic Ones Containing Spherical Inclusions", *Int. J. Engng. Sci.*, Vol. 22, 1984, pp. 845-856.
19. Taya, M. and T-W. Chou, "On Two Kinds of Ellipsoidal Inhomogeneities in an Infinite Elastic Body: An Application to a Hybrid Composite", *Int. J. Solids Structures*, Vol. 17, 1981, pp. 553-563.
20. Ju, J. W. and Chen, T. M., "Effective Elastic Moduli of Two-Phase Composites Containing Randomly Dispersed Ellipsoidal Inhomogeneities", *Acta Mechanica*, Vol. 103, 1994, pp. 103-121.
21. Ju, J. W. and Chen, T. M., "Effective Elastic Moduli of Two-Phase Composites Containing Randomly Dispersed Spherical Inhomogeneities", *Acta Mechanica*, Vol. 103, 1994, pp. 123-144.
22. Eshelby, J. D., "The Determination of the Elastic Field of an Ellipsoidal Inclusion and Related Problems", *Proc. Royal Soc. London*, Vol. A241, 1957, pp.376-396.
23. Tandon, G. P. and G. J. Weng, "Stress Distribution In and Around Spheroidal Inclusions and Voids at Finite Concentration", *J. Appl. Mech.*, Vol. 53, 1986, pp. 511-518.
24. Jeong, H., Hsu, D. K., Shannon, R. E. and P. K. Liaw, "Characterization of Anisotropic Elastic Constants of Silicon-Carbide Particulate Reinforced Aluminum Metal Matrix Composites: Part I. Experiment", *Metall. and Mater. Trans. A*, Vol. 25A, 1994, pp. 799-809.
25. Ravichandran, K. S., "Elastic Properties of Two-Phase Composites", *J. Am. Cer. Soc.*, Vol. 77, 1994, pp. 1178-1184.

UNCLASSIFIED

34

26. Mochida, T., Minoru, T. and M. Obata, "Effect of Damaged Particles on the Stiffness of a Particle/Metal Matrix Composite", JSME Int. J. Series I, Vol. 34, 1991, pp. 187-193.
27. Tsai, S. W. and Hahn, H. T., "Introduction to Composite Materials", Technomic Pub. Co. Inc., Westport, CT, 1980, pp. 9-15.
28. Wolfram, S., "Mathematica: A System for Doing Mathematics by Computer", Addison-Wesley, New York, 1989.
29. Smith, J. C., "Experimental Values for the Elastic Constants of a Particulate-Filled Glassy Polymer", J. Res. Natl. Bur. Std., Vol. 80A, 1976, pp. 45-49.
30. Yilmazer, U. and R. J. Farris, "Mechanical Behaviour and Dilatation of Particulate-Filled Thermosets in the Rubbery State", J. Appl. Polym. Sci., Vol. 28, 1983, pp. 3369-3386.
31. Hansen, J. P. and McDonald, I. R., "Theory of Simple Liquids", Academic Press, New York, 1986.
32. Pyrz, R., "Correlation of Microstructure Variability and Local Stress Field in Two-Phase Materials", Mater. Sci. and Engng., Vol. A177, 1994, pp. 253-259.
33. Richard, T. G., "The Mechanical Behaviour of a Solid Microsphere Filled Composite", J. Comp. Mater., Vol. 9, 1975, pp. 108-113.
34. Kenyon, A. S. and H. J. Duffey, "Properties of a Particulate-Filled Polymer", Polym. Eng. Sci., Vol. 7, 1967, pp. 189-193.
35. Ishai, O. and L. J. Cohen, "Elastic Properties of Filled and Porous Epoxy Composites", Int. J. Mech. Sci., Vol. 9, 1967, pp. 539-546.
36. Huang, Y., Hu, K. X., Wei, X. and A. Chandra, "A Generalized Self-Consistent Mechanics Method for Composite Materials with Multiphase Inclusions", J. Mech. Phys. Solids, Vol. 42, 1994, pp. 491-504.
37. Budiansky, B., "On the Elastic Moduli of Some Heterogeneous Materials", J. Mech. Phys. Solids, Vol. 13, 1965, pp. 223-227.
38. Schwarzl, F. R., "Mechanical Properties of Highly Filled Polymers III", Central Laboratory TNO Delft (Netherlands), CL-64/49, 1964.
39. Sumita, M., Ookuma, T., Miyasaka, K. and Ishikawa, K., J. Appl. Polym. Sci., Vol. 27, p. 3059, 1982.

UNCLASSIFIED

35

40. Maiti, S. N. and Mahapatro, P. K., "Mechanical Properties of i-PP/CaCO₃ Composites", J. Appl. Polym. Sci., Vol. 42, p. 3101, 1991.

UNCLASSIFIED

36

TABLE IElastic properties of constituent phases for particulate composites

Ref.	Matrix	Inclusion	G_o (MPa)	G_i (GPa)	ν_o	ν_i
14	polyethylene	glass bead	187	30.2	0.34	0.16
25	cobalt	tungsten-carbide	79000	293	0.31	0.194
29	epoxy	glass bead	1080	30.9	0.394	0.23
30	polyurethane	glass bead	1.4	30.2	0.499	0.16
35	epoxy	sand	725	29.4	0.4	0.25

G_o , matrix shear modulus, G_i , inclusion shear modulus, ν_o , matrix Poisson ratio, ν_i , inclusion Poisson ratio.

UNCLASSIFIED

37

TABLE IIModel input parameters for glass bead/polyurethane composites

Surface Treatment Volume Fraction	Untreated 0.3	Untreated 0.4	Untreated 0.5	Treated 0.3	Treated 0.4	Treated 0.5
Avg. rad. (μm)	12.5	12.5	12.5	12.5	12.5	12.5
Log std. dev.	0.228	0.228	0.228	0.228	0.228	0.228
c_o^i	0.30	0.40	0.50	0.30	0.40	0.50
c_o^v	0.0	0.0	0.0	0.0	0.0	0.0
G_i (GPa)	30.17	30.17	30.17	30.17	30.17	30.17
G_o (MPa)	1.40	1.40	1.40	1.40	1.40	1.40
ν_i	0.16	0.16	0.16	0.16	0.16	0.16
ν_o	0.499	0.499	0.499	0.499	0.499	0.499
P_f^a	0.7	0.7	0.7	0.7	0.7	0.7
Y_m^b	1.26	1.26	1.26	1.26	1.26	1.26
G_c :F-F ^c (J/m ²)	8	6	6	12	8	10
G_c :M-T ^d void (J/m ²)	12	8	13	16	14	21
G_c :M-T ^e vacuole (J/m ²)	12	8	14	17	14	24

a Maximum packing fraction used with F-F model.

b Interaction factor multiplier. Found by numerical trial and error.

c Adhesion energy used with F-F model. Found by numerical trial and error.

d Adhesion energy used with M-T void model. Found by numerical trial and error.

e Adhesion energy used with M-T vacuole model. Found by numerical trial and error.

c_o^i , initial inclusion volume fraction, c_o^v , initial void or vacuole volume fraction, G_i , inclusion shear modulus, G_o , matrix shear modulus, ν_i , inclusion Poisson ratio, ν_o , matrix Poisson ratio.

UNCLASSIFIED

38

TABLE III

Model input parameters for glass bead/polyethylene composites

Surface Treatment Composite No.	Untreated U2520	Untreated U2550	Treated T2520	Treated T2550	Treated T1020	Treated T1050
Avg. rad. (μm)	15.5	15.5	15.5	15.5	65	65
Log std. dev.	0.167	0.167	0.167	0.167	0.0374	0.0374
c_o^i	0.19	0.48	0.22	0.49	0.19	0.49
c_o^v	0.03	0.01	0.0	0.0	0.0	0.0
G_i (GPa)	30	30	30	30	30	30
G_o :F-F (MPa)	187	90	187	187	187	187
G_o :M-T (MPa)	187	187	187	187	187	187
ν_i	0.16	0.16	0.16	0.16	0.16	0.16
ν_o	0.34	0.34	0.34	0.34	0.34	0.34
p_f^a	0.6	0.6	0.6	0.6	0.6	0.6
Y_m^b	0.6	0.8	2.5	2.5	2.5	2.5
G_c :F-F ^c (J/m ²)	5	2.5	20	6	35	6.0
G_c :M-T ^d void (J/m ²)	4.5	2	19	12	35	10
G_c :M-T ^e vacuole (J/m ²)	4	1.8	17	11	33	10

a Maximum packing fraction used with F-F model.

b Interaction factor multiplier. Found by numerical trial and error.

c Adhesion energy used with F-F model. Found by numerical trial and error.

d Adhesion energy used with M-T void model. Found by numerical trial and error.

e Adhesion energy used with M-T vacuole model. Found by numerical trial and error.

c_o^i , initial inclusion volume fraction, c_o^v , initial void or vacuole volume fraction, G_i , inclusion shear modulus, G_o :F-F, matrix shear modulus used with F-F model, G_o :M-T, matrix shear modulus used with M-T models, ν_i , inclusion Poisson ratio, ν_o , matrix Poisson ratio.

UNCLASSIFIED

39

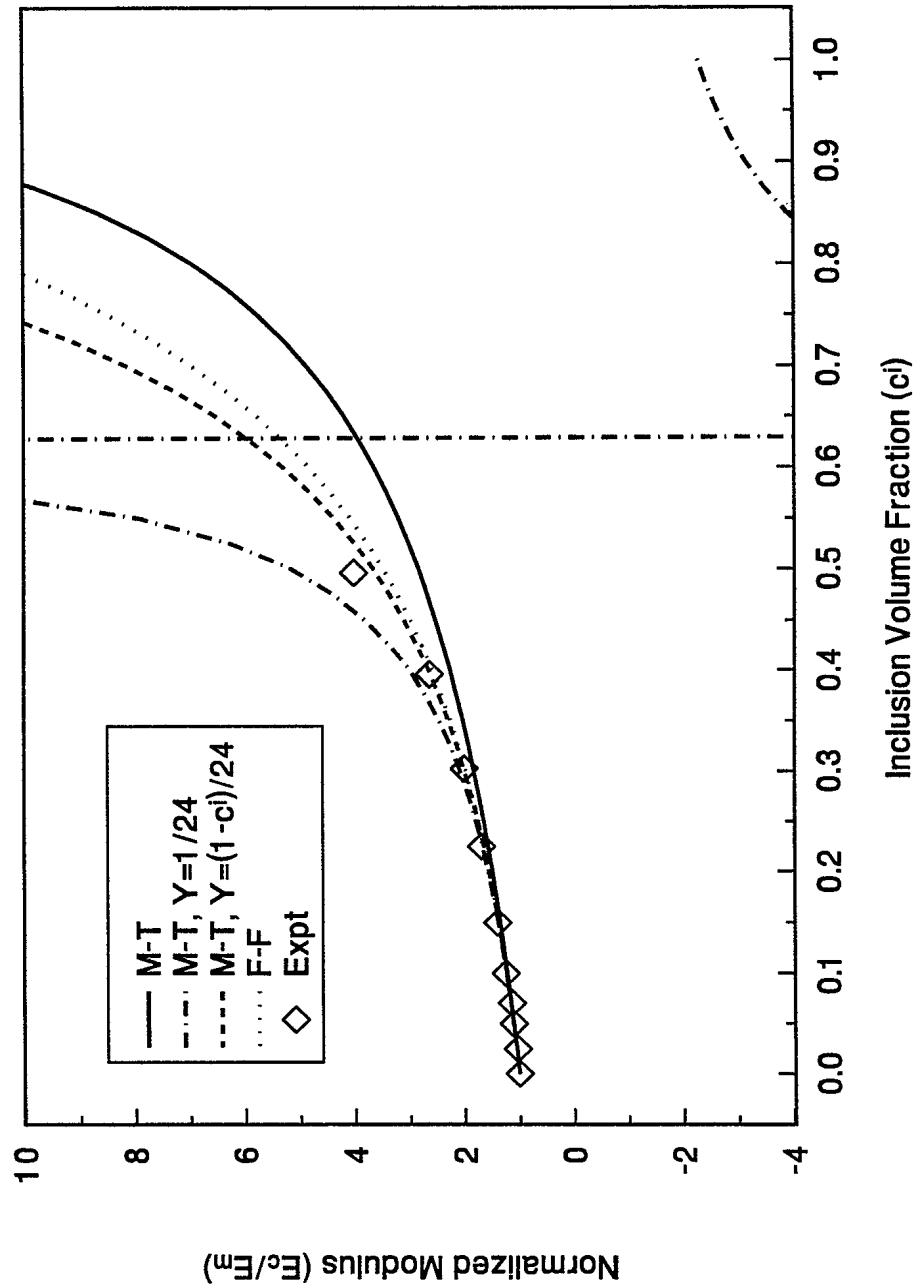


FIGURE 1 – Normalized modulus vs. volume fraction for 2-phase glass bead/epoxy composite. Experimental data from Smith (Ref. 29).

UNCLASSIFIED

40

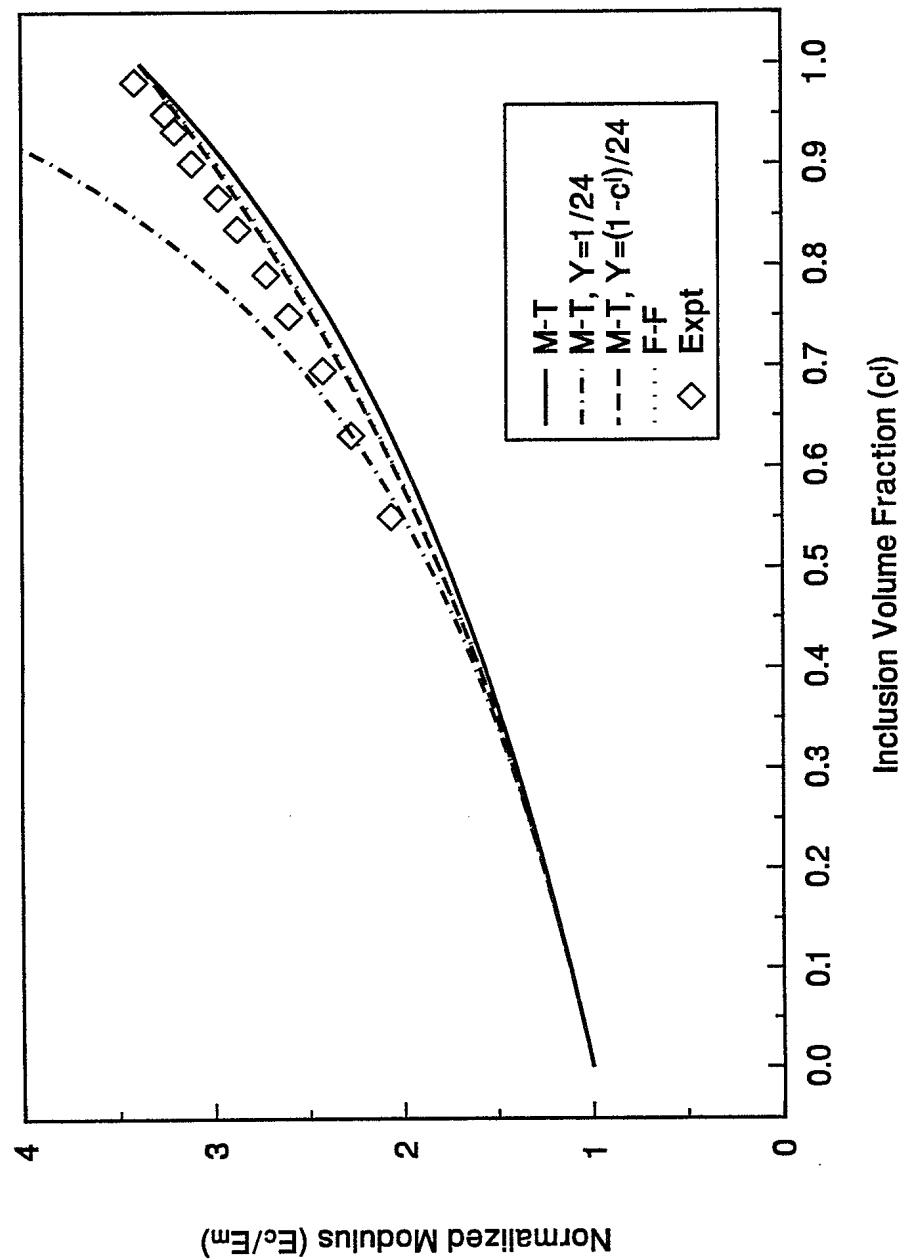


FIGURE 2 - Normalized modulus vs. volume fraction for 2-phase tungsten-carbide/cobalt cermet. Experimental data from Ravichandran (Ref. 25).

UNCLASSIFIED

41

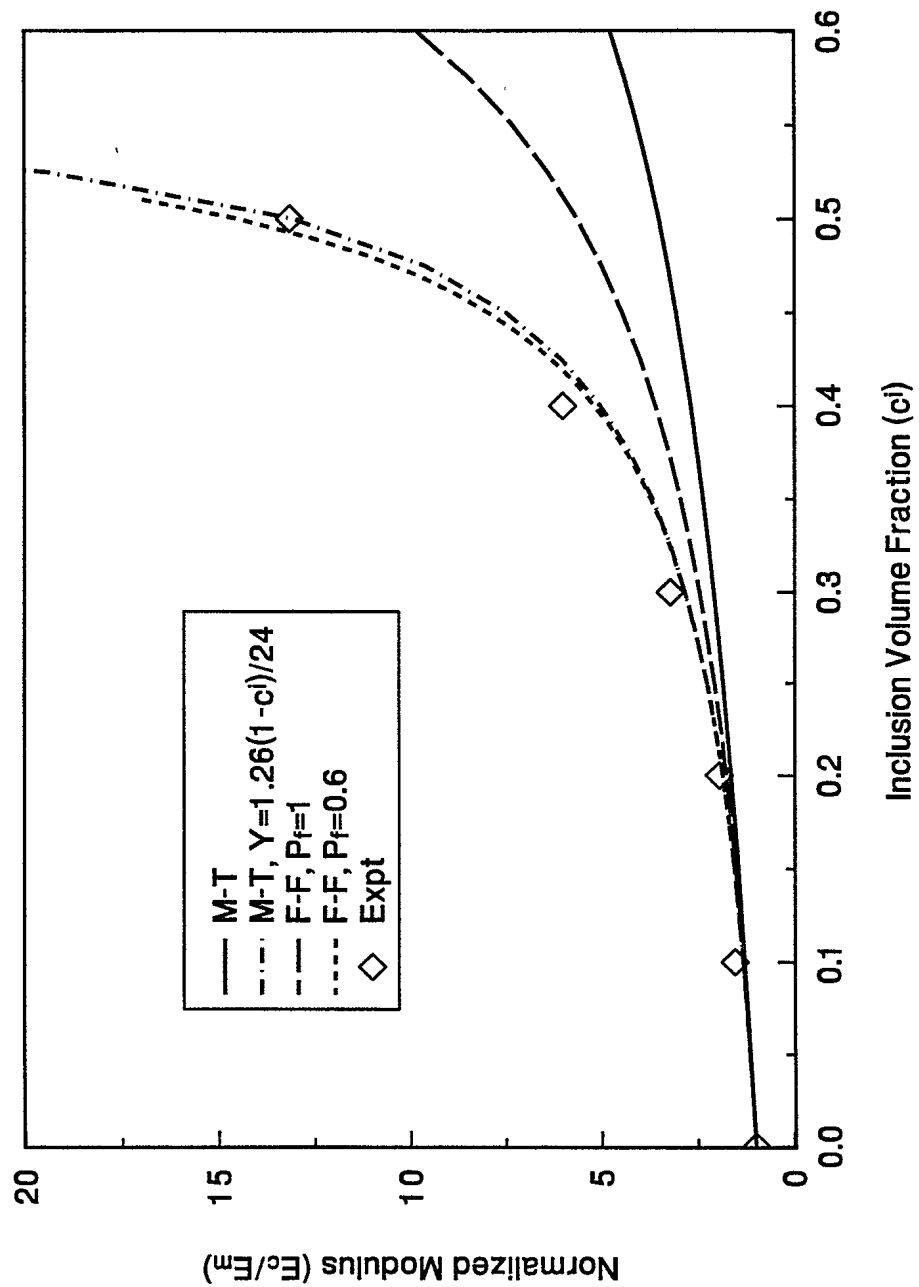


FIGURE 3 – Normalized modulus vs. volume fraction for 2-phase glass bead/polyurethane composite. Experimental data from Yilmazer (Ref. 30).

UNCLASSIFIED

42

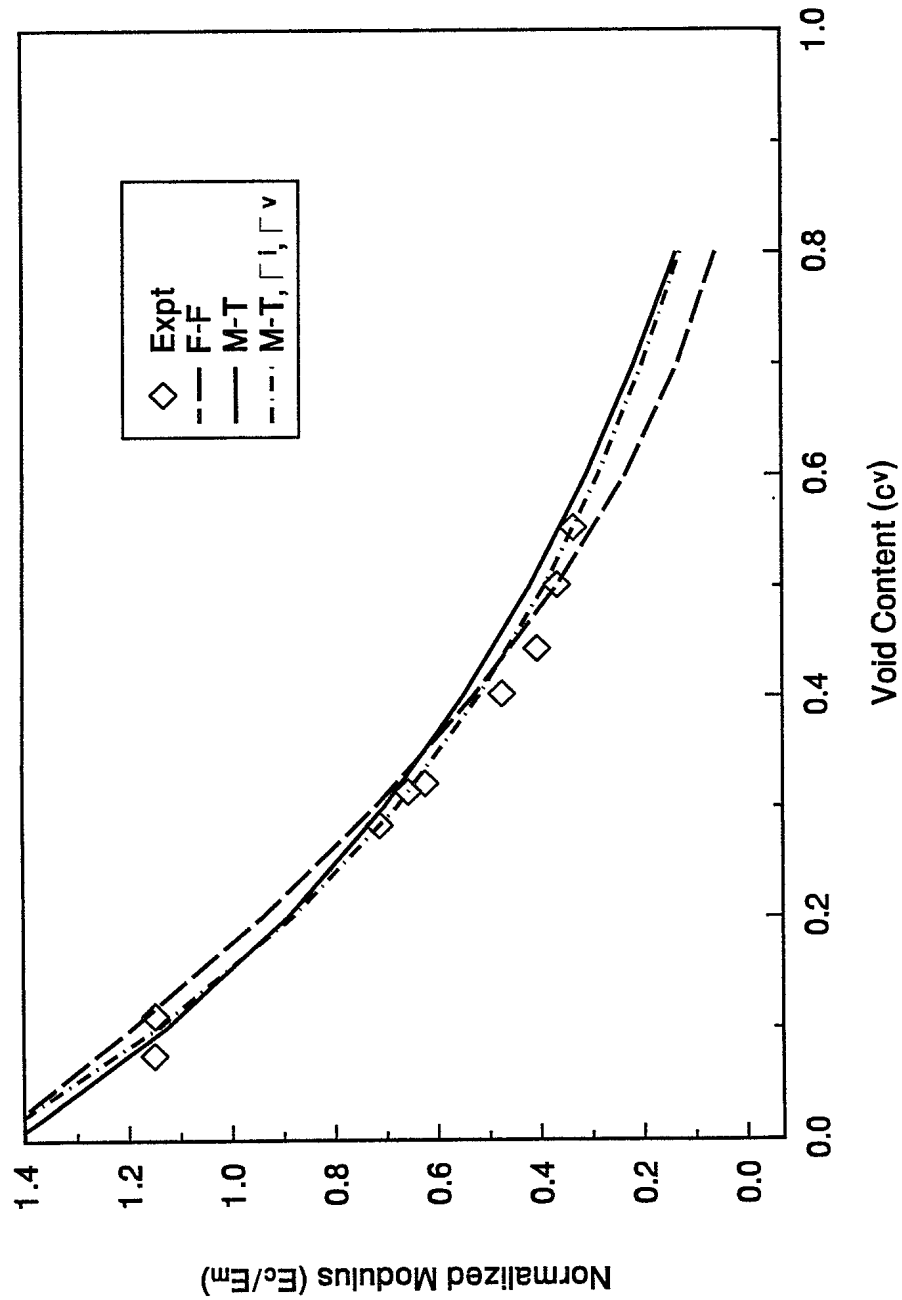


FIGURE 4 – Normalized modulus vs. volume fraction for 3-phase sand/void/epoxy composite using properties from Ref. 35. $c^i = 0.173(1 - c^v)$.

UNCLASSIFIED

43

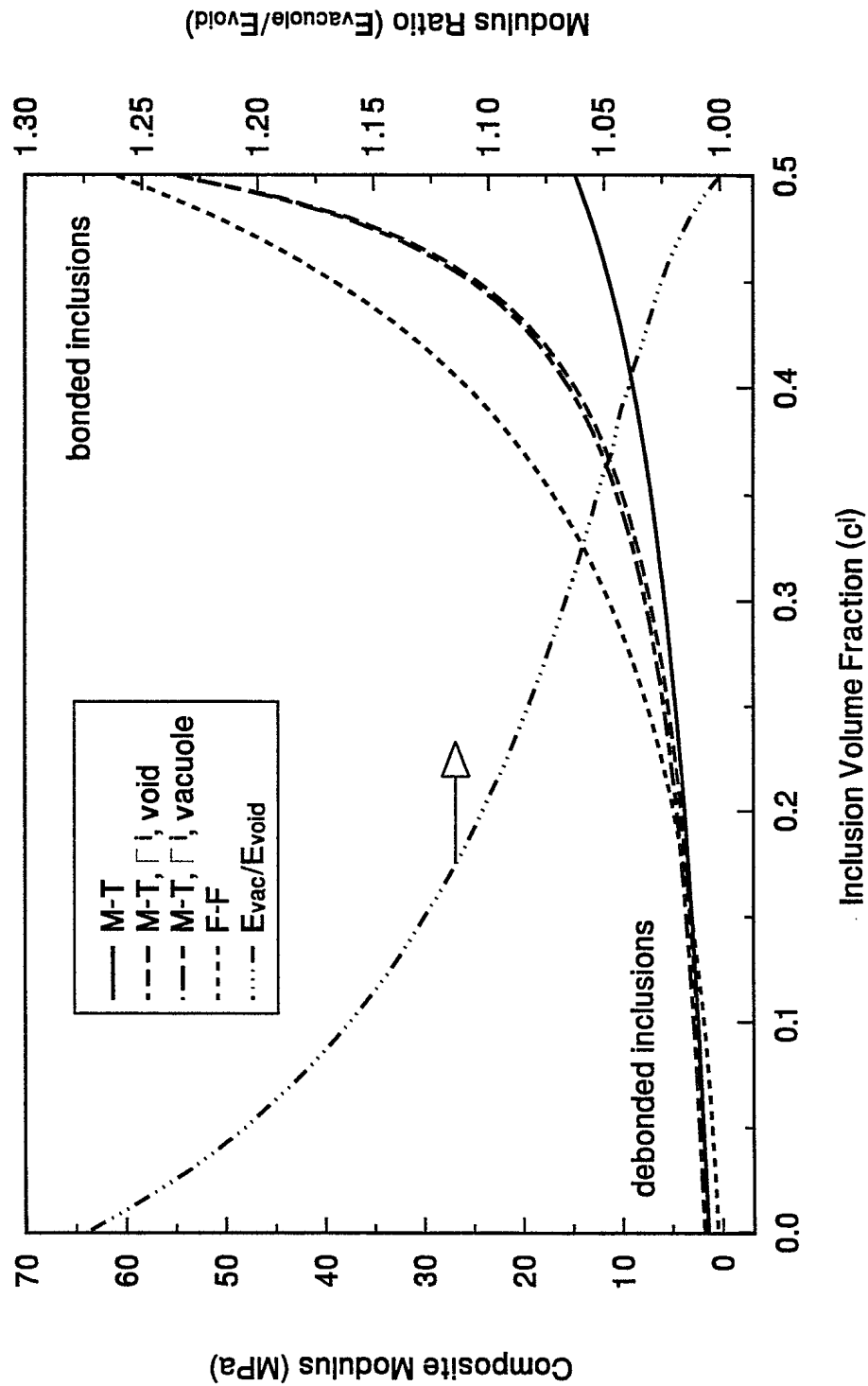


FIGURE 5 – Composite modulus vs. volume fraction for 3-phase glass bead/polyurethane/void or vacuole composite using properties from Ref. 30. $c_v^i = 0.5 - c_i^i$.

UNCLASSIFIED

44

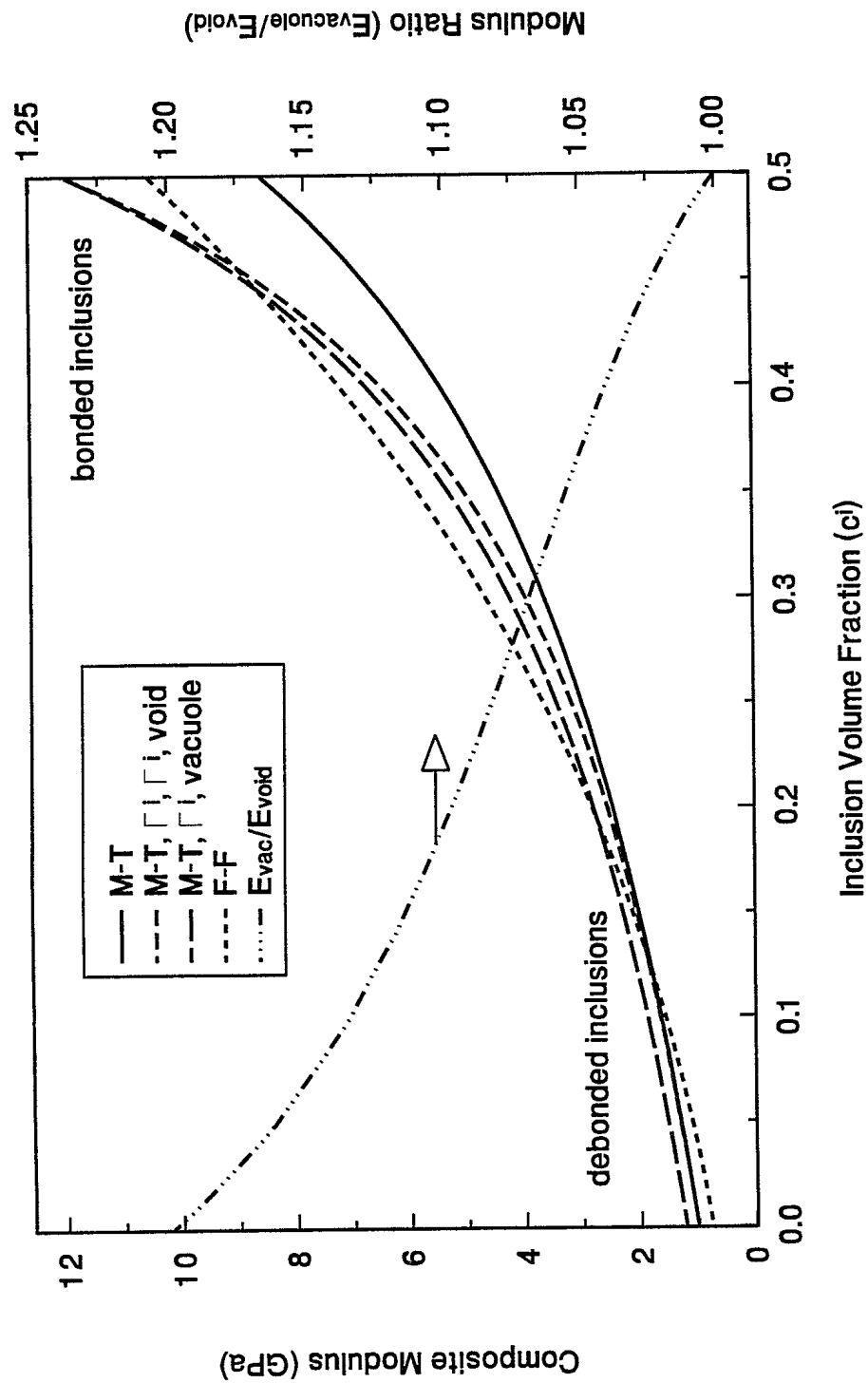


FIGURE 6 – Composite modulus vs. volume fraction for 3-phase glass bead/epoxy/void or vacuole composite using properties from Ref. 29.
 $c^v = 0.5 - c^i$.

UNCLASSIFIED

45

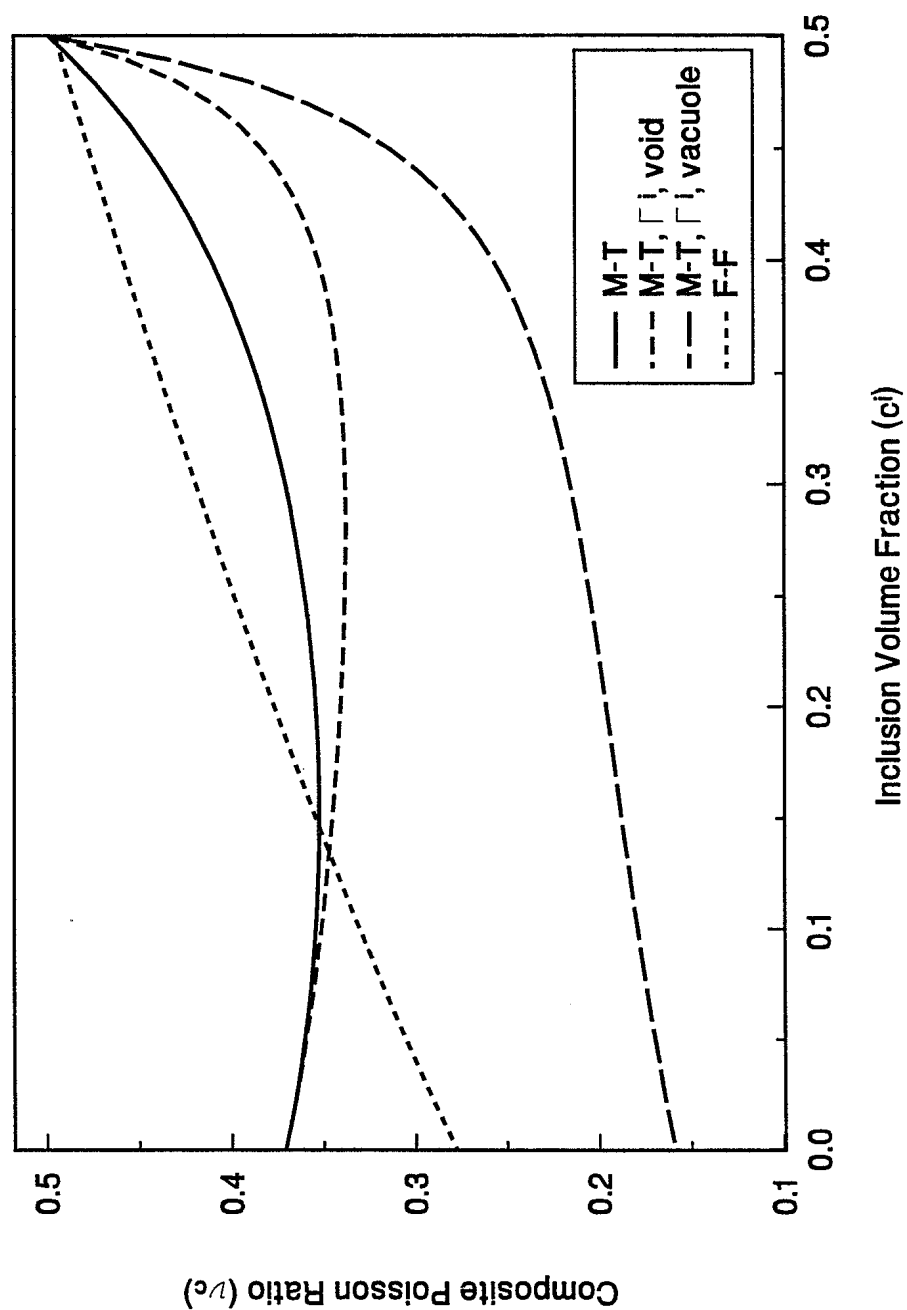


FIGURE 7 – Composite Poisson ratio vs. volume fraction for 3-phase glass bead/polyurethane/void composite using properties from Ref. 30. $c^v = 0.5 - c^i$.

UNCLASSIFIED

46

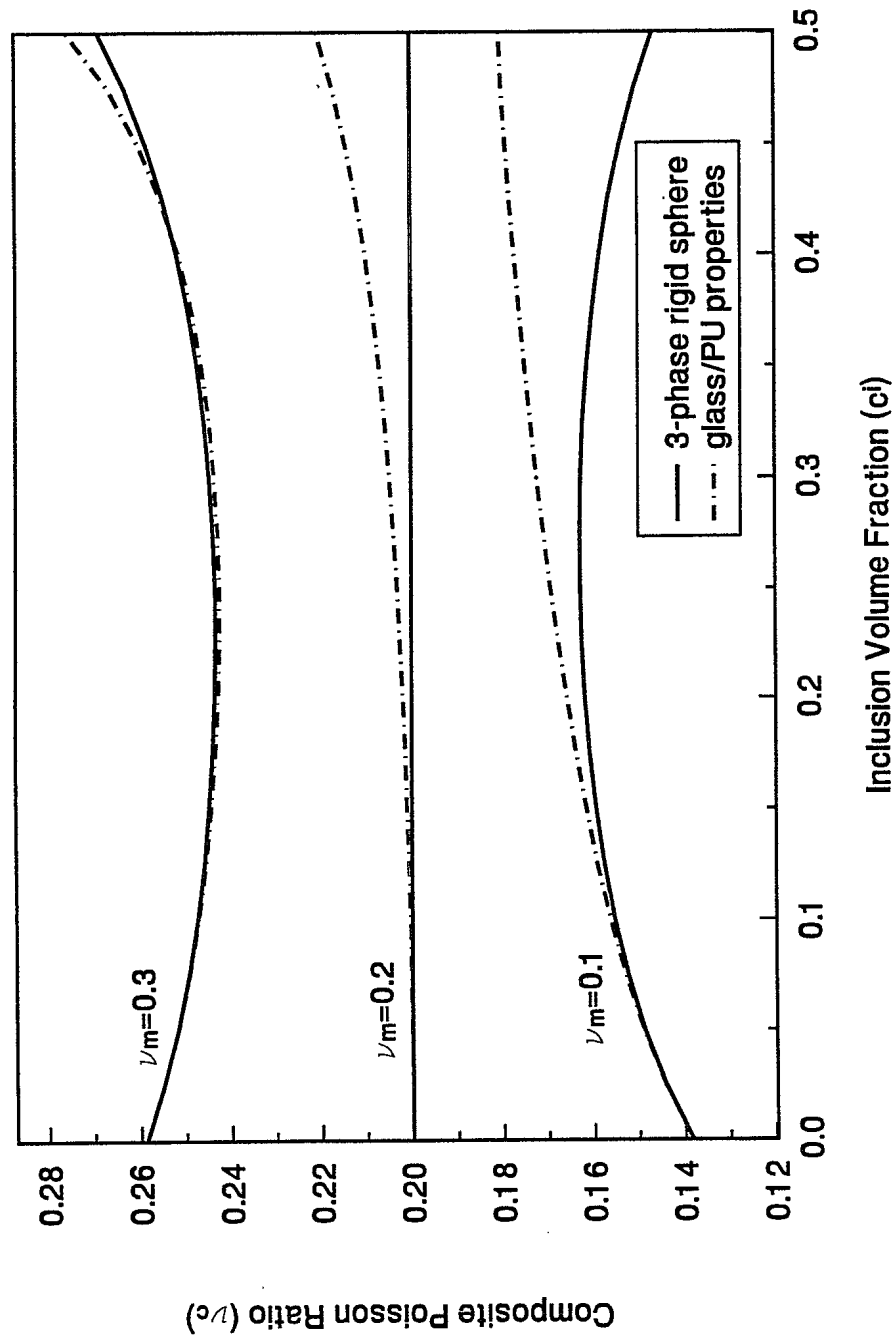


FIGURE 8 – Composite Poisson ratio vs. volume fraction for 3-phase rigid and glass bead/void/polyurethane composite with varying ν_m . $c^v = 0.5 - c^i$.

UNCLASSIFIED

47

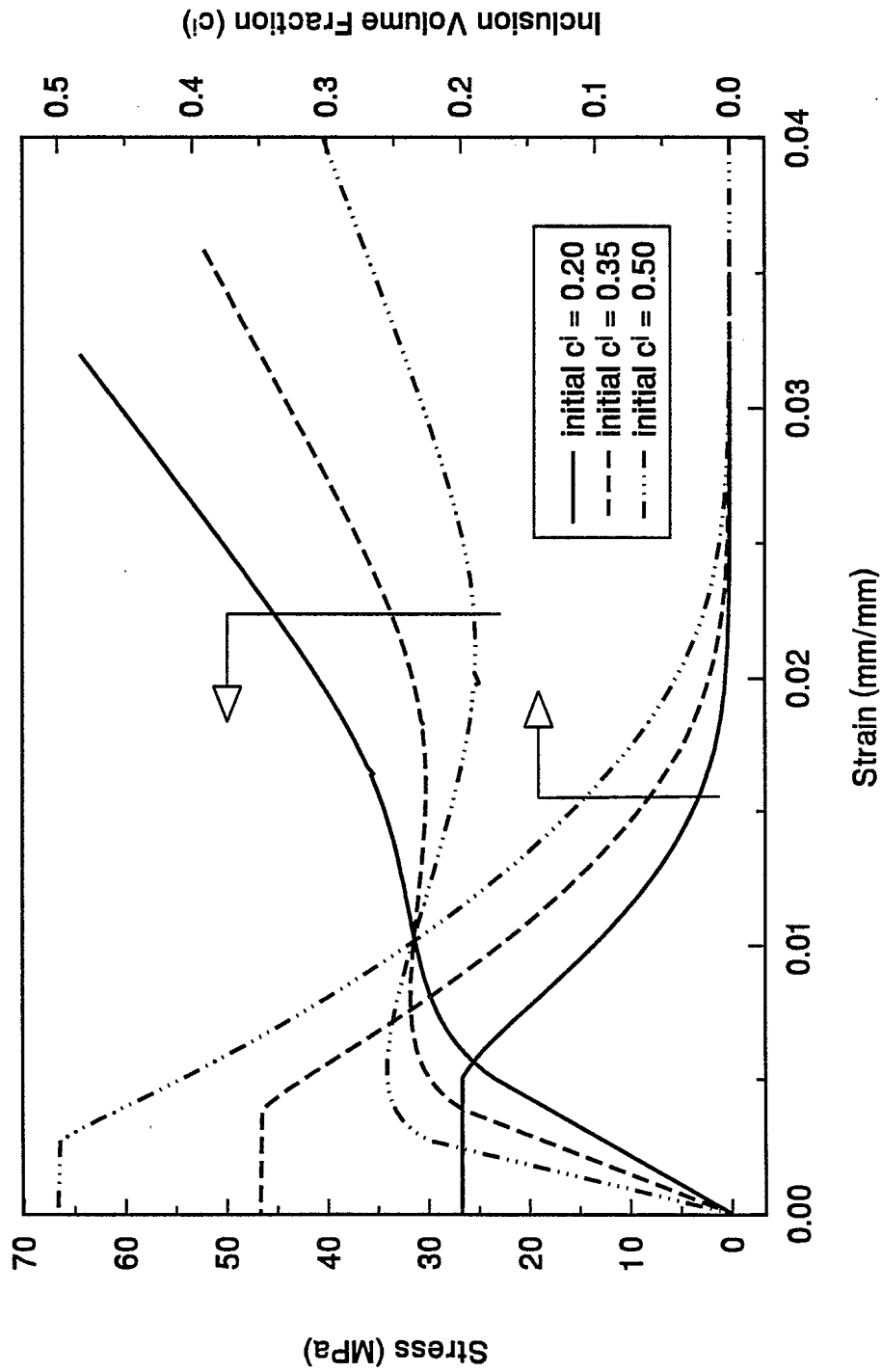


FIGURE 9 – Stress-strain and inclusion volume fraction behavior for a generic glass bead/epoxy composite containing various levels of initial inclusion volume fractions.

UNCLASSIFIED

48

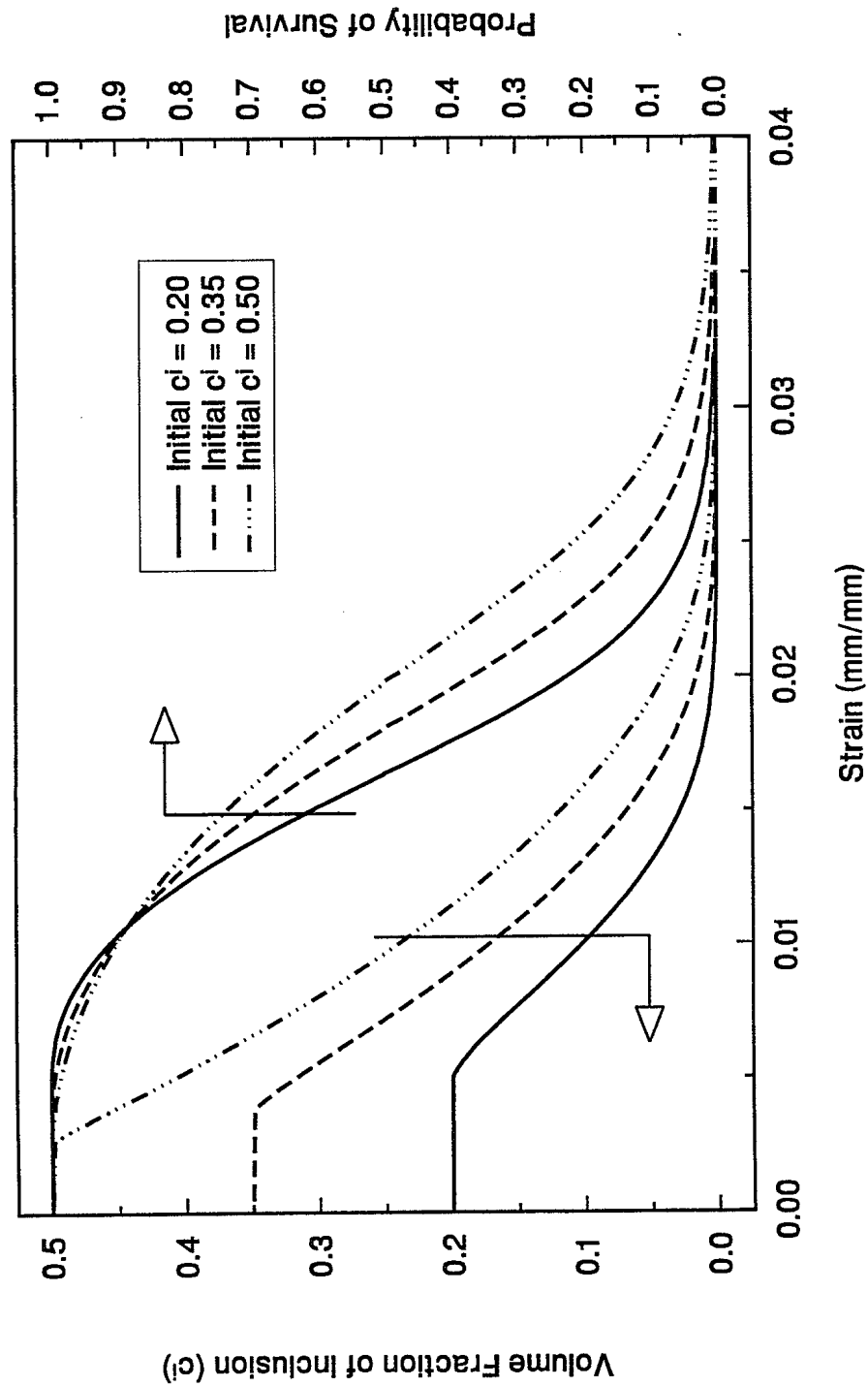


FIGURE 10 – Correspondance between inclusion volume fraction and probability of survival values as function of composite strain.

UNCLASSIFIED

49

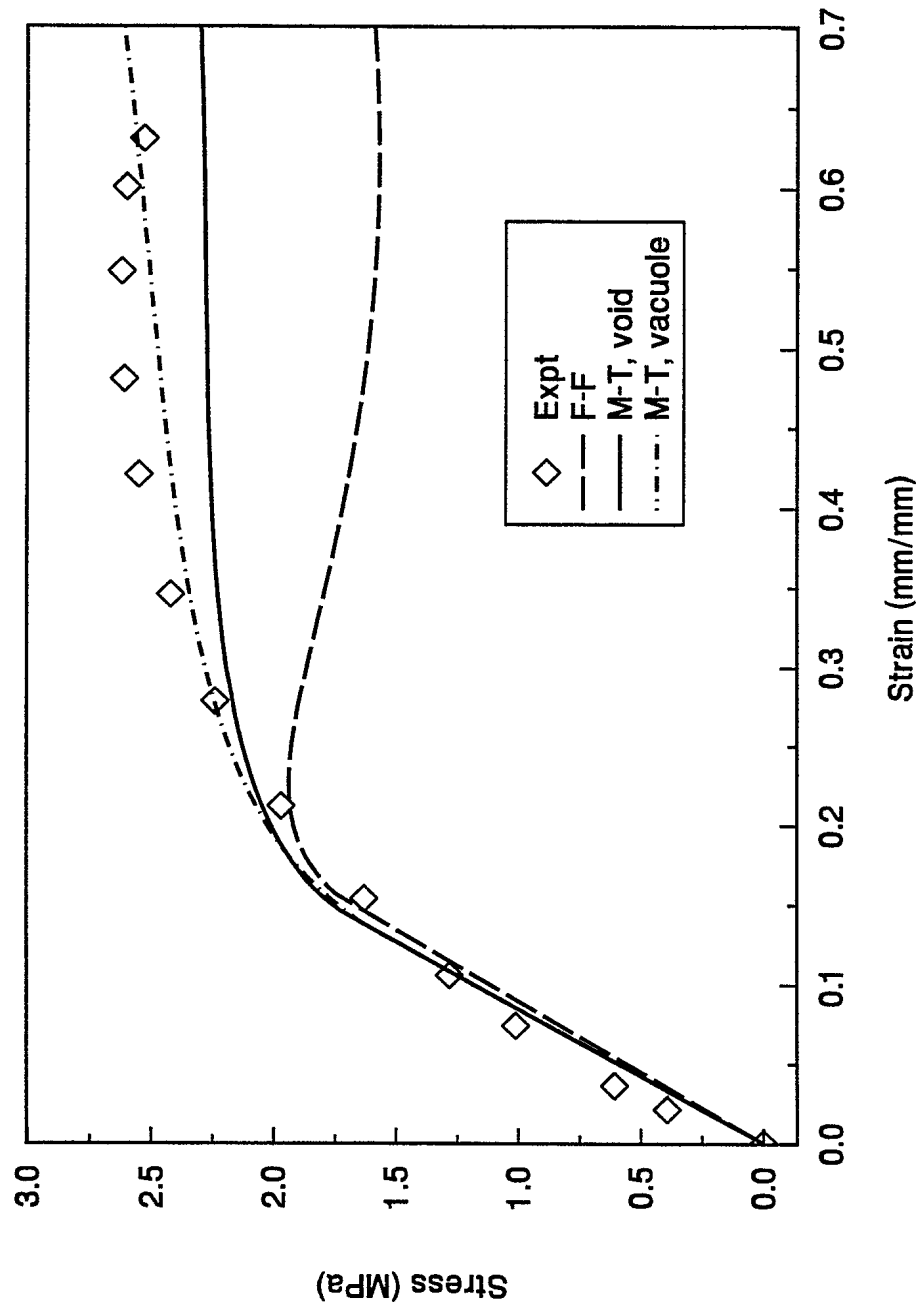


FIGURE 11 – Mechanical behavior predictions for composite containing $c_o^i = 0.3$ untreated glass beads in polyurethane (Ref. 30). $c^v = c_o^i - c^i$. Interaction between bonded particles taken into account.

UNCLASSIFIED

50

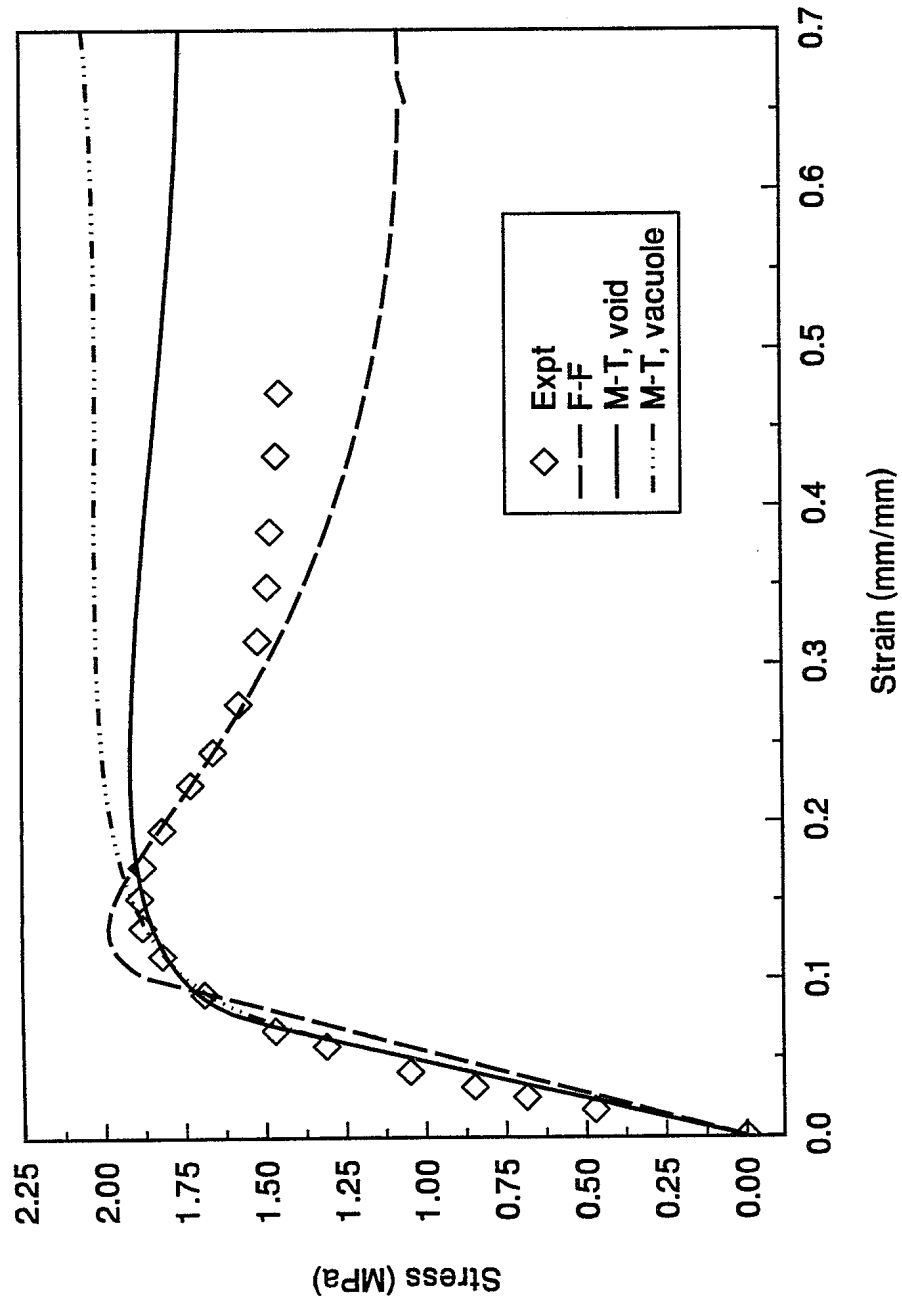


FIGURE 12 – Mechanical behavior predictions for composite containing $c_o^i = 0.4$ untreated glass beads in polyurethane (Ref. 30). $c^v = c_o^i - c^i$. Interaction between bonded particles taken into account.

UNCLASSIFIED

51

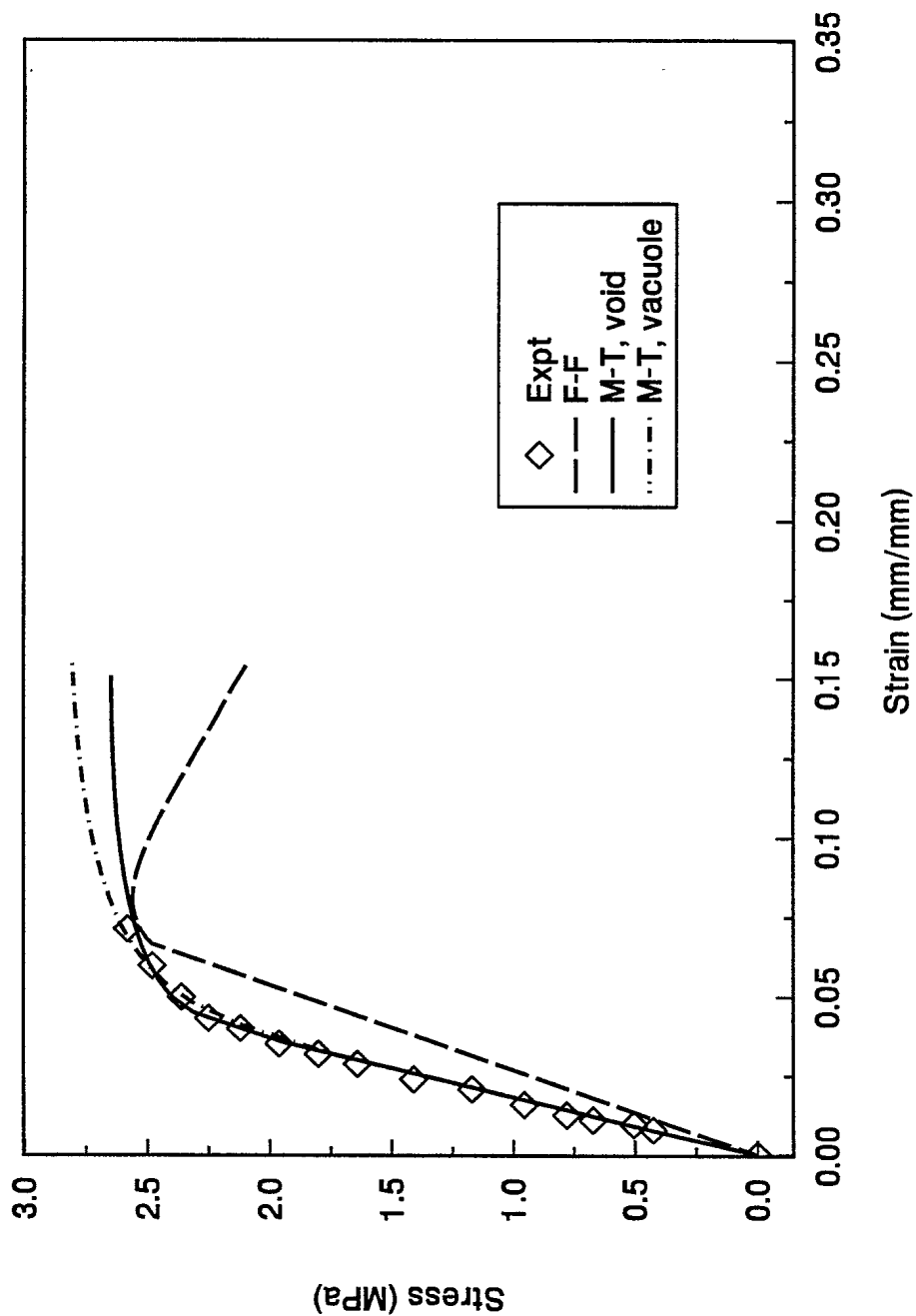


FIGURE 13 – Mechanical behavior predictions for composite containing $c_o^i = 0.5$ untreated glass beads in polyurethane (Ref. 30). $c^v = c_o^i - c^i$. Interaction between bonded particles taken into account.

UNCLASSIFIED

52

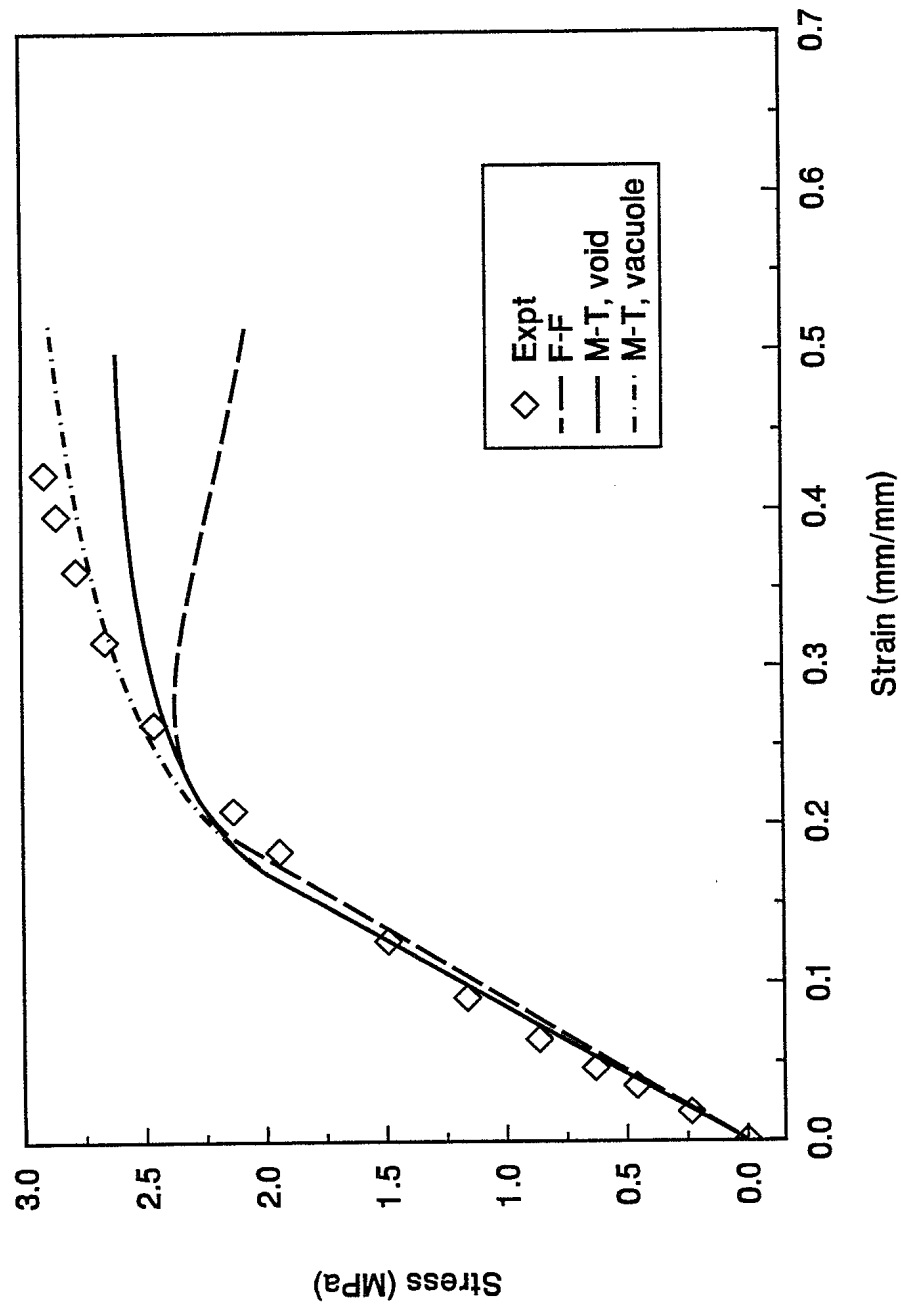


FIGURE 14 – Mechanical behavior predictions for composite containing $c_o^i = 0.3$ treated glass beads in polyurethane (Ref. 30). $c^v = c_o^i - c^i$. Interaction between bonded particles taken into account.

UNCLASSIFIED

53

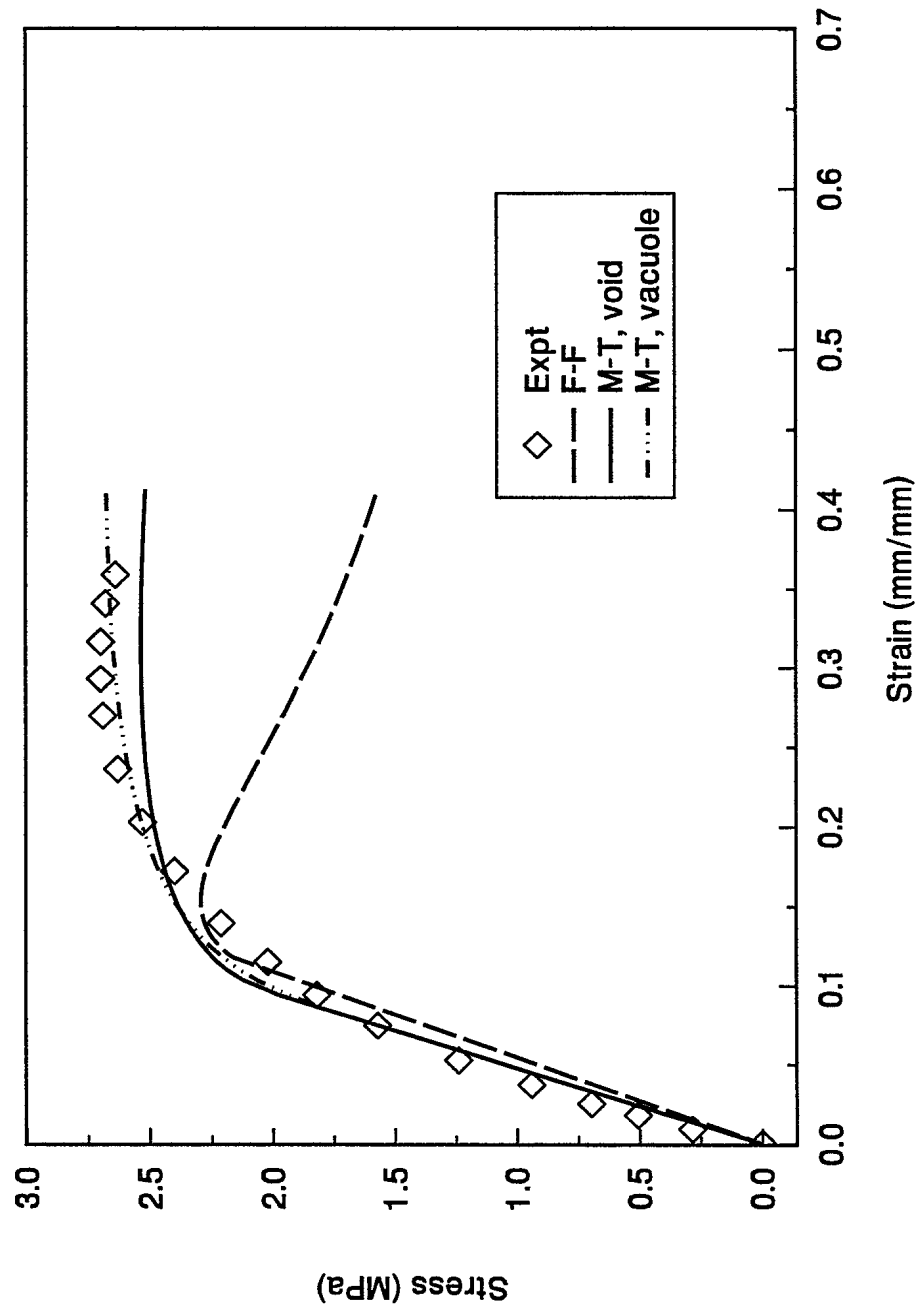


FIGURE 15 – Mechanical behavior predictions for composite containing $c_o^i = 0.4$ treated glass beads in polyurethane (Ref. 30). $c^v = c_o^i - c^i$. Interaction between bonded particles taken into account.

UNCLASSIFIED

54

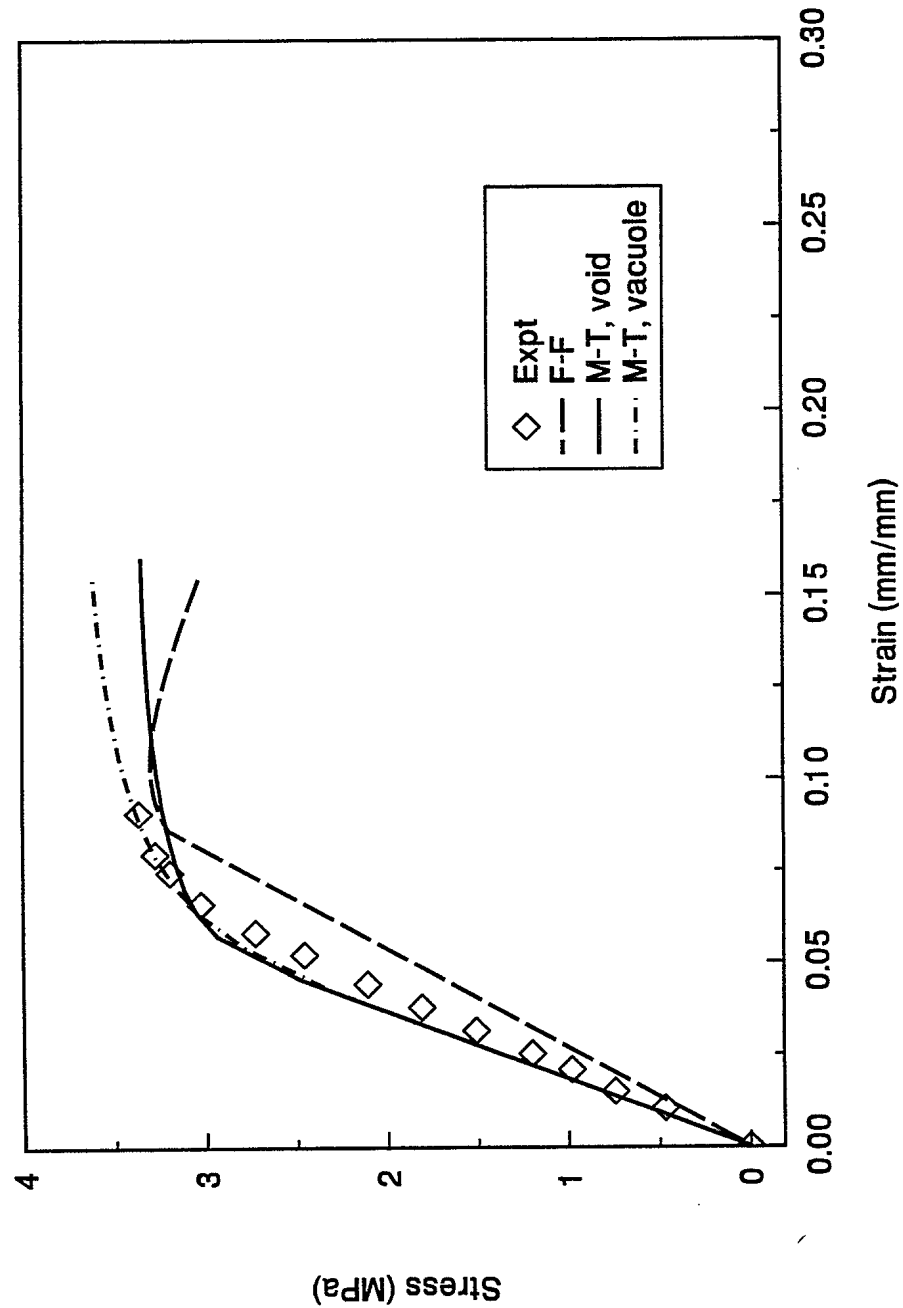


FIGURE 16 – Mechanical behavior predictions for composite containing $c_o^i = 0.5$ treated glass beads in polyurethane (Ref. 30). $c^v = c_o^i - c^i$. Interaction between bonded particles taken into account.

UNCLASSIFIED

55

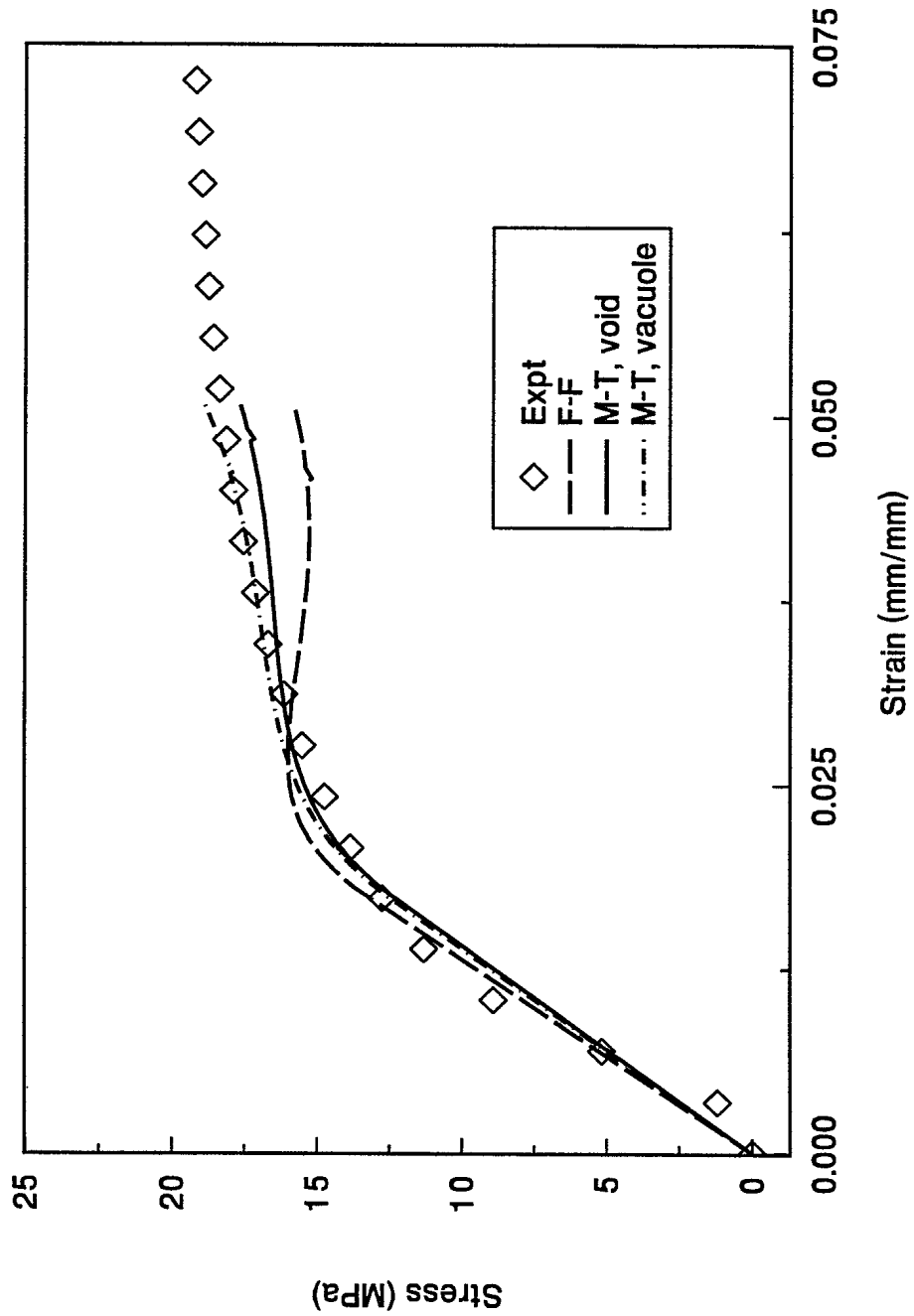


FIGURE 17 – Mechanical behavior predictions for composite containing $c_o^i = 0.19$ $31\ \mu\text{m}$ untreated glass beads in polyethylene (Ref. 14). $c^v = c_o^i - c^i$. Interaction between bonded particles taken into account.

UNCLASSIFIED

56

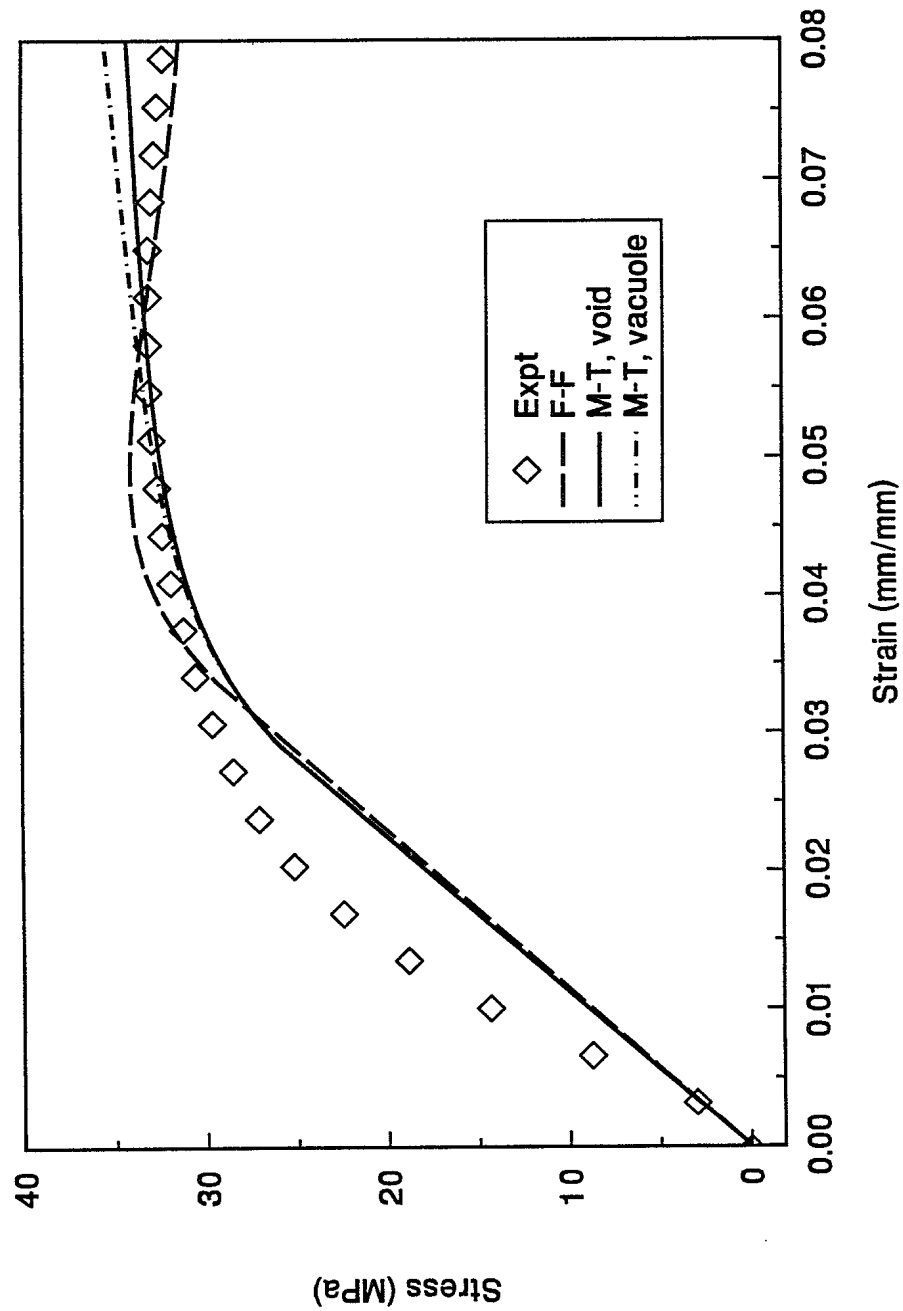


FIGURE 18 - Mechanical behavior predictions for composite containing $c_o^i = 0.22$ $31\ \mu\text{m}$ treated glass beads in polyethylene (Ref. 14). $c^v = c_o^i - c^i$. Interaction between bonded particles taken into account.

UNCLASSIFIED

57

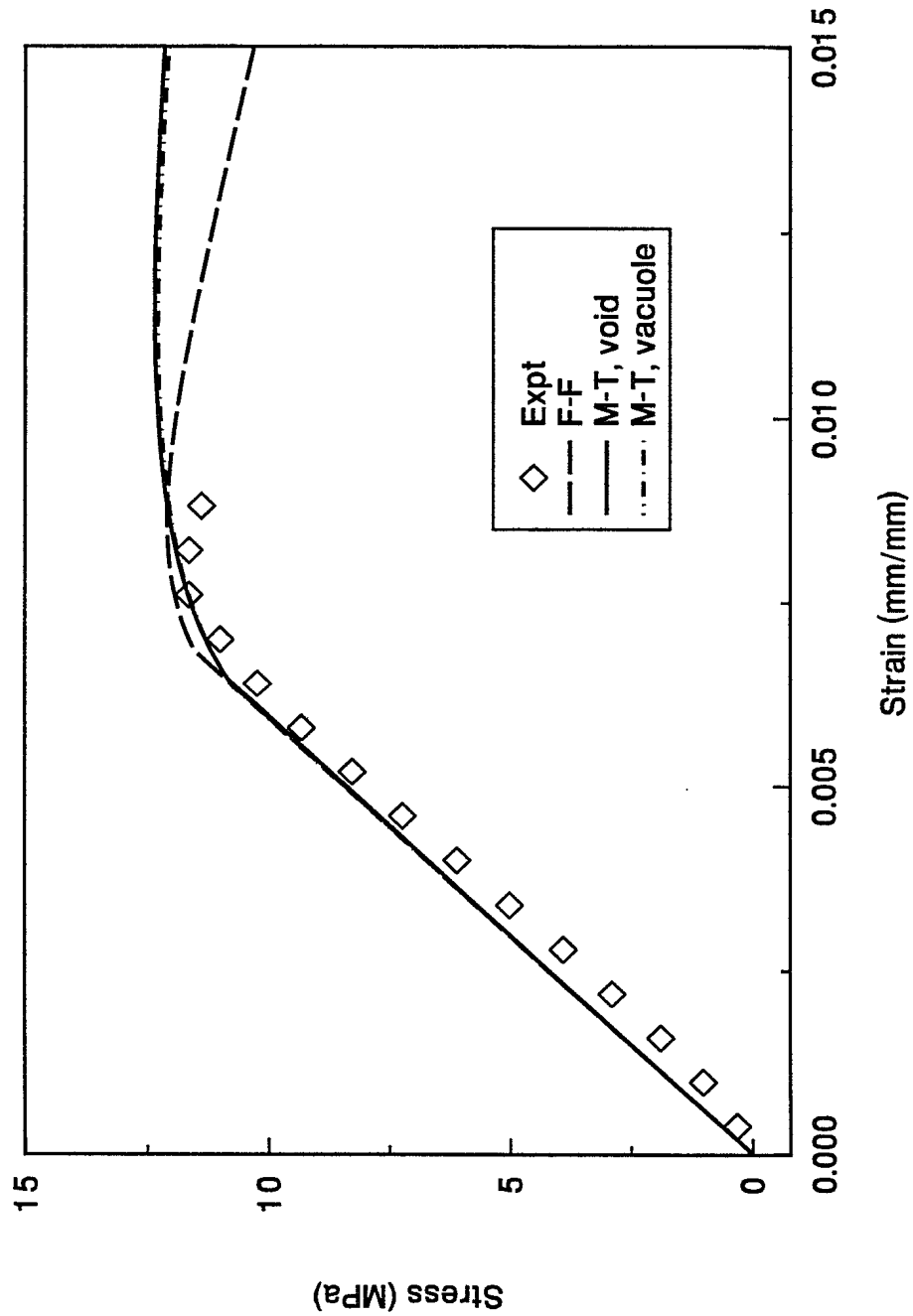


FIGURE 19 – Mechanical behavior predictions for composite containing $c_o^i = 0.48$ 31 μm untreated glass beads in polyethylene (Ref. 14). $c^v = c_o^i - c^i$. Interaction between bonded particles taken into account.

UNCLASSIFIED

58

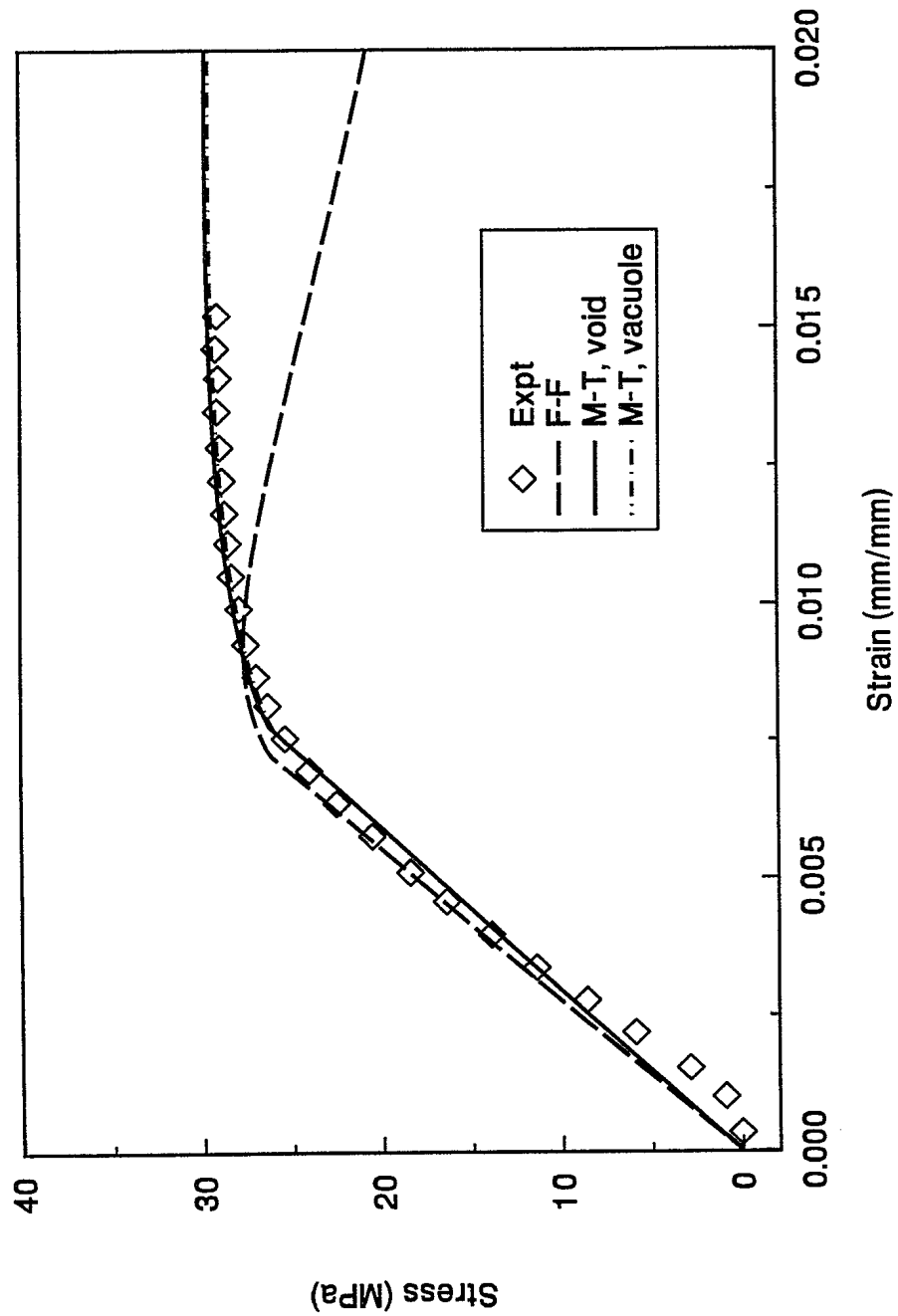


FIGURE 20 – Mechanical behavior predictions for composite containing $c_o^i = 0.49$ $31 \mu\text{m}$ treated glass beads in polyethylene (Ref. 14). $c^v = c_o^i - c^i$. Interaction between bonded particles taken into account.

UNCLASSIFIED

59

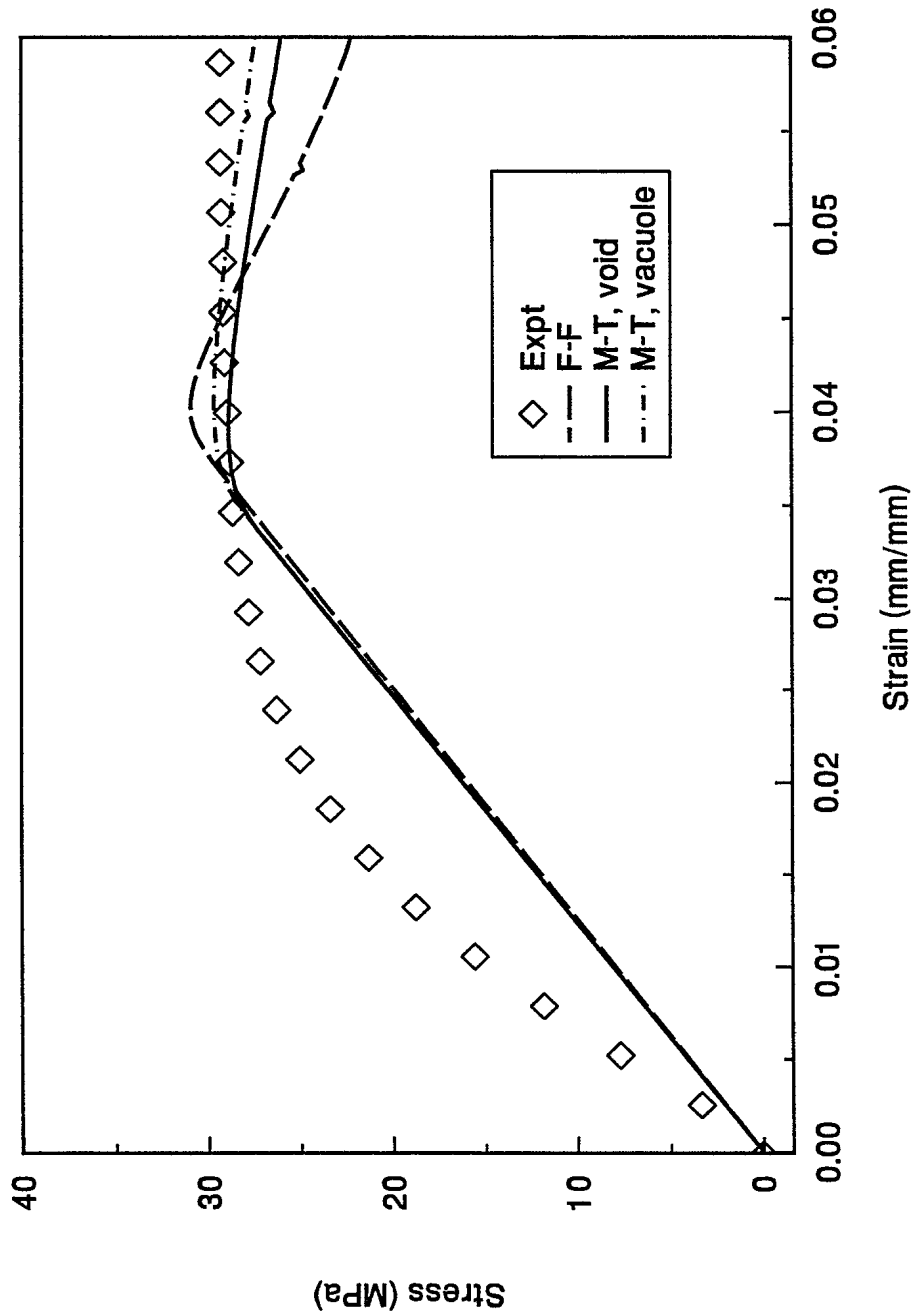


FIGURE 21 – Mechanical behavior predictions for composite containing $c_o^i = 0.19$ 130 μm treated glass beads in polyethylene (Ref. 14). $c^v = c_o^i - c^i$. Interaction between bonded particles taken into account.

UNCLASSIFIED

60

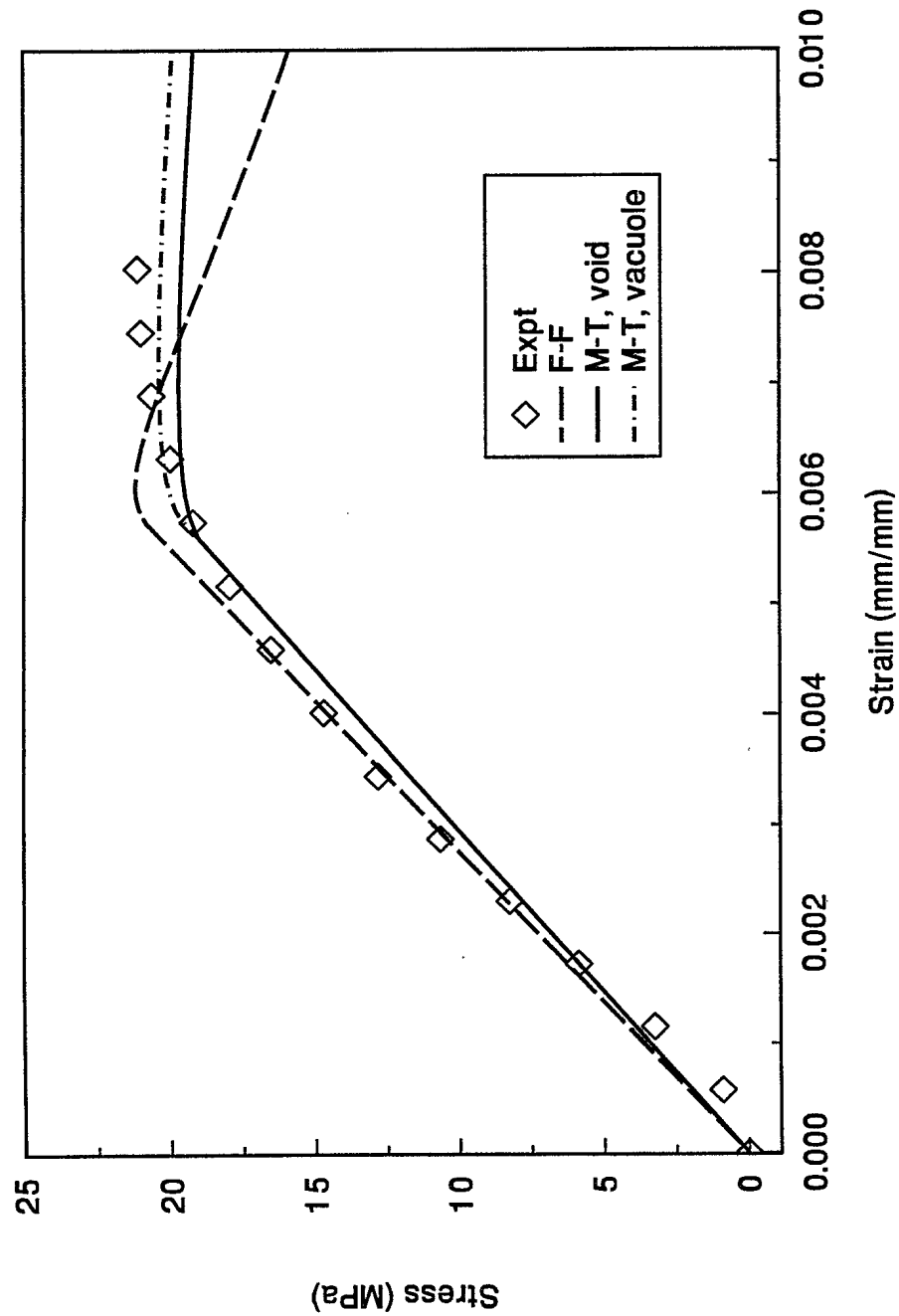


FIGURE 22 - Mechanical behavior predictions for composite containing $c_o^i = 0.49$ 130 μm treated glass beads in polyethylene (Ref. 14). $c^v = c_o^i - c^i$. Interaction between bonded particles taken into account.

UNCLASSIFIED

A.1

APPENDIX AMathematica Listing for 3-Phase Modulus ModelProgram Listing

```
(* Three-phase Mori-Tanaka model with particle interaction effects \
and void or vacuole formulation *)
```

```
(* cx - inclusion volume fraction, \
cy - void or vacuole volume fraction, \
jucor - apply ju correction (1=yes), \
voidmag - apply correction to voids (1=yes) *)
```

```
cx=0.30119; cy=0.5-cx; jucor=1; voidmag=0
```

```
(* particle interaction function \
ygr - inclusion interaction function, \
ygs - void or vacuole interaction function *)
```

```
ygr=1.26*(1-cx)/24; ygs=(1)/24
```

```
(* material constants for comparison and inclusion materials *)
```

```
(* phases in terms of tensile modulus and Poisson's ratio *)
```

```
(* em - matrix tensile modulus, \
v - matrix Poisson ratio, \
emr - inclusion tensile modulus, \
vr - inclusion Poisson ratio, \
ems - void or vacuole tensile modulus, \
vs - void or vacuole Poisson ratio, \
k - matrix bulk modulus, \
u - matrix shear modulus, \
es_ij - vacuole tensile modulus in ij-direction, \
vs_ij - vacuole Poisson ratio in ij-direction *)
```

```
(* Smith glass bead/epoxy properties *)
```

```
(* em=3.01 ; v=0.394; \
```

UNCLASSIFIED

A.2

```
emr=76 ; vr=0.23;      \  
ems=0  ; vs=0.23;      \  
k = em/(3*(1-2*v));    \  
u = em/(2*(1+v));      \  
kr = emr/(3*(1-2*vr)); \  
ur = emr/(2*(1+vr));   \  
ks = ems/(3*(1-2*vs)); \  
us = ems/(2*(1+vs));   \  
es11=0.0*ems; es22=es33=1.0*ems; \  
vs12=vs13=0; \  
vs21=vs31=vs23=vs32=vs *)
```

```
(* Ravichandran #625 *)  
(* em=207 ; v=0.31;      \  
emr=700 ; vr=0.194;      \  
ems=0  ; vs=0.194;      \  
k = em/(3*(1-2*v));      \  
u = em/(2*(1+v));        \  
kr = emr/(3*(1-2*vr));   \  
ur = emr/(2*(1+vr));     \  
ks = ems/(3*(1-2*vs));   \  
us = ems/(2*(1+vs));     \  
es11=1.0*ems; es22=es33=1.0*ems; \  
vs12=vs13=0; \  
vs21=vs31=vs23=vs32=vs *)
```

```
(* Yilmazer #351 *)  
em=4.2 ; v=0.499;      \  
emr=70000 ; vr=0.16;   \  
ems=0000  ; vs=0.16;   \  
k = em/(3*(1-2*v));    \  
u = em/(2*(1+v));      \  
kr = emr/(3*(1-2*vr)); \  
ur = emr/(2*(1+vr));   \  
ks = ems/(3*(1-2*vs)); \  
us = ems/(2*(1+vs));   \  
es11=0.0*ems; es22=es33=1.0*ems; \  
vs12=vs13=0; \  
vs21=vs31=vs23=vs32=vs *)
```

UNCLASSIFIED

A.3

```

vs12=vs13=0; \
vs21=vs31=vs23=vs32=vs

(* interaction parameters for inclusions *)
alphar = 2*(5*v-1)+10*(1-v)*(k/(kr-k)-u/(ur-u))
betar = 2*(4-5*v)+15*(1-v)*(u/(ur-u))
zetair = 12*v*(13-14*v)-(96*alphar/(3*alphar+2*betar))*(1-2*v)*(1+v)
zeta2r = 6*(25-34*v+22*v^2)-(36*alphar/(3*alphar+2*betar))*(1-2*v)*(1+v)
magr = ((5/4)/betar^2)*ygr

(* interaction parameters for voids *)
alphas = 2*(5*v-1)+10*(1-v)*(k/(ks-k)-u/(us-u))
betas = 2*(4-5*v)+15*(1-v)*(u/(us-u))
zeta1s = 12*v*(13-14*v)-(96*alphas/(3*alphas+2*betas))*(1-2*v)*(1+v)
zeta2s = 6*(25-34*v+22*v^2)-(36*alphas/(3*alphas+2*betas))*(1-2*v)*(1+v)
mags = ((5/4)/betas^2)*ygs

(* Eshelby's transformation factors for spherical particles *)
s1 = 5*v-1
s2 = 4-5*v
sdet = 15*(1-v)

(* comparison or matrix material stiffness matrix *)
c1111 = k+(4/3)*u; c1122 = k-(2/3)*u; c1133 = c1122
c2211 = c1122 ; c2222 = c1111 ; c2233 = c1122
c3311 = c1122 ; c3322 = c1122 ; c3333 = c1111

c0 = {{c1111,c1122,c1133},{c2211,c2222,c2233},{c3311,c3322,c3333}}

(* inclusion material stiffness matrix *)
cr1111 = kr+(4/3)*ur; cr1122 = kr-(2/3)*ur; cr1133 = cr1122
cr2211 = cr1122 ; cr2222 = cr1111 ; cr2233 = cr1122
cr3311 = cr1122 ; cr3322 = cr1122 ; cr3333 = cr1111

cr = {{cr1111,cr1122,cr1133},{cr2211,cr2222,cr2233},{cr3311,cr3322,cr3333}}

(* void or vacuole material stiffness matrix *)

```

UNCLASSIFIED

A.4

```

csdet = 1-vs12*vs21-vs13*vs31-vs23*vs32-vs12*vs23*vs31-vs13*vs21*vs32
cs1111 = es11(1-vs23*vs32)
cs1122 = es11(vs21+vs23*vs31)
cs1133 = es11(vs31+vs21*vs32)
cs2211 = es22(vs12+vs13*vs32)
cs2222 = es22(1-vs13*vs31)
cs2233 = es22(vs32+vs12*vs31)
cs3311 = es33(vs13+vs12*vs23)
cs3322 = es33(vs23+vs13*vs21)
cs3333 = es33(1-vs12*vs21)

```

```

cs = (1/csdet)*{{cs1111,cs1122,cs1133}, \
               {cs2211,cs2222,cs2233}, \
               {cs3311,cs3322,cs3333}}

```

(* Eshelby transformation tensor for spherical particles*)

```

s1111 = s1+2*s2; s1122 = s1      ; s1133 = s1122
s2211 = s1122   ; s2222 = s1111 ; s2233 = s1122
s3311 = s1122   ; s3322 = s1122 ; s3333 = s1111

```

```

s = (1/sdet)*{{s1111,s1122,s1133}, \
              {s2211,s2222,s2233}, \
              {s3311,s3322,s3333}}

```

(* correction factor matrix for inclusions *)

```

cwr11 = zeta1r+2*zeta2r ; cwr12 = zeta1r      ; cwr13 = cwr12
cwr21 = cwr12           ; cwr22 = cwr11      ; cwr23 = cwr12
cwr31 = cwr12           ; cwr32 = cwr12      ; cwr33 = cwr11

```

```

cwr = {{cwr11,cwr12,cwr13}, \
       {cwr21,cwr22,cwr23}, \
       {cwr31,cwr32,cwr33}}

```

(* correction factor matrix for voids *)

```

cws11 = zeta1s+2*zeta2s ; cws12 = zeta1s      ; cws13 = cws12
cws21 = cws12           ; cws22 = cws11      ; cws23 = cws12
cws31 = cws12           ; cws32 = cws12      ; cws33 = cws11

```

UNCLASSIFIED

A.5

```

cws = {{cws11,cws12,cws13}, \
       {cws21,cws22,cws23}, \
       {cws31,cws32,cws33}}

(* Identity matrix *)
i = IdentityMatrix[3]

(* A-matrices *)
ar = Inverse[cr-c0].c0
as = Inverse[cs-c0].c0

(* complete correction matrix for inclusions and voids *)
If[jucor>0,lambdar=i+magr*cx*cwr,lambdar=i]
If[voidmag>0,lambdas=i+mags*cy*cws,lambdas=i]

(* calculation of average stiffness coefficients *)
f1 = Inverse[s+ar]
f2 = Inverse[s+as]
f3 = Inverse[cx*(i-lambdar-s)+s+ar+cy*(i-lambdas-s).f2.(s+ar)]
f4 = Inverse[cy*(i-lambdas-s)+s+as+cx*(i-lambdar-s).f1.(s+as)]
fcavg = c0.(i+cx*lambdar.f3+cy*lambdas.f4)

femav = fcavg[[1,1]]-(2*fcavg[[1,2]]*fcavg[[2,1]])/(fcavg[[2,2]]+fcavg[[2,3]])
fvav = fcavg[[2,1]]/(fcavg[[2,2]]+fcavg[[2,3]])

Print["cx= ",cx]; Print["cy= ",cy]; \
Print["ju corrc= ",jucor];Print["void mag= ",voidmag]; \
Print["f eavg= ",femav]; Print["f vavg= ",fvav]

(* use for generation of modulus and Poisson ratio vs inclusion Vf *)
(* fe = N[Table[femav,{cx,0,0.5,0.01}],4] \
fv = N[Table[fvav,{cx,0,0.5,0.01}],4] *)

```


UNCLASSIFIED

B.1

APPENDIX BFORTRAN Listing for Micromechanical ModelProgram Listing

```
C==== main program
C   calculates particle size histogram with corresponding filler
C   volume fraction. uses Z-decrements for particle size
C   determination
C   user enters the following information:
C       number of points desired in stress-strain curve
C       number of particle distributions
C       avg radius and std dev of each distribution
C       volume fraction of filler and voids of each distribution
C       matrix and filler shear modulus, poisson ratio
C       void shear and bulk moduli
C       sample volume, fraction debond, w-type, m-type
C       adhesion energy and applied pressure
C   information may be entered using keyboard or by input data file.
C   three options for printing out intermediate results are available:
C       if values for no pts desired in stress-strain curve and number
C       of particle distributions are negative, data files GAUSS,
C       HISTO, DEBUG and STRESS are written.
C       if value for no pts desired in stress-strain curve is negative
C       and value for number of particle distributions is positive,
C       data files HISTO, DEBUG and STRESS are written.
C   if input data was entered using data file, the data file STRESS
C   will be renamed to the input data file's name.
C
C   to compile and link: fl p.for /link graphics.lib. the files
C   MSGRAPH.FOR and GRFDEF.FOR should be in the same directory unless
C   a temporary variable has been set up to point to the location of
C   include files. these files contain graphics routines necessary to
C   plot stress-strain curve on screen.
C
C   the indexing of the various parameters is organized as follows:
```

UNCLASSIFIED

B.2

```

C      strain - current critical strain
C      stress - current stress calc using previous E,G and crit.strain
C      Pr_surv - current no. of particles remaining
C      E,G      - moduli at current Pr_surv
C      Vf,Vv    - current filler and void volume fractions
C      dG/dc, dK/dc, dA/dc - current differential quantities
C      the total number of points is NDIS*NPTS+1 where the additional
C      point is for zero strain and stress. the first group of debonded
C      particles begins at ICNT=2.
C
C      added routine to output SQRT(r*dE/dc). dc based on total volume
C      instead of Vf+Vm. trapped zero in SQRT calc of crit. strain.
C
C      implementation of Mori-Tanaka solution extended for 3-phase and
C      particle interaction. constituent material properties
C      designated as follows: 1-inclusion,2-void or vacuole,3-matrix.
C      fraction debond (FDBND) for orthotropic properties in loading
C      direction, multiplier for rad. dist. func. (YMULT), w-type
C      designates use inclusion or void properties in
C      calc of Wv matrix (0=void, 1=inclusion), m-type determines type of
C      particle interaction used (0=none,1=inclusion, 2=inclusion and
C      void or vacuole), v-type determines isotropic or orthotropic matl
C      (0=orthotropic,1=isotropic)
C
C      last revision: 04 MAR 1995
C
C      set PTMX = NDIS*GSMX
C
      REAL LOGSTD,NPARTL,NUMPAR,NETVF,NETVV
      REAL IDENT,K,KCMP,MAG
      INTEGER GSMX,PTMX
      PARAMETER (GSMX = 250,PTMX = 750,NDIS = 3)
      COMMON /GAUS/ Z(GSMX),RADIUS(NDIS,GSMX),PROB(NDIS,GSMX)
      COMMON /DEBUG/ NUMPAR(NDIS,GSMX),VOLPAR(NDIS,GSMX),
*      NETVF(PTMX),NETVV(PTMX),DADC(PTMX),NPARTL(NDIS)
      COMMON /DIST/ RADAVG(NDIS),LOGSTD(NDIS),VLFRFO(NDIS),
*      VLFRVO(NDIS)

```


UNCLASSIFIED

B.3

```

COMMON /MATRA/ BETA(2),WI(3,3),WV(3,3),IDENT(3,3)
COMMON /MATRB/ S(3,3),CA(3,3),CB(3,3),CE(3,3),CF(3,3)
COMMON /PROPA/ K(3),G(3),E(3),POIS(3),CI(3,3),CV(3,3),CO(3,3)
COMMON /PROPB/ C11(PMX),C12(PMX),C21(PMX),C22(PMX),C23(PMX),
*   ECMP(PMX),POISC(PMX)
COMMON /RESULT/ CRTSTN(PMX),STRESS(PMX),DILAT(PMX),
*   PRBSRV(PMX),SORRAD(PMX),SORPAR(PMX),SORVLP(PMX),
*   IPDIST(PMX)
CHARACTER FILNM*8

C
C== initialize variables and arrays by BLOCK DATA INIT
C
CALL INPUT(NDIST,NTOT,VOLSMP,FDBND,YMULT,IKIND,IMORI,IPOIS,GAMM,
*   PRESS,FILNM,IWRT)
C
IABORT = 0.0
CALL STRSTN(NDIST,NTOT,NPTS,VOLSMP,FDBND,YMULT,IKIND,IMORI,IPOIS,
*   GAMM,PRESS,DILATO,IWRT,IABORT)
C
C== write out results and debug data
CALL STRWRT(NDIST,NPTS,VOLSMP,GAMM,FDBND,YMULT,IKIND,IMORI,IPOIS,
*   PRESS,DILATO,FILNM,IABORT)
IF (ABS(IWRT).GE.1) CALL DBGWRT(NDIST,NPTS,IABORT)
IF (ABS(IWRT).GE.1) CALL DBGRAT(NDIST,NPTS,IABORT)
C
CALL CRVPLT(NDIST,NPTS,IABORT)
C
END
C
C
SUBROUTINE INPUT(NDIST,NTOT,VOLSMP,FDBND,YMULT,IKIND,IMORI,IPOIS,
*   GAMM,PRESS,FILNM,IWRT)
C==== reads in problem input either by file or keyboard. if data entered
C   through a file, user inputs name only, a file extension of DAT is
C   assumed. the first line in the input file is used for a user
C   heading and is not read in, constituent material properties
C   designated as follows: 1-inclusion,2-void or vacuole,3-matrix

```

UNCLASSIFIED

B.4

```

C
C      set PTMX = NTDIS*GSMX
C
      REAL LOGSTD,NPARTL,NUMPAR,NETVF,NETVV
      REAL IDENT,K,KCMP,MAG
      INTEGER GSMX,PTMX
      PARAMETER (GSMX = 250,PTMX = 750,NTDIS = 3)
      COMMON /DIST/ RDAVG(NTDIS),LOGSTD(NTDIS),VLFRFO(NTDIS),
*      VLFRVO(NTDIS)
      COMMON /PROPA/ K(3),G(3),E(3),POIS(3),CI(3,3),CV(3,3),CO(3,3)
      CHARACTER ANS*1,FILNM*8
C
      WRITE (6,'(/,A)') ' Read data from file? (Y/N)'
      READ (5,'(A1)') ANS
C
      IF (ANS.EQ.'Y') THEN
        WRITE (6,'(A)') ' File to read? (.INP will be appended)'
        READ (5,'(A8)') FILNM
        OPEN (UNIT=7,FILE=FILNM//'.INP',FORM='FORMATTED',STATUS='OLD')
        READ (7,*)
        READ (7,*) NTOT
        READ (7,*) NDIST
        DO 10 I = 1,ABS(NDIST)
          READ (7,*) RDAVG(I)
          READ (7,*) LOGSTD(I)
          READ (7,*) VLFRFO(I),VLFRVO(I)
10      CONTINUE
        READ (7,*) VOLSMP
        READ (7,*) FDBND,YMULT,IKIND,IMORI,IPOIS
        READ (7,*) G(3),G(1)
        READ (7,*) POIS(3),POIS(1)
        READ (7,*) G(2),K(2)
        READ (7,*) GAMM,PRESS
        CLOSE (7)
      ELSE
        WRITE (6,'(/,A,I3,A)')
*      ' no. pts desired in stress-strain curve (<','GSMX,')'

```

UNCLASSIFIED

B.5

```

      READ (5,*) NTOT
      WRITE (6,'(A,I1,A)') ' no. of particle distributions (<=',
*      NTDIS,')'
      READ (5,*) NDIST
      DO 20 I = 1,ABS(NDIST)
        WRITE (6,'(A,I1,A)') ' for distribution no. ',I,
*        ' mean radius (micron)'
        READ (5,*) RADAVG(I)
        WRITE (6,'(A)') ' log normal radius std dev'
        READ (5,*) LOGSTD(I)
        WRITE (6,'(A)') ' initial volume fraction filler and void'
        READ (5,*) VLFRFO(I),VLFRVO(I)
20    CONTINUE
      WRITE (6,'(A)') ' sample volume (mm3)'
      READ (5,*) VOLSMF
      WRITE (6,'(A)') ' dbnd frac,rad dist mult,w-type,m-type,v-type'
      READ (5,*) FDBND,YMULT,IKIND,IMORI,IPOIS
      WRITE (6,'(A)') ' matrix and filler shear modulus (Pa)'
      READ (5,*) G(3),G(1)
      WRITE (6,'(A)') ' matrix and filler Poisson ratio'
      READ (5,*) POIS(3),POIS(1)
      WRITE (6,'(A)') ' void shear and bulk modulus (Pa)'
      READ (5,*) G(2),K(2)
      WRITE (6,'(A)') ' Gc (J/m2) and applied pressure (Pa)'
      READ (5,*) GAMM,PRESS
      FILNM = 'DEFAULT'
    ENDIF
C
C== set write file flag, 0=STRWRT, 1=STRWRT,DBGWRT,HSTWRT, 2=all
      IWRT = 0
      IF (NTOT.LT.0.AND.NDIST.LT.0) IWRT = 2
      IF (NTOT.LT.0.AND.NDIST.GT.0) IWRT = 1
      NDIST = ABS(NDIST)
      NTOT = ABS(NTOT)
C
      RETURN
      END

```

UNCLASSIFIED

B.6

```

C
C
      SUBROUTINE STRSTN(NDIST,NTOT,NPTS,VOLSMP,FDBND,YMULT,IKIND,IMORI,
*   IPOIS,GAMM,PRESS,DILATO,IWRT,IABORT)
C==== main subroutine which organizes particle size distribution,
C      composite property, critical strain and stress and dilation
C      calculation modules.
C
      REAL LOGSTD,NPARTL,NUMPAR,NETVF,NETVV
      INTEGER GSMX,PTMX
      PARAMETER (GSMX = 250,PTMX = 750,NTDIS = 3)
      COMMON /DEBUG/ NUMPAR(NTDIS,GSMX),VOLPAR(NTDIS,GSMX),
*   NETVF(PTMX),NETVV(PTMX),DADC(PTMX),NPARTL(NTDIS)
C
C== initialize abort flag
      IABORT = 0
C
C== create gaussian distribution of particle size
      WRITE (6,'(/,A)') ' Generating particle distribution'
      CALL GAUSS(NDIST,NTOT,NPTS,IABORT)
C== write out gaussian cumulative data
      IF (ABS(IWRT).GE.2) CALL GAUWRT(NDIST,NPTS,IABORT)
C
C== find size and number of particles to debond
      WRITE (6,'(/,A)') ' Finding particle size and number'
      CALL PARTSZ(NDIST,NPTS,VOLSMP,IABORT)
C== write out particle size and number histogram
      IF (ABS(IWRT).GE.1) CALL HSTWRT(NDIST,NPTS,IABORT)
C
      WRITE (6,'(/,A)') ' Sorting particle distributions'
      CALL SORTER(NDIST,NPTS,IABORT)
      WRITE (6,'(A)') ' Calculating vol fractions and dA/dc'
      CALL VOLFRF(NDIST,NPTS,VOLSMP,IABORT)
C
      WRITE (6,'(/,A)') ' Generating stress-strain curve'
C== calculate initial composite properties
      ICNT = 1

```

UNCLASSIFIED

B.7

```

CONCI = NETVF(ICNT)
CONCV = NETVV(ICNT)
CALL MTPRP(CONCI,CONCV,ICNT,FDBND,YMULT,IKIND,IMORI,IPOIS,IABORT)
IF (IABORT.EQ.0) WRITE (6,'(A,1X,I3,A,I3,A)')
*   ' Calculating point: ',ICNT,'/',NDIST*NPTS+1,' max'
C
C==  main routine for debonding and stress-strain calculation.
C   offset pointer ICNT by 1 to make room for unbonded state.
C
DO 10 ICNT = 2,NDIST*NPTS+1
    CONCI = NETVF(ICNT)
    CONCV = NETVV(ICNT)
    CALL MTPRP(CONCI,CONCV,ICNT,FDBND,YMULT,IKIND,IMORI,IPOIS,
*       IABORT)
    IF (IABORT.EQ.0) WRITE (6,'(A,1X,I3,A,I3,A)')
*       '+Calculating point: ',ICNT,'/',NDIST*NPTS+1,' max'
    CALL CRIT(ICNT,VOLSMP,GAMM,PRESS,IABORT)
    CALL CALVAL(ICNT,PRESS,DILATO,IABORT)
10 CONTINUE
C
    RETURN
    END
C
C
SUBROUTINE GAUSS(NDIST,NTOT,NPTS,IABORT)
C==== Program calculates the cumulative area underneath the
C   gaussian curve between the limits +/- (IEND/FACT) in increments
C   of IDELT/FACT. NTOT is used to calculate an appropriate IDELT.
C   since IDELT is rounded down, the exact number of points may be
C   greater. this is reflected in NPTS.
C   Particle radii converted from microns to millimeters.
C   An IEND of 3301 gives a cumulative distribution which starts
C   at 0.0005 and ends at 0.9995. This avoids having extremely large
C   particles when the log standard deviation is large.
C
REAL LOGSTD,NPARTL,NUMPAR,NETVF,NETVV
INTEGER GSMX,PTMX

```

UNCLASSIFIED

B.8

```

PARAMETER (GSMX = 250,PTMX = 750,NTDIS = 3)
PARAMETER (ISTART = 2,IEND = 3301,FACT = 1000,BEGNPT = 0)
EXTERNAL FUNC
COMMON /GAUS/ Z(GSMX),RADIUS(NTDIS,GSMX),PROB(NTDIS,GSMX)
COMMON /DIST/ RADAUG(NTDIS),LOGSTD(NTDIS),VLFRFO(NTDIS),
*   VLFRVO(NTDIS)

C
IMAX = GSMX/2
IDELT = 2*INT((IEND-ISTART)/NTOT)
NPTS = 2*(INT((IEND-ISTART)/IDELT)+1)
IF (NPTS.GT.IMAX) THEN
    WRITE (6,'(A)') ' Too many points: SBR GAUSS.'
    WRITE (6,'(A,I4,A)') ' Over max dim by ',NPTS-GSMX,' points.'
    IABORT = 1
    RETURN
ELSE
ENDIF

C
DO 20 J = 1,NDIST
    IPTS = 0
    DO 10 I = ISTART,IEND,IDELT
        IPTS = IPTS+1
        ENDPT = (FLOAT(I)-1)/FACT
        Z(NPTS/2+IPTS) = ENDPT
        Z(NPTS/2-IPTS+1) = -ENDPT
C== calculate upper portion of probability curve
        RADTMP = 10**((ALOG10(RADAUG(J))+ENDPT*LOGSTD(J))
        RADIUS(J,NPTS/2+IPTS) = RADTMP/1000
        CALL QSIMP(FUNC,BEGNPT,ENDPT,SURF)
        PROB(J,NPTS/2+IPTS) = 0.5+SURF
C== calculate lower portion of probability curve
        RADTMP = 10**((ALOG10(RADAUG(J))-ENDPT*LOGSTD(J))
        RADIUS(J,NPTS/2-IPTS+1) = RADTMP/1000
        PROB(J,NPTS/2-IPTS+1) = 0.5-SURF
10    CONTINUE
20 CONTINUE

C

```

UNCLASSIFIED

B.9

```

      RETURN
      END
C
      FUNCTION FUNC(X)
C==== function used for gaussian curve. called from sbr GAUSS, sbr
C      QSIMP and sbr TRAPZD.
      PI = 3.141592654
      FUNC = (1.0/SQRT(2.0*PI))*EXP(-X**2/2.0)
      RETURN
      END
C
C
      SUBROUTINE PARTSZ(NDIST,NPTS,VOLSMP,IABORT)
C==== sbr finds the total particle volume on a per particle basis.
C      from this the number of particles present in the composite is
C      calculated knowing the initial volume the particles occupy.
C      the incremental probability of the largest particles is
C      calculated using a fraction (PFRAC) of the previous probability
C      increment so that there is a smooth transition from largest to
C      smaller particle sizes in terms of number.
C
C      set PTMX = GSMX*NTDIS
C
      REAL LOGSTD,NPARTL,NUMPAR,NETVF,NETVV
      INTEGER GSMX,PTMX
      PARAMETER (GSMX = 250,PTMX = 750,NTDIS = 3)
      PARAMETER (PI = 3.1415927,PFRAC=0.75)
      COMMON /GAUS/ Z(GSMX),RADIUS(NTDIS,GSMX),PROB(NTDIS,GSMX)
      COMMON /DEBUG/ NUMPAR(NTDIS,GSMX),VOLPAR(NTDIS,GSMX),
*      NETVF(PTMX),NETVV(PTMX),DADC(PTMX),NPARTL(NTDIS)
      COMMON /DIST/ RDAVG(NTDIS),LOGSTD(NTDIS),VLFRFO(NTDIS),
*      VLFRVO(NTDIS)
C
      IF (IABORT.EQ.1) RETURN
C
C== find total number of particles in given filler volume
      DO 20 IDIST = 1,NDIST

```

UNCLASSIFIED

B.10

```
VOLTOT = 0
C  find total volume on a per particle basis
  DO 10 IPTS = 1,NPTS
    IF (IPTS.EQ.NPTS) THEN
      VOLPAR(IDIST,IPTS) = PFRAC*
*      (PROB(IDIST,IPTS)-PROB(IDIST,IPTS-1))
*      *(4.0/3.0)*PI*RADIUS(IDIST,IPTS)**3
    ELSE
      VOLPAR(IDIST,IPTS) =
*      (PROB(IDIST,IPTS+1)-PROB(IDIST,IPTS))*
*      (4.0/3.0)*PI*RADIUS(IDIST,IPTS)**3
    ENDIF
    VOLTOT = VOLTOT+VOLPAR(IDIST,IPTS)
10  CONTINUE
C  find total number of particles
  NPARTL(IDIST) = VLFRFO(IDIST)*VOLSMP/VOLTOT
20  CONTINUE
C
C  calculate volume taken up by particles of radius r
  DO 30 IDIST = 1,NDIST
    DO 40 IPTS = 1,NPTS
      IF (IPTS.EQ.NPTS) THEN
        NUMPAR(IDIST,IPTS) = NPARTL(IDIST)*
*        PFRAC*(PROB(IDIST,IPTS)-PROB(IDIST,IPTS-1))
        IF (NUMPAR(IDIST,IPTS).LT.1.0) IFLAG = 1
        VOLPAR(IDIST,IPTS) = NUMPAR(IDIST,IPTS)*
*        (4.0/3.0)*PI*RADIUS(IDIST,IPTS)**3
      ELSE
        NUMPAR(IDIST,IPTS) = NPARTL(IDIST)*
*        (PROB(IDIST,IPTS+1)-PROB(IDIST,IPTS))
        IF (NUMPAR(IDIST,IPTS).LT.1.0) IFLAG = 1
        VOLPAR(IDIST,IPTS) = NUMPAR(IDIST,IPTS)*
*        (4.0/3.0)*PI*RADIUS(IDIST,IPTS)**3
      ENDIF
C
      IF (IFLAG.EQ.1) THEN
        WRITE(6,5000)
```


UNCLASSIFIED

B.11

```

      *          IDIST,IPTS,RADIUS(IDIST,IPTS),NUMPAR(IDIST,IPTS)
      IFLAG = 0
      ELSE
      ENDIF
C
40      CONTINUE
30      CONTINUE
C
C      RETURN
5000  FORMAT(' Error SBR PARTSZ: IDIST=',I1,' IPTS=',I3,' RAD=',E11.6,
      *      ' NUMPAR=',E11.6)
      END
C
C
      SUBROUTINE SORTER(NDIST,NPTS,IABORT)
C==== loads radius, number of particles and total volume of particles
C      of radius r from each distribution in a master array to sort.
C      after sorting radii in ascending order, arrays are flipped
C      according to radius to give descending order.
C
C      set PTMX = NTDIS*GSMX
C
      REAL LOGSTD,NPARTL,NUMPAR,NETVF,NETVV
      INTEGER GSMX,PTMX
      PARAMETER (GSMX = 250,PTMX = 750,NTDIS = 3)
      COMMON /GAUS/ Z(GSMX),RADIUS(NTDIS,GSMX),PROB(NTDIS,GSMX)
      COMMON /DEBUG/ NUMPAR(NTDIS,GSMX),VOLPAR(NTDIS,GSMX),
      *      NETVF(PTMX),NETVV(PTMX),DADC(PTMX),NPARTL(NTDIS)
      COMMON /RESULT/ CRTSTN(PTMX),STRESS(PTMX),DILAT(PTMX),
      *      PRBSRV(PTMX),SORRAD(PTMX),SORPAR(PTMX),SORVLP(PTMX),
      *      IPDIST(PTMX)
C
      IF (IABORT.EQ.1) RETURN
C
C*      load master arrays
      DO 20 I = 1,NDIST
        DO 10 J = 1,NPTS

```

UNCLASSIFIED

B.12

```

        SORRAD((I-1)*NPTS+J) = RADIUS(I,J)
        SORPAR((I-1)*NPTS+J) = NUMPAR(I,J)
        SORVLP((I-1)*NPTS+J) = VOLPAR(I,J)
        IPDIST((I-1)*NPTS+J) = I
10    CONTINUE
20    CONTINUE
C
C*    sort master arrays in ascending order
      NTOT = NDIST*NPTS
      CALL SORT3(NTOT,SORRAD,SORPAR,SORVLP,IPDIST)
C
C*    sort master arrays in descending order
      DO 30 I = 1,NDIST*NPTS/2
        ATMP = SORRAD(I)
        SORRAD(I) = SORRAD(NDIST*NPTS-I+1)
        SORRAD(NDIST*NPTS-I+1) = ATMP
        BTMP = SORPAR(I)
        SORPAR(I) = SORPAR(NDIST*NPTS-I+1)
        SORPAR(NDIST*NPTS-I+1) = BTMP
        CTMP = SORVLP(I)
        SORVLP(I) = SORVLP(NDIST*NPTS-I+1)
        SORVLP(NDIST*NPTS-I+1) = CTMP
        ITMP = IPDIST(I)
        IPDIST(I) = IPDIST(NDIST*NPTS-I+1)
        IPDIST(NDIST*NPTS-I+1) = ITMP
30    CONTINUE
C
      RETURN
      END
C
C
      SUBROUTINE VOLFRG(NDIST,NPTS,VOLSMP,IABORT)
C==== calculates dA/dc, net Vf, net Vv and probability of survival for
C      given particle radius. Note: net Vf is based on total sample vol.
C      Prob of surv is based on numbers of particles.
C
C      set PTMX = NTDIS*GSMX

```

UNCLASSIFIED

B.13

C

```

REAL LOGSTD,NPARTL,NUMPAR,NETVF,NETVV
INTEGER GSMX,PTMX
PARAMETER (GSMX = 250,PTMX = 750,NTDIS = 3)
PARAMETER (PI = 3.1415927)
COMMON /DEBUG/ NUMPAR(NTDIS,GSMX),VOLPAR(NTDIS,GSMX),
*   NETVF(PTMX),NETVV(PTMX),DADC(PTMX),NPARTL(NTDIS)
COMMON /DIST/ RDAVG(NTDIS),LOGSTD(NTDIS),VLFRFO(NTDIS),
*   VLFRVO(NTDIS)
COMMON /RESULT/ CRTSTN(PTMX),STRESS(PTMX),DILAT(PTMX),
*   PRBSRV(PTMX),SORRAD(PTMX),SORPAR(PTMX),SORVLP(PTMX),
*   IPDIST(PTMX)

```

C

```

IF (IABORT.EQ.1) RETURN

```

C

```

C== calculate total volume fraction filler and void

```

```

NETVF(1) = 0
NETVV(1) = 0
DO 10 I = 1,NDIST
    NETVF(1) = NETVF(1)+VLFRFO(I)
    NETVV(1) = NETVV(1)+VLFRVO(I)

```

```

10 CONTINUE

```

```

PRBSRV(1) = 1.0

```

C

```

C== calculate net Vf and Vv, dA/dc and Prob surv. array index offset
C by 1 to leave room for initial unbonded state

```

C

```

SRVNUM = 0

```

C

```

C== find total number of particles

```

```

DO 30 ICNT = 1,NDIST
    TLNUP = TLNUP + NPARTL(ICNT)

```

```

30 CONTINUE

```

C

```

DO 20 JCNT = 2,NDIST*NPTS+1
    VLFTOT = VLFTOT - SORVLP(JCNT-1)
    NETVF(JCNT) = NETVF(JCNT-1) - SORVLP(JCNT-1)/VOLSMP

```

UNCLASSIFIED

B.14

$$\text{NETVV}(\text{JCNT}) = \text{NETVV}(\text{JCNT}-1) + \text{SORVLP}(\text{JCNT}-1)/\text{VOLSMP}$$

$$\text{SRVNUM} = \text{SRVNUM} + \text{SORPAR}(\text{JCNT}-1)$$

$$\text{PRBSRV}(\text{JCNT}) = (\text{TLNUMP} - \text{SRVNUM})/\text{TLNUMP}$$

$$\text{DADC}(\text{JCNT}) = -6.0 * \text{VOLSMP} / \text{SORRAD}(\text{JCNT}-1)$$

20 CONTINUE

C

RETURN

END

C

C

SUBROUTINE MTPRP(CONCI,CONCV,ICNT,FDBND,YMULT,IKIND,IMORI,IPOIS,

* IABORT)

C==== program for calculating composite modulus based on Mori-Tanaka.

C

FDBND=fraction debond for orthotropic properties in loading

C

direction, IKIND=use inclusion or void properties in calc of

C

Wv matrix, IMORI=type of particle interaction used 0=none,

C

1=inclusion, 2=inclusion and void or vacuole, IPOIS=type of

C

debond properties 0=orthotropic, 1=isotropic

C

REAL IDENT,K,KCMP,MAG

PARAMETER (GSMX=250,PTMX=750,NTDIS=3)

COMMON /PROPB/ C11(PTMX),C12(PTMX),C21(PTMX),C22(PTMX),C23(PTMX),

* ECMP(PTMX),POISC(PTMX)

DIMENSION CAVG(3,3)

C

IF(IABORT.EQ.1) RETURN

C

IF(ICNT.EQ.1)THEN

CALL CALCIO(IABORT)

CALL CALCCV(FDBND,IPOIS,IABORT)

CALL CMPRPO(IKIND,IMORI,IABORT)

ELSE

ENDIF

C

CALL CMPRP(CONCI,CONCV,YMULT,CAVG,IABORT)

C11(ICNT)=CAVG(1,1)

C12(ICNT)=CAVG(1,2)

UNCLASSIFIED

B.15

```

C21(ICNT)=CAVG(2,1)
C22(ICNT)=CAVG(2,2)
C23(ICNT)=CAVG(2,3)
ECMP(ICNT)=C11(ICNT)-2.0*C12(ICNT)*C21(ICNT)/((C22(ICNT)+C23(ICNT)))
POISC(ICNT)=C21(ICNT)/((C22(ICNT)+C23(ICNT)))
C
RETURN
END
C
C
SUBROUTINE CRIT(ICNT,VOLSMP,GAMM,PRESS,IABORT)
C==== calculates critical strain based on current properties because
C the energy balance requires the input work to equal the energy
C released by surface creation and the internal energy stored
C after debonding has taken place.
C
REAL LOGSTD,NPARTL,NUMPAR,NETVF,NETVV
REAL IDENT,K,KCMP,KTMP,MAG
INTEGER GSMX,PTMX
PARAMETER (GSMX = 250,PTMX = 750,NTDIS = 3)
PARAMETER (TOL = 1E-18)
COMMON /GAUS/ Z(GSMX),RADIUS(NTDIS,GSMX),PROB(NTDIS,GSMX)
COMMON /DEBUG/ NUMPAR(NTDIS,GSMX),VOLPAR(NTDIS,GSMX),
* NETVF(PTMX),NETVV(PTMX),DADC(PTMX),NPARTL(NTDIS)
COMMON /PROPB/ C11(PTMX),C12(PTMX),C21(PTMX),C22(PTMX),C23(PTMX),
* ECMP(PTMX),POISC(PTMX)
COMMON /RESULT/ CRTSTN(PTMX),STRESS(PTMX),DILAT(PTMX),
* PRBSRV(PTMX),SORRAD(PTMX),SORPAR(PTMX),SORVLP(PTMX),
* IPDIST(PTMX)
C
IF (IABORT.EQ.1) RETURN
C
CONV = 1.0E+3
C
DC = NETVF(ICNT)-NETVF(ICNT-1)
IF (ABS(DC).LT.TOL) DC = -TOL
C

```

UNCLASSIFIED

B.16

```

TC12=C12(ICNT)
TC21=C21(ICNT)
TC22=C22(ICNT)
TC23=C23(ICNT)
DC11=(C11(ICNT)-C11(ICNT-1))/DC
DC12=(C12(ICNT)-C12(ICNT-1))/DC
DC21=(C21(ICNT)-C21(ICNT-1))/DC
DC22=(C22(ICNT)-C22(ICNT-1))/DC
DC23=(C23(ICNT)-C23(ICNT-1))/DC
C
AQUAD = -DC11+2.0*((TC22+TC23)*(TC21*DC12+TC12*DC21)-
* (TC12*TC21*(DC22+DC23)))/(TC22+TC23)**2
CQUAD = CONV*2*GAMM*DADC(ICNT)/VOLSMF
C
IF (AQUAD.GE.0) THEN
    WRITE (6, '(A)') ' SBR CRIT: square root term is negative.'
    CRTSTN(ICNT) = CRTSTN(ICNT-1)
ELSE
    CRTSTN(ICNT) = SQRT(CQUAD/AQUAD)
ENDIF
C
C== for debugging
C    WRITE(6, '(A,I3)') 'ICNT: ', ICNT
C    WRITE(6, '(A,E13.6,A,E13.6,A,E13.6)') )
C    * ' DE/DC: ', DCMPE, ' GC: ', GAMM, ' DA/DC: ', DADC(ICNT)
C    WRITE(6, '(A,E13.6,A,E13.6,A,E13.6)')
C    * ' AQUAD: ', AQUAD, ' CQUAD: ', CQUAD, ' STN: ', CRTSTN(ICNT-1)
RETURN
END
C
C
SUBROUTINE CALVAL(ICNT,PRESS,DILATO,IABORT)
C==== calculates stress and dilatation at critical strain
C    properties used are those before debonding takes place
C
REAL LOGSTD,NPARTL,NUMPAR,NETVF,NETVV
REAL IDENT,K,KCMP,KTMP,MAG

```

UNCLASSIFIED

B.17

```

      INTEGER GSMX,PTMX
      PARAMETER (GSMX = 250,PTMX = 750,NTDIS = 3)
      COMMON /PROPB/ C11(PTMX),C12(PTMX),C21(PTMX),C22(PTMX),C23(PTMX),
*    ECMP(PTMX),POISC(PTMX)
      COMMON /RESULT/ CRTSTN(PTMX),STRESS(PTMX),DILAT(PTMX),
*    PRBSRV(PTMX),SORRAD(PTMX),SORPAR(PTMX),SORVLP(PTMX),
*    IPDIST(PTMX)

C
      IF (IABORT.EQ.1) RETURN

C
      TC21 = C21(ICNT-1)
      TC22 = C22(ICNT-1)
      TC23 = C23(ICNT-1)
      ETMP = ECMP(ICNT-1)
      IF (ICNT.EQ.2) DILATO = PRESS*0

C
      STRESS(ICNT) = ETMP*CRTSTN(ICNT)
C== change stress values to MPa
      STRESS(ICNT) = STRESS(ICNT)/1.0E6
      DILAT(ICNT) = (1-(2.0*TC21/(TC22+TC23)))*CRTSTN(ICNT)-DILATO

C
      RETURN
      END

C
C
      BLOCK DATA INIT
C==== initialize all variables and arrays used in program
C    check PTMX if NTDIS or GSMX are changed.
C      PTMX = NTDIS*GSMX
C
      REAL LOGSTD,NPARTL,NUMPAR,NETVF,NETVV
      REAL IDENT,K,KCMP,MAG
      INTEGER GSMX,PTMX
      PARAMETER (GSMX = 250,PTMX = 750,NTDIS = 3)
      COMMON /GAUS/ Z(GSMX),RADIUS(NTDIS,GSMX),PROB(NTDIS,GSMX)
      COMMON /DEBUG/ NUMPAR(NTDIS,GSMX),VOLPAR(NTDIS,GSMX),
*    NETVF(PTMX),NETVV(PTMX),DADC(PTMX),NPARTL(NTDIS)

```

UNCLASSIFIED

B.18

```

COMMON /DIST/ RADA VG(NTDIS),LOGSTD(NTDIS),VLFRFO(NTDIS),
*   VLFRVO(NTDIS)
COMMON /MATRA/ BETA(2),WI(3,3),WV(3,3),IDENT(3,3)
COMMON /MATRB/ S(3,3),CA(3,3),CB(3,3),CE(3,3),CF(3,3)
COMMON /PROPA/ K(3),G(3),E(3),POIS(3),CI(3,3),CV(3,3),CO(3,3)
COMMON /PROPB/ C11(PMX),C12(PMX),C21(PMX),C22(PMX),C23(PMX),
*   ECMP(PMX),POISC(PMX)
COMMON /RESULT/ CRTSTN(PMX),STRESS(PMX),DILAT(PMX),
*   PRBSRV(PMX),SORRAD(PMX),SORPAR(PMX),SORVLP(PMX),
*   IPDIST(PMX)

```

C

```

DATA Z /GSMX*0/ RADIUS /PMX*0/ PROB /PMX*0/
DATA NUMPAR /PMX*0/ VOLPAR /PMX*0/ NETVF /PMX*0/ NETVV /PMX*0/
*   DADC /PMX*0/ NPARTL /NTDIS*0/
DATA RADA VG /NTDIS*0/ LOGSTD /NTDIS*0/ VLFRFO /NTDIS*0/ VLFRVO /
*   NTDIS*0/
DATA BETA /2*0/ WI /9*0/ WV /9*0/ IDENT /1,0,0,0,1,0,0,0,1/
DATA S /9*0/ CA /9*0/ CB /9*0/ CE /9*0/ CF /9*0/
DATA K /3*0/ G /3*0/ E /3*0/ POIS /3*0/ CI /9*0/ CV /9*0/ CO /9*0/
DATA C11 /PMX*0/ C12 /PMX*0/ C21 /PMX*0/ C22 /PMX*0/
*   C23 /PMX*0/ ECMP /PMX*0/ POISC /PMX*0/
DATA CRTSTN /PMX*0/ STRESS /PMX*0/ DILAT /PMX*0/
*   PRBSRV /PMX*0/ SORRAD /PMX*0/ SORPAR /PMX*0/ SORVLP /PMX*0/
*   IPDIST /PMX*0/

```

C

END

C

C

SUBROUTINE QSIMP(FUNC,A,B,S)

```

C==== used for integration of gaussian curve in sbr GAUSS. obtained
C   from Numerical Recipes, W.H. Press, Cambridge, 1988.

```

C

EXTERNAL FUNC

PARAMETER (EPS = 1.E-6,JMAX = 20)

OST = -1.E30

OS = -1.E30

DO 10 J = 1,JMAX

UNCLASSIFIED

B.19

```

      CALL TRAPZD(FUNC,A,B,ST,J)
      S = (4.*ST-OST)/3.
      IF (ABS(S-OS).LT.EPS*ABS(OS)) RETURN
      OS = S
      OST = ST
10  CONTINUE
      PAUSE 'Too many steps: SBR QSIMP'
      END
C
C
      SUBROUTINE TRAPZD(FUNC,A,B,S,N)
C==== used for integration of gaussian curve in sbr QSIMP which is
C      called from sbr GAUSS. obtained from Numerical Recipes, W.H.
C      Press, Cambridge, 1988.
C
      EXTERNAL FUNC
      IF (N.EQ.1) THEN
        S = 0.5*(B-A)*(FUNC(A)+FUNC(B))
        IT = 1
      ELSE
        TNM = IT
        DEL = (B-A)/TNM
        X = A+0.5*DEL
        SUM = 0.
        DO 10 J = 1,IT
          SUM = SUM+FUNC(X)
          X = X+DEL
10      CONTINUE
        S = 0.5*(S+(B-A)*SUM/TNM)
        IT = 2*IT
      ENDIF
      RETURN
      END
C
C
      SUBROUTINE SORT3(N,RA,RB,RC,IRD)
C==== sorting routine from Numerical Recipes, W.H. Press, Cambridge,

```

UNCLASSIFIED
B.20

C 1988. sorts in ascending order array RA and moves elements in
C arrays RB, RC and IRD at the same time.

C

```
DIMENSION RA(N),RB(N),RC(N),IRD(N)
L = N/2+1
IR = N
10 CONTINUE
  IF (L.GT.1) THEN
    L = L-1
    RRA = RA(L)
    RRB = RB(L)
    RRC = RC(L)
    IRRD = IRD(L)
  ELSE
    RRA = RA(IR)
    RRB = RB(IR)
    RRC = RC(IR)
    IRRD = IRD(IR)
    RA(IR) = RA(1)
    RB(IR) = RB(1)
    RC(IR) = RC(1)
    IRD(IR) = IRD(1)
    IR = IR-1
    IF (IR.EQ.1) THEN
      RA(1) = RRA
      RB(1) = RRB
      RC(1) = RRC
      IRD(1) = IRRD
      RETURN
    ENDIF
  ENDIF
  I = L
  J = L+L
20 IF (J.LE.IR) THEN
  IF (J.LT.IR) THEN
    IF (RA(J).LT.RA(J+1)) J = J+1
  ENDIF
```

UNCLASSIFIED

B.21

```

      IF (RRA.LT.RA(J)) THEN
        RA(I) = RA(J)
        RB(I) = RB(J)
        RC(I) = RC(J)
        IRD(I) = IRD(J)
        I = J
        J = J+J
      ELSE
        J = IR+1
      ENDIF
      GOTO 20
    ENDIF
    RA(I) = RRA
    RB(I) = RRB
    RC(I) = RRC
    IRD(I) = IRRD
    GOTO 10
  END

C
C
      SUBROUTINE CALCIO(IABORT)
C==== calculate the property matrix for inclusion and matrix,
C      isotropic relations
C
      REAL IDENT,K,KCMP,MAG
      COMMON /PROPA/ K(3),G(3),E(3),POIS(3),CI(3,3),CV(3,3),CO(3,3)
C
      IF(IABORT.EQ.1) RETURN
C
      K(1)=(2.0*G(1)*(1+POIS(1)))/(3.0*(1.0-2.0*POIS(1)))
      E(1)=G(1)*(2.0*(1+POIS(1)))
      K(3)=(2.0*G(3)*(1+POIS(3)))/(3.0*(1.0-2.0*POIS(3)))
      E(3)=G(3)*(2.0*(1+POIS(3)))
      C1=K(1)+(4.0/3.0)*G(1)
      C2=K(1)-(2.0/3.0)*G(1)
      C3=K(3)+(4.0/3.0)*G(3)
      C4=K(3)-(2.0/3.0)*G(3)

```

UNCLASSIFIED
B.22

```

      DO 11 I=1,3
        DO 21 J=1,3
          CI(I,J)=C2
          CO(I,J)=C4
          IF(I.EQ.J) CI(I,J)=C1
          IF(I.EQ.J) CO(I,J)=C3
21      CONTINUE
11      CONTINUE
C
      RETURN
      END
C
C
      SUBROUTINE CALCCV(FDBND,IPOIS,IABORT)
C==== calculate the property matrix for debonded particle,
C      orthotropic relations, FDBND is debond fraction for vacuole
C      IPOIS determines whether orthotropic or isotropic
C
      REAL IDENT,K,KCMP,MAG
      COMMON /PROPA/ K(3),G(3),E(3),POIS(3),CI(3,3),CV(3,3),CO(3,3)
C
      IF(IABORT.EQ.1) RETURN
C
      IF(K(2).NE.0.AND.G(2).NE.0) THEN
        POIS(2) = (3.0*K(2)-2.0*G(2))/(2.0*(3.0*K(2)+G(2)))
        E(2) = 9.0*K(2)*G(2)/(3.0*K(2)+G(2))
      ELSE
        E(2) = 0.0
        POIS(2) = 0.0
      ENDIF
C
      PCON=REAL(IPOIS)
      DETM = 1-POIS(2)**2-PCON*2*(POIS(2)**2+POIS(2)**3)
      CV(1,1)=(FDBND*E(2)*(1-POIS(2)**2))/DETM
      CV(1,2)=(FDBND*E(2)*(POIS(2)+POIS(2)**2))/DETM
      CV(1,3)=CV(1,2)
      CV(2,1)=(E(2)*PCON*POIS(2)*(1+POIS(2)))/DETM

```

UNCLASSIFIED

B.23

```

CV(2,2)=(E(2)*(1-PCON*POIS(2)**2))/DETM
CV(2,3)=(E(2)*(POIS(2)+PCON*POIS(2)**2))/DETM
CV(3,1)=CV(2,1)
CV(3,2)=CV(2,3)
CV(3,3)=CV(2,2)

```

C

```

RETURN
END

```

C

C

```

SUBROUTINE CMPRPO(IKIND,IMORI,IABORT)

```

```

C==== calculate constants in composite equation

```

C

```

REAL IDENT,K,KCMP,MAG
COMMON /MATRB/ S(3,3),CA(3,3),CB(3,3),CE(3,3),CF(3,3)
COMMON /PROPA/ K(3),G(3),E(3),POIS(3),CI(3,3),CV(3,3),CO(3,3)
DIMENSION CTEMPA(3,3),CTEMPB(3,3)

```

C

```

IF(IABORT.EQ.1) RETURN

```

C

```

CALL CALCW(IKIND,IMORI,IABORT)
CALL CALCS(IABORT)
CALL SUB(CTEMPA,CI,CO)
CALL INVERT(CTEMPB,CTEMPA,IABORT)
CALL MULT(CA,CTEMPB,CO)
CALL SUB(CTEMPA,CV,CO)
CALL INVERT(CTEMPB,CTEMPA,IABORT)
CALL MULT(CB,CTEMPB,CO)
CALL ADD(CE,S,CB)
CALL ADD(CF,S,CA)

```

C

```

RETURN
END

```

C

```

SUBROUTINE CMPRP(CONCI,CONCV,YMULT,CAVG,IABORT)

```

```

C== calculate composite properties, ITYPE identifies inclusion

```

C

```

or void

```

UNCLASSIFIED

B.24

```

REAL IDENT,K,KCMP,MAG
COMMON /MATRA/ BETA(2),WI(3,3),WV(3,3),IDENT(3,3)
COMMON /MATRB/ S(3,3),CA(3,3),CB(3,3),CE(3,3),CF(3,3)
COMMON /PROPA/ K(3),G(3),E(3),POIS(3),CI(3,3),CV(3,3),CO(3,3)
DIMENSION CC(3,3),CD(3,3),CG(3,3),CH(3,3)
DIMENSION CTEMPA(3,3),CTEMPB(3,3),CTEMPC(3,3),CAVG(3,3)

C
C== calculate phase-dependent components of composite equation
C calculate first half
C calculate phase-i components
  ITYPE = 1
  CALL GAMMA(CG,CONCI,ITYPE,YMULT,IABORT)
  CALL SUB(CTEMPA,IDENT,S)
  CALL SUB(CTEMPB,CTEMPA,CG)
  DO 11 I=1,3
    DO 21 J=1,3
      CC(I,J)=CONCI*CTEMPB(I,J)
21  CONTINUE
11 CONTINUE
C calculate phase-v components
  ITYPE = 2
  CALL GAMMA(CH,CONCV,ITYPE,YMULT,IABORT)
  CALL SUB(CTEMPA,IDENT,S)
  CALL SUB(CTEMPB,CTEMPA,CH)
  DO 31 I=1,3
    DO 41 J=1,3
      CD(I,J)=CONCV*CTEMPB(I,J)
41  CONTINUE
31 CONTINUE
  CALL INVERT(CTEMPA,CE,IABORT)
  CALL MULT(CTEMPB,CD,CTEMPA)
  CALL MULT(CTEMPA,CTEMPB,CF)
C combine phase-i and phase-v components
  CALL ADD(CTEMPB,CTEMPA,CA)
  CALL ADD(CTEMPA,CTEMPB,S)
  CALL ADD(CTEMPB,CTEMPA,CC)
  CALL INVERT(CTEMPA,CTEMPB,IABORT)

```

UNCLASSIFIED

B.25

```

      CALL MULT(CTEMPB,CG,CTEMPA)
      DO 51 I=1,3
        DO 61 J=1,3
          CTEMPC(I,J)=CONCI*CTEMPB(I,J)
61      CONTINUE
51 CONTINUE
C      calculate second half
      CALL INVERT(CTEMPA,CF,IABORT)
      CALL MULT(CTEMPB,CC,CTEMPA)
      CALL MULT(CTEMPA,CTEMPB,CE)
C      combine phase-i and phase-v components
      CALL ADD(CTEMPB,CTEMPA,CB)
      CALL ADD(CTEMPA,CTEMPB,S)
      CALL ADD(CTEMPB,CTEMPA,CD)
      CALL INVERT(CTEMPA,CTEMPB,IABORT)
      CALL MULT(CTEMPB,CH,CTEMPA)
      DO 71 I=1,3
        DO 81 J=1,3
          CTEMPA(I,J)=CONCV*CTEMPB(I,J)
81      CONTINUE
71 CONTINUE
C=     combine all components
      CALL ADD(CTEMPB,CTEMPC,CTEMPA)
      CALL ADD(CTEMPA,CTEMPB,IDENT)
      CALL MULT(CAVG,CO,CTEMPA)
C
      RETURN
      END
C
C
      SUBROUTINE CALCW(IKIND,IMORI,IABORT)
C==== calculate correction matrices WI and WV and BETA for
C      use in sbr GAMMA, IKIND determines inclusion or void for vacuole
C      IMORI determines if correction matrix used, 0=none,1=inclusion
C      2=inclusion and void
C
      REAL IDENT,K,KCMP,MAG

```

UNCLASSIFIED

B.26

```

REAL KTEMP,KMAT
COMMON /MATRA/ BETA(2),WI(3,3),WV(3,3),IDENT(3,3)
COMMON /MATRB/ S(3,3),CA(3,3),CB(3,3),CE(3,3),CF(3,3)
COMMON /PROPA/ K(3),G(3),E(3),POIS(3),CI(3,3),CV(3,3),CO(3,3)

C
IF(IABORT.EQ.1) RETURN

C
POISM = POIS(3)
KMAT = K(3)
GMAT = G(3)

C
KTEMP=K(1)
GTEMP=G(1)
DO 11 INCL=1,2
  IF(INCL.EQ.2.AND.IKIND.EQ.0)THEN
    GTEMP=0.0
    KTEMP=0.0
  ELSE
    GTEMP=G(INCL)
    KTEMP=K(INCL)
  ENDIF

C
ALPHA = 2.0*(5.0*POISM-1)+10.0*(1-POISM)*
*      (KMAT/(KTEMP-KMAT)-GMAT/(GTEMP-GMAT))
BETA(INCL) = 2.0*(4.0-5.0*POISM)+15.0*(1-POISM)*
*      (GMAT/(GTEMP-GMAT))
ZETA1 = 12.0*(13.0*POISM-14.0*POISM**2)-(96.0*ALPHA/
*      (3.0*ALPHA+2.0*BETA(INCL)))*(1-2.0*POISM)*(1+POISM)
ZETA2 = 6.0*(25.0-34.0*POISM+22.0*POISM**2)-(36.0*ALPHA/
*      (3.0*ALPHA+2.0*BETA(INCL)))*(1-2.0*POISM)*(1+POISM)

C
DO 21 I=1,3
  DO 31 J=1,3
    IF(INCL.EQ.1.AND.IMORI.NE.0)THEN
      WI(I,J)=ZETA1
      IF(I.EQ.J) WI(I,J)=ZETA1+2*ZETA2
    ELSEIF(INCL.EQ.1.AND.IMORI.EQ.0)THEN

```


UNCLASSIFIED

B.27

```

                WI(I,J)=0.0
                ELSEIF(INCL.EQ.2.AND.IMORI.EQ.2)THEN
                    WV(I,J)=ZETA1
                    IF(I.EQ.J) WV(I,J)=ZETA1+2*ZETA2
                ELSE
                    WV(I,J)=0.0
                ENDIF
31      CONTINUE
21      CONTINUE
11      CONTINUE
C
    RETURN
    END
C
C
    SUBROUTINE CALCS(IABORT)
C==== calculate Eshelby matrices SI and SV
    COMMON /MATRB/ S(3,3),CA(3,3),CB(3,3),CE(3,3),CF(3,3)
    COMMON /PROPA/ K(3),G(3),E(3),POIS(3),CI(3,3),CV(3,3),CO(3,3)
C
    IF(IABORT.EQ.1) RETURN
C
    POISM = POIS(3)
    SDET = 15.0*(1-POISM)
C
    S1 = 5.0*POISM-1
    S2 = 4.0-5.0*POISM
C
    DO 11 I=1,3
        DO 21 J=1,3
            S(I,J)=S1/SDET
            IF(I.EQ.J) S(I,J)=(S1+2.0*S2)/SDET
21      CONTINUE
11      CONTINUE
C
    RETURN
    END

```

UNCLASSIFIED

B.28

```

C
C
      SUBROUTINE GAMMA(A,CONC,ITYPE,YMULT,IABORT)
C==== calculate correction matrix A given inclusion I and its
C      concentration CONC, Y depends on microstructural features
C      ITYPE identifies inclusion or void
      REAL IDENT,K,KCMP,MAG
      COMMON /MATRA/ BETA(2),WI(3,3),WV(3,3),IDENT(3,3)
      DIMENSION A(3,3)
C
      IF(IABORT.EQ.1) RETURN
C
      Y=YMULT*(1-CONC)/24.0
      MAG = 5.0*CONC*Y/(4.0*BETA(ITYPE)**2)
      DO 11 I=1,3
        DO 21 J=1,3
          IF(ITYPE.EQ.1) A(I,J)=IDENT(I,J)+MAG*WI(I,J)
          IF(ITYPE.EQ.2) A(I,J)=IDENT(I,J)+MAG*WV(I,J)
21      CONTINUE
11 CONTINUE
C
      RETURN
      END
C
C
      SUBROUTINE ADD(C,A,B)
C==== subroutine for adding two square matrices C=A+B
      DIMENSION A(3,3),B(3,3),C(3,3)
C
      DO 11 I=1,3
        DO 21 J=1,3
          C(I,J) = A(I,J)+B(I,J)
21      CONTINUE
11 CONTINUE
C
      RETURN
      END

```

UNCLASSIFIED

B.29

C

C

SUBROUTINE SUB(C,A,B)

C==== subroutine for adding two square matrices C=A-B

DIMENSION A(3,3),B(3,3),C(3,3)

C

DO 11 I=1,3

DO 21 J=1,3

C(I,J) = A(I,J)-B(I,J)

21 CONTINUE

11 CONTINUE

C

RETURN

END

C

C

SUBROUTINE MULT(C,A,B)

C==== subroutine for multiplying two square matrices C=A.B

DIMENSION A(3,3),B(3,3),C(3,3)

C

DO 11 I=1,3

DO 21 J=1,3

C(I,J) = 0

DO 31 K=1,3

C(I,J) = C(I,J)+A(I,K)*B(K,J)

31 CONTINUE

21 CONTINUE

11 CONTINUE

C

RETURN

END

C

C

SUBROUTINE INVERT(AI,A,IABORT)

C==== subroutine used for inverting matrix A to give AI

DIMENSION A(3,3),AI(3,3)

C

UNCLASSIFIED

B.30

```

      IF(IABORT.EQ.1) RETURN
C
      DETA = -(A(1,3)*A(2,2)*A(3,1)) + A(1,2)*A(2,3)*A(3,1)
*      + A(1,3)*A(2,1)*A(3,2) - A(1,1)*A(2,3)*A(3,2)
*      - A(1,2)*A(2,1)*A(3,3) + A(1,1)*A(2,2)*A(3,3)
C
      IF(DETA.NE.0)THEN
        AI(1,1) = (-(A(2,3)*A(3,2)) + A(2,2)*A(3,3))/DETA
        AI(1,2) = (A(1,3)*A(3,2) - A(1,2)*A(3,3))/DETA
        AI(1,3) = (-(A(1,3)*A(2,2)) + A(1,2)*A(2,3))/DETA
        AI(2,1) = (A(2,3)*A(3,1) - A(2,1)*A(3,3))/DETA
        AI(2,2) = (-(A(1,3)*A(3,1)) + A(1,1)*A(3,3))/DETA
        AI(2,3) = (A(1,3)*A(2,1) - A(1,1)*A(2,3))/DETA
        AI(3,1) = (-(A(2,2)*A(3,1)) + A(2,1)*A(3,2))/DETA
        AI(3,2) = (A(1,2)*A(3,1) - A(1,1)*A(3,2))/DETA
        AI(3,3) = (-(A(1,2)*A(2,1)) + A(1,1)*A(2,2))/DETA
      ELSE
        IABORT = 1
        WRITE(6,'(A)') 'SBR INVERT: indeterminate matrix'
      ENDIF
C
      RETURN
      END
C
C
      SUBROUTINE GAUWRT(NDIST,NPTS,IABORT)
C==== write out cumulative distribution data.
C      for some reason, cannot print out PROBs correctly using
C      F format, numbers end up getting multiplied by ten.
C
C      set PTMX = NTDIS*GSMX
C
      REAL LOGSTD,NPARTL,NUMPAR,NETVF,NETVV
      INTEGER GSMX,PTMX
      PARAMETER (GSMX = 250,PTMX = 750,NTDIS = 3)
      COMMON /GAUS/ Z(GSMX),RADIUS(NTDIS,GSMX),PROB(NTDIS,GSMX)
C

```

UNCLASSIFIED

B.31

```

      IF (IABORT.EQ.1) RETURN
      WRITE (6, '(A)') ' Writing GAUSS.DAT'
C
      OPEN (UNIT=7, FILE='_GAUSS.DAT', FORM='FORMATTED', STATUS='UNKNOWN')
      WRITE (7, 5000)
      DO 10 IPTS = 1, NPTS
          WRITE (7, 5100) Z(IPTS), (PROB(IDIST, IPTS), RADIUS(IDIST, IPTS),
*           IDIST = 1, NDIST)
10 CONTINUE
      CLOSE (7)
C
      RETURN
5000 FORMAT ('      Z           Pr           Radius(mm)           Pr
*      Radius(mm)           Pr           Radius(mm)')
5100 FORMAT (1X, F6.3, 6(3X, OPE13.6))
      END
C
C
      SUBROUTINE HSTWRT(NDIST, NPTS, IABORT)
C==== write out histogram and tracking data
C
      REAL LOGSTD, NPARTL, NUMPAR, NETVF, NETVV
      INTEGER GSMX, PTMX
      PARAMETER (GSMX = 250, PTMX = 750, NTDIS = 3)
      COMMON /GAUS/ Z(GSMX), RADIUS(NTDIS, GSMX), PROB(NTDIS, GSMX)
      COMMON /DEBUG/ NUMPAR(NTDIS, GSMX), VOLPAR(NTDIS, GSMX),
*      NETVF(PTMX), NETVV(PTMX), DADC(PTMX), NPARTL(NTDIS)
C
      IF (IABORT.EQ.1) RETURN
      WRITE (6, '(A)') ' Writing HISTO.DAT'
C
      OPEN (UNIT=7, FILE='_HISTO.DAT', FORM='FORMATTED', STATUS='UNKNOWN')
      NPRTOT = 0
      VOLTOT = 0
      DO 30 IDIST = 1, NDIST
          DO 40 IHST = 1, NPTS
              NPRTOT = NPRTOT + NUMPAR(IDIST, IHST)

```

UNCLASSIFIED

B.32

```

          VOLTOT = VOLTOT + VOLPAR(IDIST,IHST)
40      CONTINUE
30      CONTINUE
C
      CUMVOL = 0.0
      DO 20 IDIST = 1,NDIST
          WRITE (7,5000)
          DO 10 IHST = 1,NPTS
              PERNPR = 100*REAL(NUMPAR(IDIST,IHST))/REAL(NPRTOT)
              PERVOL = 100*VOLPAR(IDIST,IHST)/VOLTOT
              CUMVOL = CUMVOL + PERVOL
              WRITE (7,5100) IHST,RADIUS(IDIST,IHST),
*                  ALOG10(NUMPAR(IDIST,IHST)),VOLPAR(IDIST,IHST),PERNPR,
*                  PERVOL,PROB(IDIST,IHST),CUMVOL
10      CONTINUE
20      CONTINUE
      CLOSE (7)
C
      RETURN
5000 FORMAT (' Point      avg R(mm)      log # part.      volume(mm3) %no.
*particles % part.volume cum. prob.      cum. vol.>')
5100 FORMAT (2X,I3,3X,7(1PE13.6,2X))
      END
C
C
      SUBROUTINE STRWRT(NDIST,NPTS,VOLSMP,GAMM,FDBND,YMULT,IKIND,IMORI,
*      IPOIS,PRESS,DILATO,FILNM,IABORT)
C==== write out stress and dilatation results versus critical strain
C      include probability survival, radius, no. particles and
C      distribution info.
C
      REAL LOGSTD,NPARTL,NUMPAR,NETVF,NETVV
      REAL IDENT,K,KCMP,MAG
      INTEGER GSMX,PTMX
      PARAMETER (GSMX = 250,PTMX = 750,NTDIS = 3)
      COMMON /DIST/ RDAVG(NTDIS),LOGSTD(NTDIS),VLFRFO(NTDIS),
*      VLFRVO(NTDIS)

```

UNCLASSIFIED

B.33

```

COMMON /DEBUG/ NUNPAR(NTDIS,GSMX),VOLPAR(NTDIS,GSMX),
*   NETVF(PMX),NETVV(PMX),DADC(PMX),NPARTL(NTDIS)
COMMON /PROPA/ K(3),G(3),E(3),POIS(3),CI(3,3),CV(3,3),CO(3,3)
COMMON /PROPB/ C11(PMX),C12(PMX),C21(PMX),C22(PMX),C23(PMX),
*   ECMP(PMX),POISC(PMX)
COMMON /RESULT/ CRTSTN(PMX),STRESS(PMX),DILAT(PMX),
*   PRBSRV(PMX),SORRAD(PMX),SORPAR(PMX),SORVLP(PMX),
*   IPDIST(PMX)
CHARACTER FILNM*8

C
  IF (IABORT.EQ.1) RETURN

C
  IF (FILNM.EQ.'DEFAULT') FILNM = '_STRESS'
  WRITE (6,'(/,A,A8,A)') ' Writing to ',FILNM,'.DAT'

C
  OPEN (UNIT=7,FILE=FILNM//'_DAT',STATUS='UNKNOWN')
  WRITE (7,5000)
  DO 10 I = 1,NDIST
    WRITE (7,'(1X,I1,4(3X,OPE11.4))') I,RADAVG(I),LOGSTD(I),
*      VLFRFO(I),VLFRVO(I)
10 CONTINUE

C
  WRITE (7,5100) G(3),G(1),POIS(3),POIS(1),G(2),K(2)
  WRITE (7,5200) VOLSMF,FDBND,YMULT,IKIND,IMORI,IPOIS
  WRITE (7,5300) PRESS,GAMM,DILATO
  WRITE (7,5400)
  DO 20 I = 1,NDIST*NPTS+1
    ETMP = ECMP(I)/1E6
    WRITE (7,5600) I,CRTSTN(I),STRESS(I),DILAT(I),PRBSRV(I),ETMP,
*      POISC(I),NETVF(I),NETVV(I),IPDIST(I-1)
20 CONTINUE

C
  CLOSE (7)
  RETURN

5000 FORMAT (' #      avg Rad(um)      std dev      Vf      Vv')
5100 FORMAT (' Gm(Pa)=',OPE11.4,' Gf(Pa)=',OPE11.4,' vm=',OPE11.4,
*   ' vf=',OPE11.4,' Gv(Pa)=',OPE11.4,' Kv=',OPE11.4)

```

UNCLASSIFIED

B.34

```

5200 FORMAT (' V(mm3) =',OPE11.4,' frac dbnd=',OPE11.4,' Y-mult=',
*   OPE11.4,' w-type=',I3,' m-type=',I3,' v-type=',I3)
5300 FORMAT (' P0(Pa)=',OPE11.4,' Gc(Pa-m)=',OPE11.4,' (dV/V)0=',OPE11
*   .4)
5400 FORMAT (' Point  crit strn      stress(MPa)      dV/V      Pr|surv
*   E_c(MPa)      Poisson      V_f      V_v      dist')
5600 FORMAT (1X,I3,3X,8(1PE11.4,2X),1X,I1)
C
      END
C
C
      SUBROUTINE DBGWRT(NDIST,NPTS,IABORT)
C==== write out additional data for debugging purposes
C
C      set PTMX = NTDIS*GSMX
C
      REAL LOGSTD,NPARTL,NUMPAR,NETVF,NETVV
      REAL IDENT,K,KCMP,MAG
      INTEGER GSMX,PTMX
      PARAMETER (GSMX = 250,PTMX = 750,NTDIS = 3)
      COMMON /GAUS/ Z(GSMX),RADIUS(NTDIS,GSMX),PROB(NTDIS,GSMX)
      COMMON /DEBUG/ NUMPAR(NTDIS,GSMX),VOLPAR(NTDIS,GSMX),
*   NETVF(PTMX),NETVV(PTMX),DADC(PTMX),NPARTL(NTDIS)
      COMMON /PROPB/ C11(PTMX),C12(PTMX),C21(PTMX),C22(PTMX),C23(PTMX),
*   ECMP(PTMX),POISC(PTMX)
      COMMON /RESULT/ CRTSTN(PTMX),STRESS(PTMX),DILAT(PTMX),
*   PRBSRV(PTMX),SORRAD(PTMX),SORPAR(PTMX),SORVLP(PTMX),
*   IPDIST(PTMX)
C
      IF (IABORT.EQ.1) RETURN
      WRITE (6,'(A)') ' Writing DEBUG.DAT'
C
      OPEN (UNIT=7,FILE='_DEBUG.DAT',FORM='FORMATTED',STATUS='UNKNOWN')
      WRITE (7,5000)
      DO 10 IHST = 1,NDIST*NPTS+1
          WRITE (7,5100) IHST,NETVF(IHST),NETVV(IHST),DADC(IHST),
*   C11(IHST),C12(IHST),C21(IHST),C22(IHST),C23(IHST),

```


UNCLASSIFIED

B.35

```

      *      PRBSRV(IHST)
10  CONTINUE
      CLOSE (7)
C
      RETURN
5000 FORMAT (' Point      net Vf      net Vv      dA/dc
      * C11      C12      C21      C22      C23
      *      Pr|surv')
5100 FORMAT (2X,I3,3X,9(OPE13.6,2X))
      END
C
C
      SUBROUTINE DBGRAT(NDIST,NPTS,IABORT)
C==== write out additional data for debugging purposes
C      along with stress-strain data outputs radius and the factor
C      SQRT(RAD*dG/dc) to look at its relationship with crit. strain
C
C      set PTMX = NTDIS*GSMX
C
      REAL LOGSTD,NPARTL,NUMPAR,NETVF,NETVV
      REAL IDENT,K,KCMP,KTMP,MAG
      INTEGER GSMX,PTMX
      PARAMETER (GSMX = 250,PTMX = 750,NTDIS = 3)
      COMMON /GAUS/ Z(GSMX),RADIUS(NTDIS,GSMX),PROB(NTDIS,GSMX)
      COMMON /DEBUG/ NUMPAR(NTDIS,GSMX),VOLPAR(NTDIS,GSMX),
      *   NETVF(PTMX),NETVV(PTMX),DADC(PTMX),NPARTL(NTDIS)
      COMMON /PROPB/ C11(PTMX),C12(PTMX),C21(PTMX),C22(PTMX),C23(PTMX),
      *   ECMP(PTMX),POISC(PTMX)
      COMMON /RESULT/ CRTSTN(PTMX),STRESS(PTMX),DILAT(PTMX),
      *   PRBSRV(PTMX),SORRAD(PTMX),SORPAR(PTMX),SORVLP(PTMX),
      *   IPDIST(PTMX)
C
      IF (IABORT.EQ.1) RETURN
      WRITE (6,'(A)') ' Writing DERAT.DAT'
C
      OPEN (UNIT=7,FILE='_DERAT.DAT',FORM='FORMATTED',STATUS='UNKNOWN')
      WRITE (7,5000)

```

UNCLASSIFIED

B.36

```

DO 10 IHST = 1,NDIST*NPTS+1
  ETMP = ECMP(IHST)
  RAD = 0.0
  DNETF = 0.0
  DNETV = 0.0
  DETMP = 0.0
  IF(IHST.GT.1) RAD = SORRAD(IHST-1)
  IF(IHST.GT.1) DNETF = ABS(NETVF(IHST) - NETVF(IHST-1))
  IF(IHST.GT.1) DNETV = ABS(NETVV(IHST) - NETVV(IHST-1))
  IF(IHST.GT.1) DETMP = ABS(ECMP(IHST) - ECMP(IHST-1))
  FACT = SQRT(RAD*DETM)
  WRITE (7,5100) IHST,CRTSTN(IHST),STRESS(IHST),RAD,PRBSRV(IHST),
*      ETMP,POISC(IHST),DNETF,DNETV,FACT
10 CONTINUE
  CLOSE (7)
C
  RETURN
5000 FORMAT (' Point   crit strn   stress(MPa)  Avg r(mm)   Pr|surv
*      E_c(MPa)   Poisson   dV_f         dV_v         fact')
5100 FORMAT (1X,I3,3X,9(1PE11.4,2X))
END
C
C
  INCLUDE 'MSGRAPH.FOR'
C
  SUBROUTINE CRVPLT(NDIST,NPTS,IABORT)
C==== driver routine for plotting curve on screen, keep the
C      INCLUDE 'MSGRAPH.FOR' with this module.
C
C      set PTMX = NTDIS*GSMX
C
  REAL LOGSTD,NPARTL,NUMPAR,NETVF,NETVV
  INTEGER GSMX,PTMX
  PARAMETER (GSMX = 250,PTMX = 750,NTDIS = 3)
  COMMON /RESULT/ CRTSTN(PTMX),STRESS(PTMX),DILAT(PTMX),
*      PRBSRV(PTMX),SORRAD(PTMX),SORPAR(PTMX),SORVLP(PTMX),
*      IPDIST(PTMX)

```

UNCLASSIFIED

B.37

```
DIMENSION X(PTMX),Y1(PTMX),Y2(PTMX)
CHARACTER ANS*1
C
IF (IABORT.EQ.1) RETURN
C
10 CONTINUE
WRITE (6,'(/,A)') ' Graph results on screen? (Y/N)'
READ (5,'(A1)') ANS
C
NTOT = NDIST*NPTS+1
DO 20 ICNT = 1,NTOT
    X(ICNT) = CRTSTN(ICNT)
    Y1(ICNT) = STRESS(ICNT)
    Y2(ICNT) = DILAT(ICNT)
20 CONTINUE
C
IF (ANS.EQ.'Y') THEN
    WRITE (6,'(A)') ' Strain, Stress and dV/V end pts'
    READ (5,*) XEND,YSEND,YDEND
    CALL GRAF(NTOT,X,Y1,Y2,XEND,YSEND,YDEND)
ELSE
ENDIF
C
IF (ANS.EQ.'Y') GOTO 10
C
RETURN
END
C
C
SUBROUTINE GRAF(N,X,Y1,Y2,XEND,YSEND,YDEND)
C
C    set PTMX = NTDIS*GSMX
C
INTEGER PTMX
PARAMETER (GSMX = 250,PTMX = 750,NTDIS = 3)
DIMENSION X(PTMX),Y1(PTMX),Y2(PTMX)
C
```

UNCLASSIFIED

B.38

```
      INCLUDE 'GRFDEF.FOR'
C
      CALL VIDEO(MAXX,MAXY,NOGRAF)
      IF (NOGRAF.EQ.0) THEN
C
          CALL VWPORT(MAXX,MAXY)
C
          XBEG = 0
          YBEG = 0
          CALL WINDOW(XBEG,YBEG,XEND,YSEND)
          ICURV = 1
          XLAB = 'strain'
          YLAB = 'strs (MPa)'
          CALL ATTRIB(ICURV,ILNCOL,ILNSTY)
          CALL LABELS(ICURV,ILNCOL,XLAB,YLAB,XBEG,YBEG,XEND,YSEND)
C
          ICURV = 1
          CALL ATTRIB(ICURV,ILNCOL,ILNSTY)
          CALL CURVE(X,Y1,N,ILNCOL,ILNSTY)
          CALL WINDOW(XBEG,YBEG,XEND,YDEND)
          ICURV = 3
          XLAB = 'strain'
          YLAB = 'dV/V'
          CALL ATTRIB(ICURV,ILNCOL,ILNSTY)
          CALL LABELS(ICURV,ILNCOL,XLAB,YLAB,XBEG,YBEG,XEND,YDEND)
          ICURV = 3
          CALL ATTRIB(ICURV,ILNCOL,ILNSTY)
          CALL CURVE(X,Y2,N,ILNCOL,ILNSTY)
C
          CALL ENDGRF()
      ELSE
          WRITE (6,'(A)') ' SBR GRAF: problem with graphics'
      ENDIF
C
      RETURN
      END
```

UNCLASSIFIED

INTERNAL DISTRIBUTION

DREV R-9514

1 - Deputy Director General
1 - H/EM Section
6 - Document Library
1 - F.C. Wong (Author)
1 - P. Brousseau
1 - Dr. S. Thiboutot
1 - S. Villeneuve
1 - G. Bérubé
1 - M. Bolduc
1 - Dr. D. Nandlall

UNCLASSIFIED

EXTERNAL DISTRIBUTION

DREV R-9514

- 2 - DSIS
- 1 - CRAD
- 1 - DSAL
- 1 - DSAA
- 1 - DSAM
- 1 - DAEPM(FT)
- 1 - DLR
- 1 - DMCS
- 1 - DARFT
- 1 - DNR

- 1 - Bristol Aerospace Ltd.
Rockets and Space Division
P.O. Box 874
Winnipeg, MB
R3C 2S4
Attn: Engineering Library

- 1 - National Research Council Canada
National Aeronautical Establishment
Structures and Materials Laboratory
Ottawa, Ontario
Attn: Dr. W. Wallace

- 1 - U. S. Army Missile Command
AMSMI-RD-PR-M (B. Marsh)
Redstone Arsenal, AL 35898-5249
United States of America
Attn: Commander

UNCLASSIFIED

EXTERNAL DISTRIBUTION

DREV R-9514

- 1 - Aeronautical and Maritime Research Laboratory
Explosives Ordnance Division
Salisbury, SA 5108
Attn: Dr. Sook Ying Ho
- 2 - Defence Research Agency
Propulsion Research
Fort Halstead
Sevenoaks, Kent TN 14 7BP
United Kingdom
Attn: Dr. Jim Buswell, Dr. M. Hinton
- 1 - Dept. of Materials Engineering
Composite Group
The University of British Columbia
23324 Main Mall
Vancouver, B.C.
V6T 1Z4
Attn: Dr. A. Poursarstip

UNCLASSIFIED
SECURITY CLASSIFICATION OF FORM
 (Highest classification of Title, Abstract, Keywords)

DOCUMENT CONTROL DATA

1. ORIGINATOR (name and address) DREV P.O. Box 8800 Courcellette, Qc GOA 1R0	2. SECURITY CLASSIFICATION (Including special warning terms if applicable) UNCLASSIFIED	
3. TITLE (Its classification should be indicated by the appropriate abbreviation (S,C,R or U) On the Prediction of Mechanical Behavior of Particulate Composites Using an Improved Mori-Tanaka Method		
4. AUTHORS (Last name, first name, middle initial. If military, show rank, e.g. Doe, Maj. John E.) Wong, Franklin, C.		
5. DATE OF PUBLICATION (month and year)	6a. NO. OF PAGES 64	6b. NO. OF REFERENCES 39
7. DESCRIPTIVE NOTES (the category of the document, e.g. technical report, technical note or memorandum. Give the inclusive dates when a specific reporting period is covered.) Technical Report		
8. SPONSORING ACTIVITY (name and address)		
9a. PROJECT OR GRANT NO. (Please specify whether project or grant)	9b. CONTRACT NO.	
10a. ORIGINATOR'S DOCUMENT NUMBER R-9514	10b. OTHER DOCUMENT NOS. N/A	
11. DOCUMENT AVAILABILITY (any limitations on further dissemination of the document, other than those imposed by security classification) <ul style="list-style-type: none"> <input checked="" type="checkbox"/> Unlimited distribution <input type="checkbox"/> Contractors in approved countries (specify) <input type="checkbox"/> Canadian contractors (with need-to-know) <input type="checkbox"/> Government (with need-to-know) <input type="checkbox"/> Defence departments <input type="checkbox"/> Other (please specify) : 		
12. DOCUMENT ANNOUNCEMENT (any limitation to the bibliographic announcement of this document. This will normally correspond to the Document Availability (11). However, where further distribution (beyond the audience specified in 11) is possible, a wider announcement audience may be selected.)		

UNCLASSIFIED
SECURITY CLASSIFICATION OF FORM

UNCLASSIFIED
SECURITY CLASSIFICATION OF FORM

13. **ABSTRACT** (a brief and factual summary of the document. It may also appear elsewhere in the body of the document itself. It is highly desirable that the abstract of classified documents be unclassified. Each paragraph of the abstract shall begin with an indication of the security classification of the information in the paragraph (unless the document itself is unclassified) represented as (S), (C), (R), or (U). It is not necessary to include here abstracts in both official languages unless the text is bilingual).

New micromechanical models for the prediction of particulate composite mechanical behavior have been developed. The models use an energy balance concept to account for nonlinear behavior due to particle debonding and incorporate a composite modulus prediction routine based on an improved Mori-Takana method. This method permits particle interaction effects to be taken into account and allows the stiffness matrix for voids or vacuoles to be explicitly stated in the model. To demonstrate the characteristics of the improved Mori-Takana method, comparisons with 2-phase and 3-phase modulus data were made. The micromechanical models developed for void and vacuole formation were evaluated against available mechanical behavior data. Comparisons showed that the model derived for vacuole formation predicted the mechanical behavior correctly for a range of composites which contained inclusion volume fractions ranging from 0.2 to 0.4. The inability of the models to predict the initial stress-strain behavior of a composite containing a volume fraction of 0.22 of well bonded particles suggests nonlinear matrix effects need to be included in the present model formulation.

14. **KEYWORDS, DESCRIPTORS or IDENTIFIERS** (technically meaningful terms or short phrases that characterize a document and could be helpful in cataloging the document. They should be selected so that no security classification is required. Identifiers, such as equipment model designation, trade name, military project code name, geographic location may also be included. If possible keywords should be selected from a published thesaurus. e.g. Thesaurus of Engineering and Scientific Terms (TEST) and that thesaurus-identified. If it is not possible to select indexing terms which are Unclassified, the classification of each should be indicated as with the title.)

Micromechanics, Mori-Takana, particle interaction, debond, 2-phase, 3-phase, void, vacuole, Eshelby, elastic properties, prediction, energy balance, mechanical behavior, eigenstrain.

501263

UNCLASSIFIED
SECURITY CLASSIFICATION OF FORM